N-glycosylation of fibulin-4 regulates tropoelastin interaction and assembly

Chae Syng Lee

Department of Anatomy and Cell Biology, Faculty of Medicine

McGill University

Montreal, Quebec, CANADA

April, 2015

A thesis submitted to McGill University in partial fulfillment of the requirements of

the degree of Master of Science

TABLE OF CONTENTS

TABLE OF CONTENTS ..... **i**
TABLE OF FIGURES ..... **iii**
LIST OF TABLES ..... **v**
ACKNOWLEDGEMENTS ..... **vi**
CONTRIBUTIONS ..... **viii**
ABBREVIATIONS ..... **ix**
1 ABSTRACT AND RÉSUMÉ **1**
1.1 Abstract 1
1.2 Résumé 3
2 LITERATURE REVIEW AND INTRODUCTION **5**
2.1 The extracellular matrix 5
2.2 Elastic fibers 5
2.3 Elastin 6
2.4 Microfibrils 8
2.5 Short fibulins 10
2.5.1 Characteristics and properties 10
2.5.2 Human mutations and mouse models of fibulin-4 12
2.5.3 Human mutations and mouse models of fibulin-5 13
2.5.4 Fibulin-4 and -5 in elastogenesis 14
2.6 N-linked glycosylation 17
2.7 Unfolded protein response 19
3 OBJECTIVES **22**
4 MATERIALS AND METHODS **23**
4.1 Antibodies 23
4.2 Generation of fibulin-4 N-linked glycosylation site mutants 24
4.3 Cell culture 25
4.3.1 Cell lines 25
4.3.2 Cell transfection procedures 25
4.4 Recombinant protein purification 26

4.5 Sodium Dodecyl Sulphate-Polyacrylamide Gel Electrophoresis 27
4.6 Western blotting 28
4.7 Peptide -N-Glycosidase F deglycosylation assay 29
4.8 Solid phase binding assay 29
4.9 Indirect immunofluorescence assay 30
4.10 Enzyme-linked immunosorbent assay 30
4.11 Reverse transcription polymerase chain reaction 31
4.12 Dot blot assay 31
5 RESULTS 32
5.1 Fibulin-4 exhibits enhanced binding upon deglycosylation 32
5.2 Generation of the mutants of fibulin-4 lacking N-linked glycosylation sites 35
5.3 Analysis of Western blotting and Coomassie blue staining of the recombinantly-expressed fibulin-4 wild-type and the N-linked glycosylation site mutants 39
5.4 Comparison of cell surface deposition between fibulin-4 wild-type and glycosylation site mutants 43
5.5 Analysis of XBP1 mRNA 46
5.6 Analysis on established cell lines for their elastogenic properties 48
5.6.1 Analysis of ARPE-19 48
5.6.2 Analysis of RFL-6 53
5.6.3 Analysis of FBC 53
5.6.4 Analysis of PAC1 53
5.7 Overexpression of fibulin-4 glycosylation site mutants induces more secretion and assembly of tropoelastin into fibers 56
5.8 Overexpression of fibulin-4 wild-type and glycosylation site mutants enhance secretion of tropoelastin into ECM but does not increase expression of tropoelastin 64
5.9 Additional results related to the project 67
6 RATIONALE, DISCUSSIONS, AND FUTURE DIRECTIONS 71
6.1 Rationale 71
6.2 Disrupted secretory pathway 72
6.3 Impact on elastogenesis 74
6.4 Working models 78
6.5 Conclusions 81
7 REFERENCES 82

TABLE OF FIGURES

Figure 1. Schematic overview of human tropoelastin domain structures 7
Figure 2. Formation of microfibrils in non-elastic and elastic tissues 9
Figure 3. Schematic overview of the human short fibulins 11
Figure 4. Model of role of fibulin-4 and -5 in early elastogenesis 15
Figure 5. Overview of the process of N-linked glycosylation 18
Figure 6. Overview of the unfolded protein response 20
Figure 7. Enzymatically deglycosylated fibulin-4 shows enhanced binding to tropoelastin 33
Figure 8. Schematic overview of the generation of fibulin-4 N-linked glycosylation mutants expression plasmids. 36
Figure 9. Experimental overview of the generation of fibulin-4 N-linked glycosylation mutants expression plasmids outlined in figure 8 37
Figure 10. Confirmation of the desired Asn-Gln mutations by the Sanger sequencing chromatograms 38
Figure 11. Comparison between fibulin-4 wild-type and N-glycosylation site mutants 40
Figure 12. Densitometric comparison between fibulin-4 wild-type and the N-linked glycosylation site mutants 42
Figure 13. Fibulin-4 glycosylation site mutants exhibit less deposition onto the HEK293H cell surface 44
Figure 14. HEK293H cells transfected with N-linked glycosylation site mutant constructs demonstrate UPR 47
Figure 15. Analysis of cell lines for elastogenic properties 50
Figure 16. Elastic fiber assembly in PAC1 55
Figure 17. Analysis of recombinant overexpression of fibulin-4 wild-type and N-linked Glycosylation site mutants in PAC1 cells 57
Figure 18. Addition of exogenous fibulin-4 slightly enhances elastic fiber assembly 62
Figure 19. Analysis of mRNA and secreted protein levels in transfected PAC1 cells 65
Figure 20. ELISA analysis using different antibodies against fibulin-4 wild-type and the fibulin-4_N-1 fragment 68
Figure 21. Western blotting comparison between the anti-fibulin-4 antibody and

affinity purified anti-fibulin-4_AP-N antibody 70
Figure 22. Working model of fibulin-4 wild-type and the N-linked glycosylation site mutant secretory pathway in HEK293H cells 79
Figure 23. Working model of fibulin-4 wild-type and the N-linked glycosylation site mutant secretory pathway in PAC1 cells 80

LIST OF TABLES

Table 1. Summary of the analysis of cell lines for their elastogenic components 49

ACKNOWLEDGEMENTS

Foremost, I would express my sincere gratitude to my supervisor, Dr. Dieter Reinhardt, for his thoughtful advice, generous and patient guidance, as well as his sharp and helpful critics and kind encouragements, which all motivated and inspired me to go through this journey of master's program. I truly appreciate being a graduate student in his lab, conducting research here helped me greatly to become a scientific researcher. Additionally, I thank Dr. Reinhardt for thoughtful and invaluable inputs for my thesis. Without his support and patience, this all could not have been possible.

Next, I would like to thank the past and current Reinhardt laboratory members who were a constant source of pleasure during the program. Jelena Djokic, a past MSc student and a research assistant, introduced me to all the important techniques, and provided a kind guidance for any questions I had during the first one and a half years. I thank Amelie Pagliuzza, a past lab manager, for preparing such an organized and enthusiastic lab environment to conduct experiments, and to socialize. I further thank my current lab members including Dr. Valentin Nelea, Heena Kumra, Hong Pham, and Karina Zeyer, as well as a laboratory neighbour Hidetaka Ishii, for being not only great lab mates but true friends. I always appreciate their presences and thank God for giving such wonderful people around me.

I thank my committee members, Dr. Natalie Lamarche-Vane, Dr. John Presley, and Dr. Lisbet Haglund, for their time during my committee meeting, which greatly helped me and guided my project in every positive ways with their precious input.

I would like to give a special thanks to Dr. Elaine Davis who provided two elastogenic cell lines, fetal bovine chondroblasts and rat pulmonary arterial smooth muscle cells, for my experiments.

Furthermore, I thank the department of Anatomy and Cell Biology at McGill University for providing me such a wonderful opportunity to explore the world of scientific research.

Last but not least, I would like to thank my family, including my dad (Kwang Jin Lee), my mom (Yun Wha Lee), my brother (Chae Won Lee), and my girlfriend (Unkyung Shin) for their everyday prayers which always encourage me to move on, constantly caring about my health and happiness to do research, and for their unconditional support throughout this master's program.

And above all, I give all the glory to my God.

CONTRIBUTIONS

I planned and performed all the experiments and data analysis included in this thesis, with the exceptions listed below.

Dr. Dieter Reinhardt guided and mentored this project. He contributed in providing ideas for experiments, trouble-shootings, and discussions. Dr. Dieter Reinhardt critically and thoroughly proof-read this thesis.

The preparation of the wild-type fibulin-4 construct and subsequent transfection into mammalian cells were performed by a former lab manager, Christine Fagotto-Kaufmann. She also generated the anti-fibulin-4 and -5 antibodies.

Dr. Valentine Nelea performed the Biacore analyses of wild-type and deglycosylated fibulin-4 binding to tropoelastin.

ABBREVIATIONS

ATF6	Activating transcription factor 6
AP-N	Affinity-purified fibulin-4 antibody against N-1 fragment
APS	Ammonium persulfate
BCA	Bicinchoninic acid
BiP	Immunoglobulin-binding protein
BSA	Bovine serum albumin
C	Carboxyl terminal
cbEGF	Calcium-binding epidermal growth factor
cDNA	Complementary deoxyribonucleic acid
dH_2O	Deionized water
DAPI	4',6-diamidino-2-phenylindole
DMEM	Dulbecco's Modified Eagle medium
DNA	Deoxyribonucleic acid
DTT	Dithiothreitol
ECM	Extracellular matrix
ELISA	Enzyme-linked immunosorbent assay
ELN	Elastin
Endo	Endogenous
ER	Endoplasmic reticulum
ERAD	Endoplasmic reticulum-associated degradation
FBN-1	Fibrillin-1

FBS	Fetal bovine serum
FN	Fibronectin
G418	Gentamicin sulfate antibiotic
GAPDH	Glyceraldehyde 3-phosphate dehydrogenase
HEK293	Human embryonic kidney
HEPES	4-(2-hydroxyethyl)-1-1-piperazineethanesulfonic acid
hFBLN4	human fibulin-4
hFBLN4_I-II	N-terminus to cbEGF6 domain fragment
hFBLN4_N-1	N-terminus to cbEGF1 domain fragment
IgG	Immunoglobulin G
IRE1	Inositol-requiring kinase 1
kDa	kiloDalton
KO	Knock-out
LOX	Lysyl oxidase
LOXL1	Lysyl oxidase-like-1
LTBP	Latent TGFβ binding protein
MMP	Matrix metalloproteinase
mRNA	Messenger ribonucleic acid
Mut1, 2, T	fibulin-4 N-linked glycosylation site mutant 1, 2, T
N	Amino terminal
N.C.	Negative control
NT	Non-transfected cells
PBS	Phosphate-buffered saline

PCR	Polymerase chain reaction
PERK	Protein kinase R (PKR)-like endoplasmic reticulum kinase
PMSF	Phenylmethanesulfonylfluoride
PNGaseF	Peptide -N-glycosidase F
PSG	Penicillin-streptomycin-glutamine
Rec	Recombinant
RGD	Arginine-Glycine-Aspartic Acid
SDS	Sodium dodecyl sulfate
SDS-PAGE	Sodium dodecyl sulfate-polyacrylamide gel electrophoresis
TBS	Tris-buffered saline
TBST	Tris-buffered saline containing Tween-20
TEMED	Tetramethylethylenediamine
TGFβ	Transforming growth factor beta
UPR	Unfolded protein responses
WT	Wild-type
XBP1	X-box binding protein 1

1 ABSTRACT AND RÉSUMÉ

1.1 Abstract

The fibulin family is a group of eight extracellular glycoproteins, characterized by a variable number of calcium-binding epidermal growth factor (cbEGF) domains followed by a fibulin-type module at the C-terminus. Fibulin-3, -4, and -5 are referred to as the short fibulins, and consist of six cbEGF domains followed by the C-terminal domain. The short fibulins are expressed in various elastic tissues, including blood vessels, lungs and skin, and are known to play important roles in elastogenesis. Fibulin-4 is of great interest as mutations lead to cardiovascular and skin disease in humans. Its absence results in perinatal death in the corresponding knockout mouse model. Human fibulin-4 contains two N-linked glycans of unknown function, one in the third cbEGF domain at Asn^{198}, and one in the C-terminal domain at Asn^{394}.

The recombinant histidine-tagged human fibulin-4 was expressed in the mammalian HEK293H expression system and purified the protein by chelating (Ni^{2+}) chromatography. After fibulin-4 was enzymatically deglycosylated, it exhibited enhanced binding to tropoelastin, the soluble form of elastin, as compared to the fully glycosylated fibulin-4. Based on these results, it was hypothesized that fibulin-4 N-glycosylation plays a critical role in elastic fiber formation. To test this hypothesis, Mutants of fibulin-4 lacking the N-linked glycosylation site i) at Asn^{198}, ii) at Asn^{394}, and iii) at both sites were generated. The mutant constructs were transfected into HEK293H cells to ensure proper post-translational modifications. All glycosylation mutants were secreted in significantly lower amounts compared to the wild-type protein, and showed enhanced activation of the unfolded protein response pathway, indicating that folding in the endoplasmic reticulum was stalled. This demonstrates that N-linked glycosylation of fibulin-4 is important for proper secretion of the protein into the extracellular matrix. To identify a suitable cell culture model for elastogenesis, several cell lines were surveyed by immunofluorescent staining of relevant elastogenic proteins. Pulmonary aortic smooth muscle cells (PAC1) showed expression of fibronectin, fibrillin-1, and tropoelastin. The fibulin-4 wild-type and the glycosylation mutants were transfected in PAC1 cells to study their consequences on elastic fiber formation. It was found that overexpression of fibulin-4 enhances tropoelastin secretion from these cells. All glycosylation

mutants enhanced the assembly of tropoelastin into extracellular fibers significantly more than the wild-type fibulin-4. The data suggest that the fibulin-4 interaction with tropoelastin is regulated by the presence of N-linked glycans, possibly within the secretory pathway as a chaperone function. The data further indicate that the N-linked fibulin-4 glycans inhibit the extracellular formation of elastic fibers.

1.2 Résumé

La famille des fibulines comprend huit glycoprotéines extracellulaires, caractérisées par un nombre variable de domaines de type « calcium-binding epidermal growth factor » (cbEGF), suivis de modules de type fibuline en C-terminal. Les fibulines-3, -4 et -5 consistent en six domaines cbEGF suivis par le domaine C-terminal. Ces fibulines sont exprimées dans divers tissus élastiques, incluant les vaisseaux sanguins, les poumons et la peau, et jouent un rôle important dans l'élastogénèse. Notamment, des mutations dans la fibuline-4 sont responsables de maladies cardiovasculaires et cutanées, et son absence dans les modèles de souris cause une mort prénatale. La fibuline-4 humaine contient deux groupes glycanes de fonction inconnue, un situé dans le cbEGF à la position Asn^{198}, et le second dans le domaine C-terminal à la position Asn^{394}.

La fibuline-4 recombinante comportant un tag histidine a été exprimée dans des cellules HEK293H, puis purifiée par chromatographie d'affinité. L'affinité de la fibuline-4 pour la tropoelastine après déglycosylation enzymatique étant augmentée, nous avons supposé que la glycosylation de la fibuline-4 joue un rôle essentiel dans la formation des fibres élastiques. Pour tester cette hypothèse, nous avons généré des mutants de la fibuline-4 dépourvue d'un ou des deux sites de N-glycosylation. Les constructions encodant les mutants ont été transfectées dans des cellules HEK293H pour s`assurer que les modifications post-traductionnelles étaient adéquates. Tous les mutants étaient sécrétés en quantité significativement inférieure à la protéine normale, et montraient une activation de la réponse aux protéines malformées, indiquant que le processus repliement conformationnel de conformation de la protéine au sein du réticulum endoplasmique était bloqué. Ce résultat démontre que la N-glycosylation de la fibuline-4 est important pour assurer la sécrétion de la protéine dans la matrice extracellulaire. Afin d'identifier un bon modèle de culture cellulaire pour l'étude de l'élastogénèse, l'expression de protéines élastogéniques a été analysée par immunofluorescence dans plusieurs lignées cellulaires. Les cellules musculaires lisses aortiques de rats (PAC1) ont été sélectionnées et transfectées avec la fibuline-4 de type sauvage ou mutante afin d'étudier l'impact de la glycosylation sur la formation des fibres élastiques. Nous avons découvert que la surexpression de la fibuline-4 augmente la sécrétion de tropoélastine, et que les mutants induisent un meilleur assemblage de la tropoélastine dans les fibres extracellulaires. Ces données suggèrent que l'intéraction de la fibuline-4 avec la tropoélastine est régulée par la présence de glycosylation, possiblement par une fonction de

chaperonne dans la voie de sécrétion, et que les N-glycanes inhibent la formation de fibres élastiques dans l'espace extracellulaire.

2 LITERATURE REVIEW AND INTRODUCTION

2.1 The extracellular matrix

The extracellular matrix (ECM) acts as a dynamic micro-environment surrounding the cells in multicellular organisms. Functions of the ECM include 1) providing adhesive substrates for cells, 2) conferring structural integrity to tissues and organs, 3) enabling communications between cells and tissues through cell-surface receptors or through mechanical forces, and 4) acting as a reservoir for numerous growth factors, providing them upon needs (Rozario and DeSimone, 2010). The ECM is composed of various molecules, including collagen and non-collagenous glycoproteins, glycosaminoglycans and proteoglycans, and elastin (Aumailley and Gayraud, 1998). ECM constantly undergoes remodeling processes where the components of the matrix are deposited, modified, and degraded, and these dynamic changes are tightly regulated (Lu et al., 2011). Failure in the regulation of ECM dynamics may result in abnormal cell proliferation and invasion which can further develop into pathogenesis, including fibrosis and cancer (Ihn, 2002; Muschler and Streuli, 2010). Therefore, it is extremely important to understand the dynamic mechanisms of the ECM.

2.2 Elastic fibers

Elastic fibers are one of the major ECM fibers in connective tissues which require elasticity, such as aorta, arteries, skin, lung, ligaments, and auricular cartilage (Mecham and Davis, 1994). Structurally, they are composed of the mature cross-linked elastin core (~90%) and a remaining portion of ~10% is constituted by microfibrils surrounding the core (Hubmacher and Reinhardt, 2011; Kozel et al., 2011). Functionally, elastic fibers serve the following three major functions in vertebrates (Kielty, 2006). First, they maintain all elastic tissues structurally by providing physical elasticity. Second, they regulate the availability of growth factors of the transforming growth factor beta (TGFβ) superfamily in elastic tissues. Third, elastic fibers mediate cell attachment which can further lead to regulation of cell differentiation, migration, and survival. The molecular composition of elastic fibers also include the elastic fiber interface connecting the elastic fiber with microfibrils which includes latent TGFβ binding protein-2 and -4 (LTBP-2 and -4), fibulin-2, -4

and -5, and emilin-1 (Gibson et al., 1995; McLaughlin et al., 2006; Nakamura et al., 2002; Noda et al., 2013; Yanagisawa et al., 2002; Zanetti et al., 2004).

2.3 Elastin

Tropoelastin with a molecular mass of ~65-70kDa mainly contains hydrophobic amino acid residues, including alanine, leucine, and valine which compose the typical hydrophobic domains (~40%), as well as glycine (~33%) and proline (~10-13%) (Kozel et al., 2011). There are also lysine-containing cross-linking domains which constitutes pairs of lysine residues separated by two or three alanine (KA) or proline (KP) residues. Tropoelastin is highly expressed during development from mid-gestation to the post-natal period, and declines drastically thereafter (Holzenberger et al., 1993; Keeley, 1979). Tropoelastin is an extremely durable protein, with a life span of ~80 years, measured by aspartic acid racemization and ^{14}C turnover (Shapiro et al., 1991). In adult tissue, the expression of tropoelastin is suppressed through a post-translational mechanism which mediates rapid decay of the messenger ribonucleic acid (mRNA) (Parks, 1997).

Tropoelastin is secreted as a soluble molecule in the ECM. Due to the hydrophobic domains, soluble tropoelastin tends to interact between each other through the hydrophobic domains. This results in tropoelastin coacervation, or molecules correctly-aligning and aggregating with each other (Rapaka and Urry, 1978). When tropoelastin is properly coacervated in the ECM, the lysine/alanine or lysine/proline-rich hydrophilic domains are cross-linked by lysyl oxidase (LOX) which forms covalent linkages between the maturing elastin molecules (Kagan and Sullivan, 1982; Mithieux and Weiss, 2005). Two of the covalent linkages can further condense with each other, forming desmosine or isodesmosine crosslinks (Partridge et al., 1963).

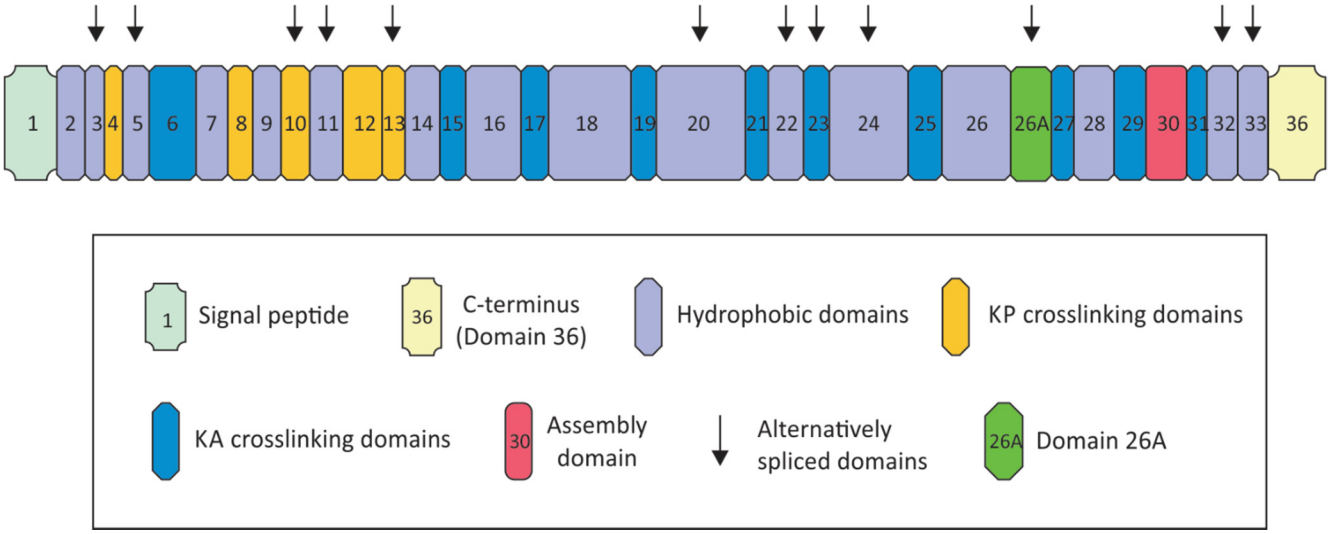

Figure 1. Schematic overview of human tropoelastin domain structures

Human tropoelastin consists of 34 domains, and the hydrophobic and hydrophilic domains are alternatively arrayed. Human tropoelastin lacks exon 34 and 35 which are found in other mammalian tropoelastins. Purple boxes represent domains composed of hydrophobic amino acid residues, whereas orange and blue boxes represent hydrophilic domains either rich in lysine-alanine (KA) or lysine-proline (KP). The arrows indicate exons that are alternatively spliced.

Homozygous elastin knock-out (KO) mice die perinatally due to subendothelial cell proliferation and reorganization of smooth muscle cells, resulting in lethal obstructive arterial disease (Li et al., 1998a). Heterozygous elastin mice are viable with ~50% reduction in both elastin mRNA and protein, and exhibited supravalvular aortic stenosis (Li et al., 1998b). Human mutations in the elastin gene have been reported to lead to cardiovascular and other elasticity-related diseases, including supravalvular aortic stenosis, William-Beuren syndrome, and autosomal dominant cutis laxa (Curran et al., 1993; Ewart et al., 1993; Tassabehji et al., 1998).

2.4 Microfibrils

Microfibrils are ~10-12nm in diameter formed adjacent to cells producing elastin and parallel to the developing elastic fiber (Mithieux and Weiss, 2005). They are composed of polymerized fibrillin-1, -2 and -3 and associated with numerous accessory proteins (Corson et al., 2004; Kielty, 2006; Sakai et al., 1986; Zhang et al., 1994). Tissue or cell culture extracts, visualized by electron microscopy after rotary shadowing revealed that microfibrils appear as a bead-on-a-string structure with bead periodicity of ~56nm (Keene et al., 1991; Wess et al., 1998). Whereas microfibrils are tightly associated on the surface of elastic fibers in blood vessels, lung, and skin, they are also found in non-elastic tissues in the absence of elastic fibers such as the ciliary zonules of the eye, superficial regions of the skin, and kidney (Kriz et al., 1990; Raviola, 1971). The main functions of microfibrils are 1) to provide structural integrity to tissues in zones close to basement membranes, 2) to act as a scaffold for elastin to be deposited and assembled, and 3) to regulate the availability of growth factors such as TGFβ and bone morphogenetic proteins (Hubmacher and Reinhardt, 2011; Ramirez and Sakai, 2010).

The assembly and formation of fibrillin-containing microfibrils require several steps, including protein processing as well as interaction with other ECM molecules. First, fibrillins are secreted from mesenchymal cells, such as fibroblasts as propeptides and become processed into mature fibrillin through furin-type convertases (Milewicz et al., 1995). Oligomerization of fibrillins mediated through their carboxyl terminal (C-terminal) region forms the basic bead unit of

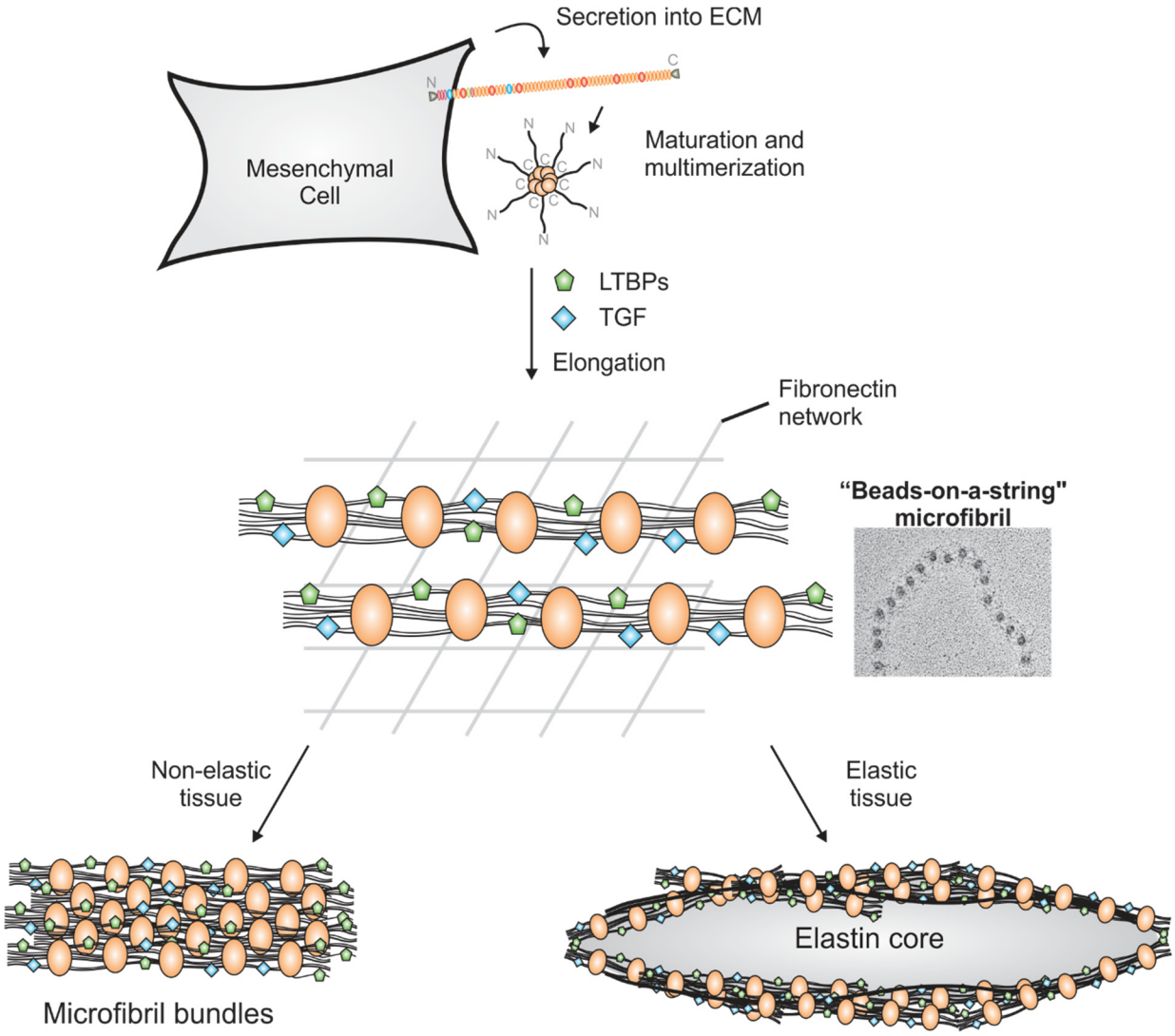

Figure 2. Formation of microfibrils in non-elastic and elastic tissues

Fibrillins are secreted from mesenchymal cells, such as fibroblasts. The secreted fibrillins undergo maturation through multimerization through both C-C-terminal and C-N-terminal interactions which result in formation of "beads-on-a-string" microfibrils. This process requires a fibronectin network. The assembled microfibrils can either form microfibril bundles in non-elastic tissues, such as ciliary zonules of the eyes, or form elastic fibers in elastic tissues, such as blood vessels and lung.

microfibrils with high avidity to bind other bead units to result in the typical beads-on-the string microfibrils (Hubmacher et al., 2008).

Human mutations in fibrillins have been reported to lead to various connective tissue disorders, which are generally referred to as fibrillinopathies. Mutations in fibrillin-1 lead to Marfan syndrome, dominant Weill-Marchesani syndrome, or stiff skin syndrome, whereas mutations in fibrillin-2 cause congenital contractural arachnodactyly or Beals-Hecht syndrome (Loeys et al., 2010; Robinson et al., 2006; Viljoen et al., 1991). Mice lacking fibrillin-1 die perinatally due to aortic aneurysm, impaired pulmonary function and/or diaphragmatic rupture, whereas fibrillin-2 KO mice develop morphologically normal aorta (Carta et al., 2006). Mice deficient for both fibrillin-1 and -2 die around E14.5 *in utero* - due to impaired or delayed elastogenesis in the medial layer of the aorta compared to the wild-type mice (Carta et al., 2006).

2.5 Short fibulins

2.5.1 Characteristics and properties

Fibulins are a family of extracellular glycoproteins with eight members (Segade, 2010; Yanagisawa and Davis, 2010). Among the eight members, fibulin-3, -4 and -5 are grouped as "short fibulin" (Fig. 3). The genes of the short fibulins are evolutionarily conserved between many species, from sea squirts to vertebrates, including humans (Segade, 2010). Fibulin-4 and -5 have been extensively studied and are known to play critical roles in elastic fiber formation, or elastogenesis (Papke and Yanagisawa, 2014). The predicted molecular masses for fibulin-4 and -5 are 54 and 52kDa each, and they are composed of six tandem arrays of calcium-binding epidermal growth factor-like domains (cbEGF domains) followed by a fibulin-type module at their C-termini (Giltay et al., 1999; Jones et al., 2010; Nakamura et al., 1999). Fibulin-4 and -5 are also characterized by an amino-terminal (N-terminal) linker of 28 and 44 amino acids between the fourth and fifth cysteine in the first cbEGF domain (Kobayashi et al., 2007). Additionally, fibulin-4 and -5 contain two predicted evolutionarily well conserved N-linked glycosylation sites, suggesting important but yet unknown functions.

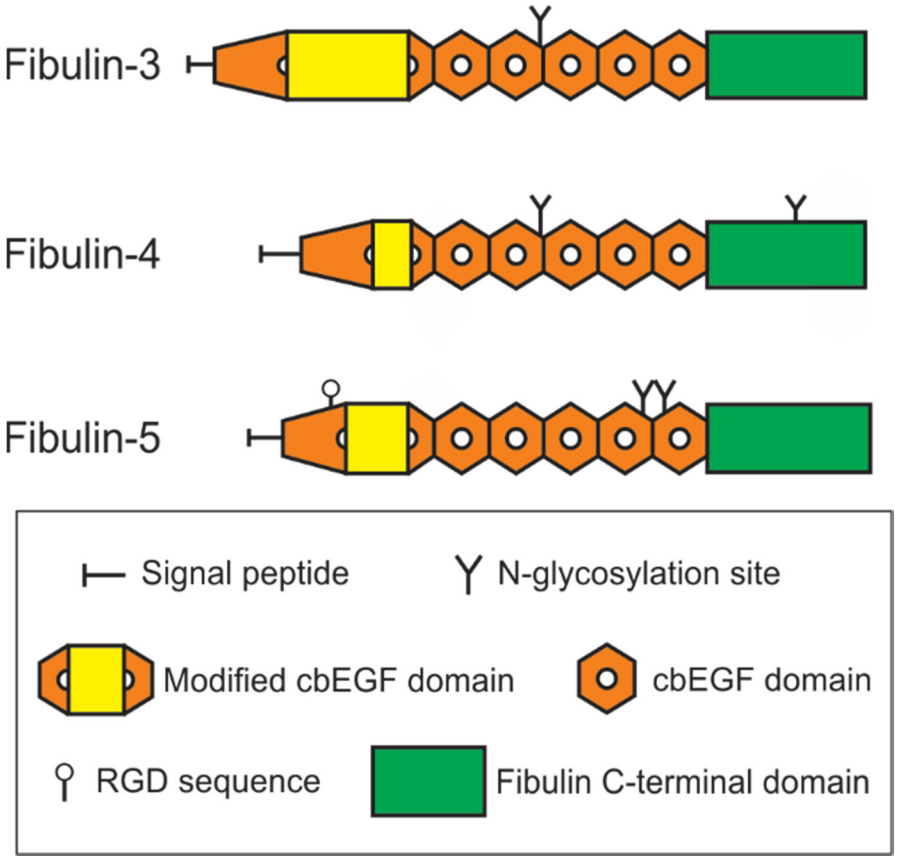

Figure 3. Schematic overview of the human short fibulins

The short fibulins are composed of six tandem arrays of cbEGF domains, followed by fibulin-type module at the C-terminus. Fibulin-3 contains one predicted N-glycosylation site whereas fibulin-4 and -5 contain two predicted sites. The short fibulins contain varying lengths of N-terminal linker region in the first cbEGF domain between fourth and fifth cysteines. Only fibulin-5 contains an RGD sequence which mediates cell-integrin interactions.

Recombinantly expressed and purified full-length human fibulin-4 shows a double band at 65 and 61kDa, whereas when it is enzymatically deglycosylated the size shifts to 57kDa, suggesting that the two glycosylation sites in recombinant human fibulin-4 are either single- or double-occupied by glycans (Djokic et al., 2013). Only fibulin-5 contains an arginine-glycine-aspartic acid (RGD) sequence in its first cbEGF domain which mediates cell interaction through several integrins including α4β1, α5β1, and αVβ3 (Kobayashi et al., 2007; Lomas et al., 2007). Both fibulin-4 and -5 are expressed in various tissues which require the expression of elastic fibers, such as aorta, large blood vessels, lung, skin, heart, and skeletal muscles (Giltay et al., 1999; Kobayashi et al., 2007).

2.5.2 Human mutations and mouse models of fibulin-4

Humans with mutations in fibulin-4 have been reported with autosomal recessive cutis laxa, a heterogeneous group of connective tissue disorders characterized by abnormalities in elastic connective tissues (Hebson et al., 2014). Most patients exhibit aortic aneurysms, dilation and tortuosity of arteries, and skin defects, whereas a smaller group show deficiencies in lungs and bone. Depending on the severities of the disease, patients live different lifespans, some die perinatally whereas others develop to the adult age.

A fibulin-4 complete KO mouse has been generated through targeted disruption of the fibulin-4 gene (McLaughlin et al., 2006). These mice die perinatally at postnatal day 2. They show severe vascular and lung phenotypes. Several arterial irregularities including aneurysms, dilatation, rupture, tortuosity, narrowing and hemorrhages were observed. The distal airspaces were significantly enlarged, resembling a lung emphysema phenotype. The abnormalities appeared as early as embryonic day 12.5 and it was found that these mice show deficiencies in elastogenesis, with severely reduced amount of mature elastin and low contents of desmosine.

Huang et al. generated a conditional fibulin-4 KO mouse model in smooth muscle cell- ($Fbln4^{SMKO}$) to determine the mechanism of aneurysm formation (Huang et al., 2010). These mice die after about 2 months. The ascending aortas show aneurysms whereas the descending aortas were elongated. These data demonstrate that the formation of aortic aneurysms as well as aorta elongation were due to the absence of fibulin-4 in the smooth muscle cells.

In order to study the role of fibulin-4 in later stages of life, another mouse model with reduced expression of fibulin-4 was generated (Hanada et al., 2007). The heterozygous (fibulin-$4^{+/R}$) mice express about 2 fold less fibulin-4 RNA whereas the homozygous (fibulin-$4^{R/R}$) mice express about 4 fold less compared to the wild-type mice. Both fibulin-$4^{+/R}$ and fibulin-$4^{R/R}$ mice do not die perinatally and they only show cardiovascular phenotypes, but not lung or skin defects. The ascending aortas of fibulin-$4^{+/R}$ mice were occasionally dilated with the formation of small aneurysms whereas the fibulin-$4^{R/R}$ aortas were significantly more dilated and elongated. The descending aortas of fibulin-$4^{R/R}$ mice were narrowed as well. Furthermore, the hearts of fibulin-$4^{R/R}$ mice showed defects in their function with increased pressure and stroke volumes. Transcriptome comparisons between the wild-type, fibulin-$4^{+/R}$ and fibulin-$4^{R/R}$ mice revealed that numerous inflammatory/immune and apoptotic genes undergo significant changes due to the reduction in fibulin-4. Many differentially expressed genes were found to be related to the TGFβ signaling pathway, suggesting an additional role of fibulin-4 in regulation of TGFβ signaling (Hanada et al., 2007).

2.5.3 Human mutations and mouse models of fibulin-5

Patients with mutations in fibulin-5 have also been reported with autosomal recessive cutis laxa, however, the severity of the symptoms are much milder than what was observed for fibulin-4 mutations (Hu et al., 2006; Loeys et al., 2002). The clinical symptoms include loose skin with only mild cardiovascular defects. Interestingly, two fibulin-5 mutations have been reported to decrease binding affinity for tropoelastin (Hu et al., 2006; Kobayashi et al., 2007), suggesting a possible pathogenetic mechanism by interfering with elastogenesis. Other mutations in fibulin-5 have been reported to result in age-related macular degeneration (Stone et al., 2004). Accumulations of proteins and lipids beneath the retinal pigment epithelium and within the Bruch's membrane can result in loss of central vision.

Fibulin-5 KO mice are viable, and they develop abnormally lax skin with folds, sagging jowls, large cheeks and senescent appearances (Nakamura et al., 2002; Yanagisawa et al., 2002). Fibulin-$5^{-/-}$ mice show characteristics of elongation and tortuosity of the arteries which is accompanied by loss of compliances in blood vessels. Interestingly, fibulin-$5^{-/-}$ mice do not develop aortic

aneurysms. However pulmonary enlargement and disruption of distal airspaces were commonly observed. A hallmark at the histological level is disruptions of the elastic laminae in the ascending aortas and skin. Overall, these data suggest that fibulin-5 plays critical roles in elastogenesis.

2.5.4 Fibulin-4 and -5 in elastogenesis

The expression profile, the associated human disorders, as well as the mouse studies clearly demonstrate that fibulin-4 and -5 play critical roles in elastic tissues and organs. Although the exact elastogenic mechanisms of the two fibulins are not clear, several studies have been performed to investigate the molecular roles of short fibulins in elastogenesis. Figure 4 graphically summarizes these data.

Fibulin-4 has been shown to interact with several extracellular proteins which are involved in elastic fiber formation, including tropoelastin, LOX, and fibrillin-1 (Choudhury et al., 2009; Horiguchi et al., 2009; Kobayashi et al., 2007; McLaughlin et al., 2006). It shows moderate binding affinity for tropoelastin, and the binding site was mapped to a region of the C-terminus fibulin-type module. Fibulin-4 shows strong binding affinity for LOX (Choudhury et al., 2009). Interestingly, pre-incubation of fibulin-4 with LOX enhanced the interaction between fibulin-4 and tropoelastin (Choudhury et al., 2009). Horiguchi et al. supported this observation by showing that LOX does not interact with tropoelastin in the absence of fibulin-4 (Horiguchi et al., 2009). This suggests that fibulin-4 may act as a facilitator for tropoelastin to undergo cross-linking by LOX. Fibulin-4 was found to interact with LTBP-4 and this is required for a proper deposition onto microfibrils (Bultmann-Mellin et al., 2015). The N-terminal half of fibulin-4 contains an interaction site for a fibrillin-1 N-terminal fragment, suggesting that fibulin-4 may also be involved in an interaction with microfibrils (Choudhury et al., 2009). However, this interaction inhibits fibulin-4 from binding to tropoelastin and LOX. Surprisingly, Kobayashi et al., noted that fibulin-4 does not interact with fibronectin, which is known as a master organizer of fibrillin-containing microfibril formation (Kobayashi et al., 2007; Sabatier et al., 2009). Fibulin-4 also interacts with various cell types, including skin and lung fibroblasts as well as umbilical vein and umbilical artery smooth muscle cells (Djokic et al., 2013). Interaction between fibulin-4 and heparin was observed,

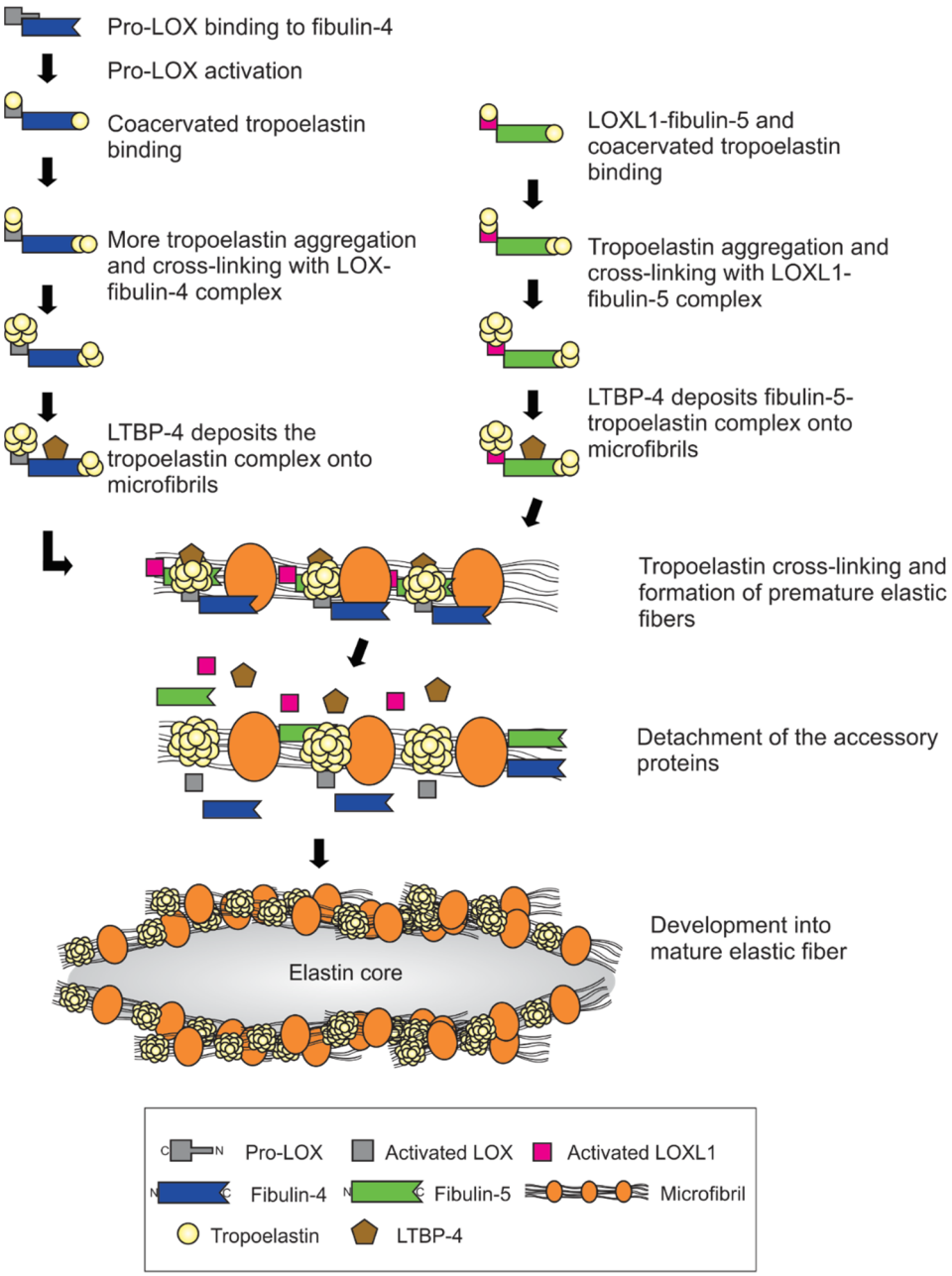

Figure 4. Model of role of fibulin-4 and -5 in early elastogenesis

Represented is the summary of studies investigating the roles of fibulin-4 and -5 in early elastic fiber assembly. First, inactive LOX is activated via interaction with fibulin-4 and this interaction enables binding of the complex to the coacervated tropoelastin. Activated LOX cross-links the tropoelastin into mature form, and cross-linked tropoelastin is delivered and deposited onto fibrillins-containing microfibrils. The accessory proteins are detached from tropoelastin and returned to the ECM. Fibulin-5 acts in similar manner except that it interacts with LOX-like I enzyme.

which is often used as a model of cell-surface heparan sulfate, suggesting an integrin-independent cell binding mechanism of fibulin-4 (Djokic et al., 2013).

Studies have shown that tropoelastin interacts with fibulin-5 stronger than fibulin-4 (Choudhury et al., 2009; Wachi et al., 2008). This observation was supported by the co-localization of fibulin-5 with tropoelastin in fetal bovine chondrocytes which express tropoelastin (Zheng et al., 2007). Fibulin-5 was found to bind weakly to LOX, however it exhibited binding affinity to LOX-like 1 protein (LOXL1) through its C-terminal region (Liu et al., 2004; Wachi et al., 2008). This suggests that there may exist an interaction specificity of substrates between fibulin-4 and -5 (Yanagisawa and Davis, 2010). Interestingly, fibulin-5 was found to bind fibulin-4 with moderate affinity, suggesting that the two proteins may communicate with each other to facilitate elastic fiber formation (Choudhury et al., 2009). Fibulin-5 was also found to interact with LTBP-2, and this negatively affects the interaction between fibulin-5 and tropoelastin, impacting elastogenesis (Hirai et al., 2007; Sideek et al., 2014). Furthermore, LTBP-4 interacts with fibulin-5 and this interaction is required in deposition of fibulin-5 and tropoelastin complex onto microfibrils (Bultmann-Mellin et al., 2015; Noda et al., 2013). Like fibulin-4, fibulin-5 also interacts with the N-terminal portion of fibrillin-1 via both the N- and the C-terminus, and also did not bind to fibronectin (Choudhury et al., 2009; Kobayashi et al., 2007). Through the RGD site, fibulin-5 also interacts with α4β1, α5β1, and αVβ3 integrins (Kobayashi et al., 2007; Lomas et al., 2007). It also shows binding affinity to heparin but slightly weaker than fibulin-4 (Djokic et al., 2013).

A cell culture study was performed to elucidate the possible role of fibulin-5 in elastogenesis (Nonaka et al., 2009). An elastogenic cell line, ARPE-19, or human retinal pigment epithelial cells, which express elastic fiber components such as fibrillin-1 and LOX but not tropoelastin, could form elastic fiber networks in a dose-dependent manner when exogenous tropoelastin was added (Wachi et al., 2005). In this study, fibulin-5 was overexpressed and then exogenous tropoelastin was supplied to evaluate the role of fibulin-5 in elastogenesis. The fibulin-5 overexpression did not affect mRNA expressions of other components. The cells formed elastic fiber networks upon the addition of exogenous tropoelastin and this was slightly enhanced in the fibulin-5-overexpressing ARPE-19 cells. Fibulin-5 formed fibrous networks which were co-localized with

tropoelastin and fibrillin-1, suggesting that these proteins form complexes in the ECM. Interestingly, although there was only a slight increase in elastogenesis upon fibulin-5 overexpression, the amount of desmosine in the matrix increased significantly, indicating that overexpression of fibulin-5 not only enhances deposition of tropoelastin into the ECM but it also increases cross-linking of tropoelastin. These results demonstrate that fibulin-5 may participate in elastogenesis through deposition and maturation of tropoelastin in the ECM.

2.6 N-linked glycosylation

Newly synthesized ECM proteins often require proper modifications in the endoplasmic reticulum (ER) in order to acquire the active conformation or to reach the destination (Schroder and Kaufman, 2005). Among important post-translational modifications, such as disulfide bond formation, glycosylation of asparagine residues, or N-linked glycosylation, stands as one of the most important and critical modification for secretory proteins (Schroder and Kaufman, 2005). N-linked glycosylation functions through increasing the solubility of proteins, generating signals which recruit important regulatory factors for the folding of the glycosylated proteins (glycoproteins), shielding the attachment sites of the proteins against non-specific interactions, as well as stabilizing the proteins' conformations (Tannous et al., 2014; Wormald and Dwek, 1999). Proteins which are not properly folded and modified confront two fates: either they remain inside the ER until they are properly folded with the assistance of the ER-resident chaperones or they undergo ER-associated degradation (ERAD) (Ellgaard and Helenius, 2003).

Polypeptides undergoing N-linked glycosylation contain the consensus sequence consisting of asparagine-any amino acid except proline-serine/threonine (N-X-S/T) (Hart et al., 1979) (Fig. 5). Upon entering the lumen of the ER, the asparagine residue of this consensus sequence is recognized and modified through the attachment of an oligosaccharide molecule composed of three glucose residues, nine mannose residues, and two N-acetylglucosamine residues (Kornfeld and Kornfeld, 1985). Immediately, the outermost glucose residue is trimmed by α-glucosidase I, an ER transmembrane protein containing a catalytic domain at the lumen of the ER (Kornfeld and Kornfeld, 1985). Di-glucosylated polypeptides are bound to malectin, a membrane-bound ER protein, which verifies the correct conformation of the polypeptides at early glycosylation stages

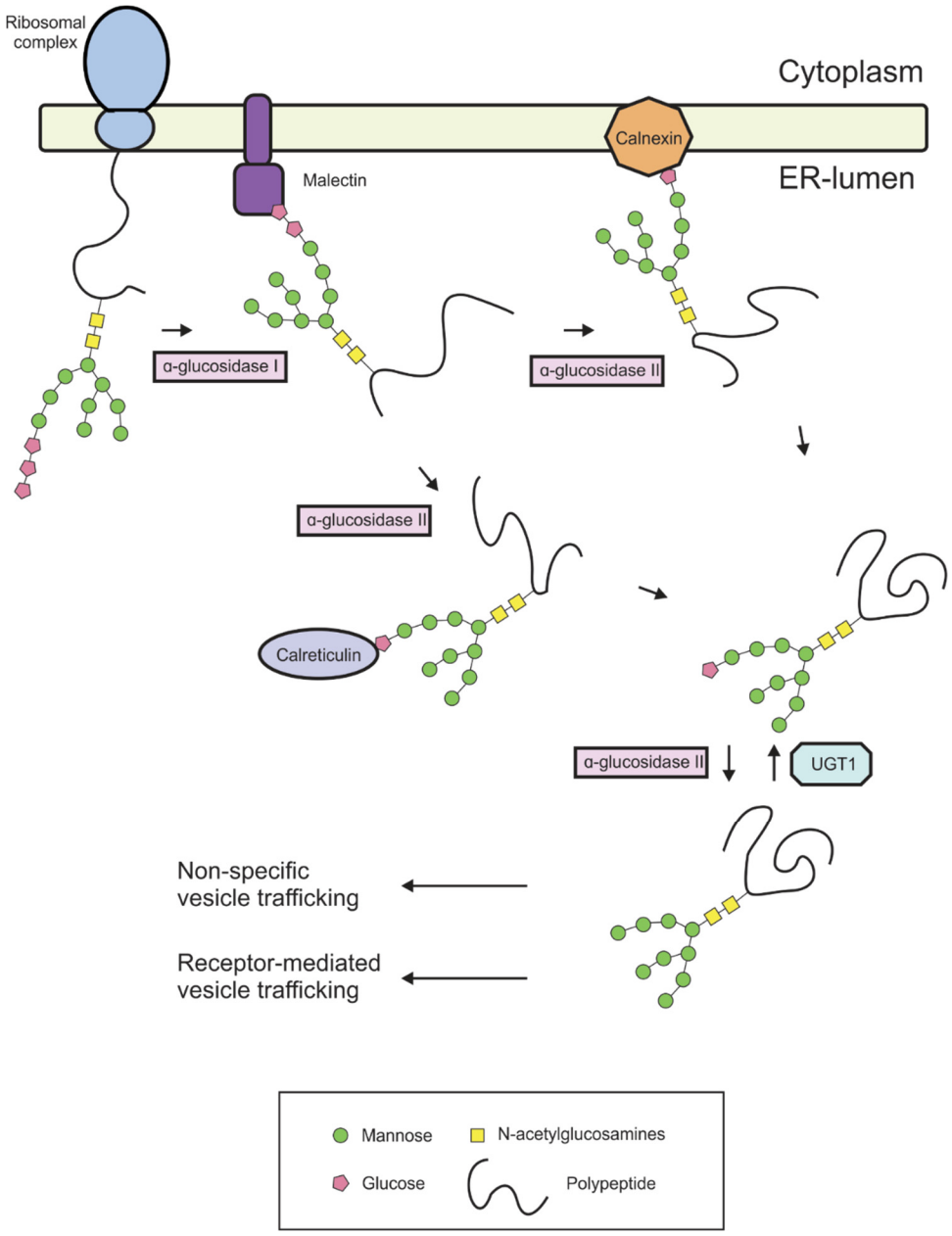

Figure 5. Overview of the process of N-linked glycosylation

Represented is the overview of the process of N-linked glycosylation. Upon entering the lumen of ER, the N-X-S/T consensus sequences in polypeptides are recognized and used to attach an oligosaccharide of three glucose residues, nine mannose residues, and two N-acetylglucosamine residues. α-glucosidase I immediately cleaves the first glucose residue which is then recognized by malectin. An additional glucose residue is cleaved by α-glucosidase II and subsequently the mono-glucosylated polypeptides interact with calnexin or calreticulin for further modification. The last glucose residue is also cleaved by α-glucosidase II, but UGT1 may attach a glucose residue back to the polypeptides if not properly folded. The properly-folded polypeptide is then transported to the Golgi, either via non-specific vesicle-mediated or specific receptor-mediated transport.

(Galli et al., 2011; Schallus et al., 2008). Subsequently, the second glucose residue of the oligosaccharide molecule is trimmed by α-glucosidase II, and this enables the mono-glucosylated polypeptides to interact with the lectin chaperones, calnexin and calreticulin, processing proteins with additional intramolecular modifications, including formation of native disulfide bonds and peptidyl-prolyl bonds isomerization (Cannon and Helenius, 1999; Hubbard and Robbins, 1979). Another glucose residue-trimming by α-glucosidase II releases the proteins from binding to these lectin chaperones. However, if the polypeptides are still immature to be exported, UDP-glucose glycoprotein glucosyltransferase I, another ER-resident protein, transfers a glucose residue onto the glycans and forces the polypeptides to interact with the lectin chaperones again (Trombetta and Helenius, 2000). Properly-folded polypeptides are exported to the Golgi compartment and eventually to the ECM through the secretory pathway either in non-specific vesicle trafficking process or in a specific receptor-mediated process (Tannous et al., 2014).

2.7 Unfolded protein response

The unfolded protein response (URP) is a regulatory consequence the ER exerts when there is an imbalance between the load of proteins in the ER requiring proper folding process versus the capacity of the ER to manage this folding (Ron and Walter, 2007) (Fig. 6). An ER chaperone, the immunoglobulin-binding protein (BiP), serves as a chaperone for protein processing in the ER (Gething, 1999). Simultaneously BiP binds to ER -resident transmembrane protein kinases, such as the protein kinase RNA-like ER kinase (PERK), the inositol-requiring kinase 1 (IRE1), and the activating transcription factor 6 (ATF6) and maintain these kinases in an inactive state (Ron and Walter, 2007). In the presence of excess amount of unfolded proteins in the ER, kinase-bound BiP becomes released to assist as a chaperone. Consequently, this activates the transmembrane kinases and mediates downstream signaling pathways in order to recover the homeostatic state of protein synthesis (Bertolotti et al., 2000). For an example, upon release of BiP from IRE1, the activated IRE1 uses its endoribonuclease activity at the cytoplasmic domain to excise an intron from mRNA of a transcription factor, x-box binding protein1 or XBP1 (Shang and Lehrman, 2004). The spliced XBP1, lacking 26-nucleotides, translocates into the nucleus where it binds to the regulatory regions of its target sequences which may restore proper ER function, including ER-associated protein degradation (ERAD) (Shang and Lehrman, 2004). Persisting activations of PERK and ATF6 lead

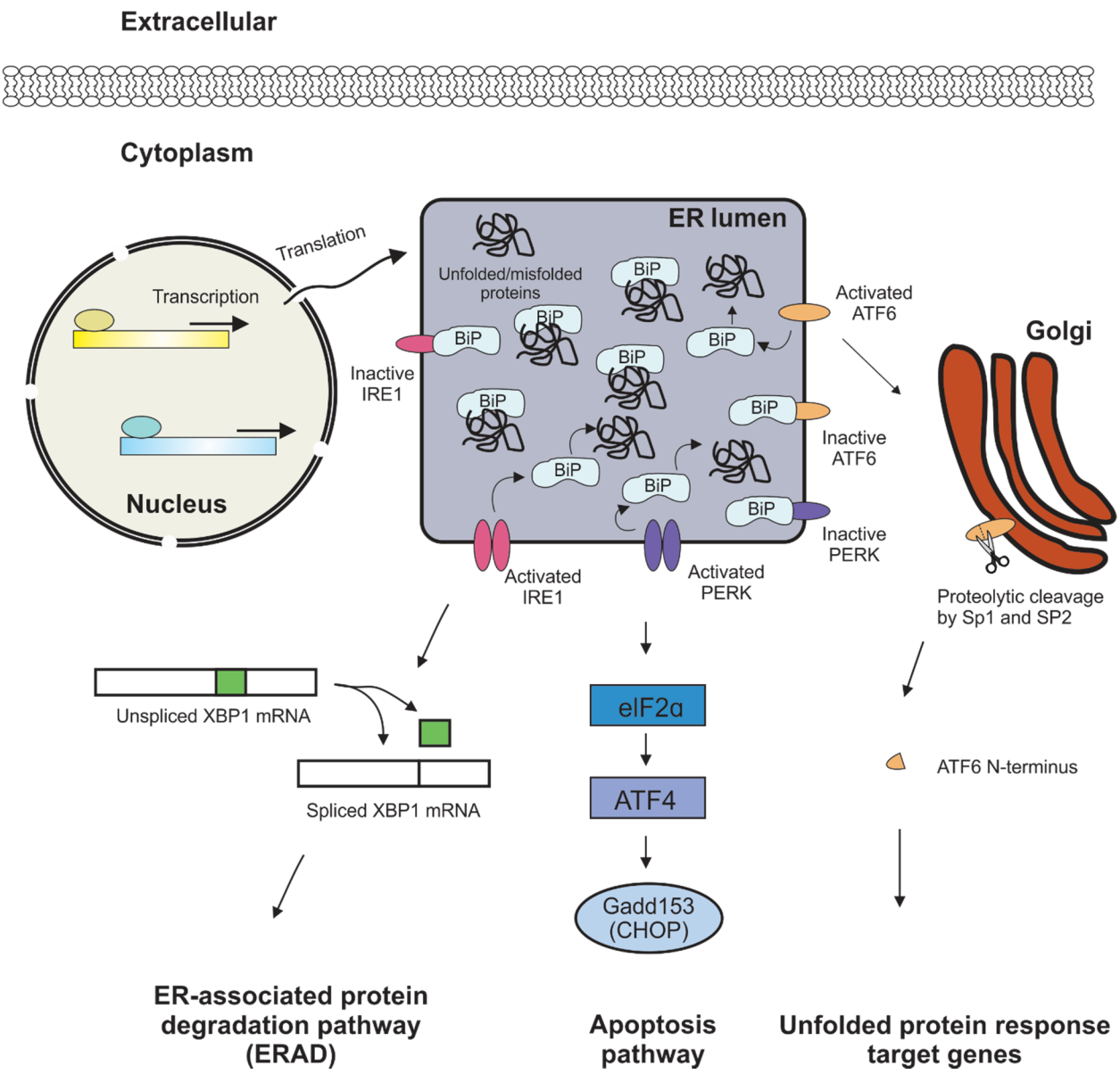

Figure 6. Overview of the unfolded protein response

Unfolded protein responses occur when there is imbalance between the amount of the ER-resident folding chaperones, BiP, and the amount of unfolded/misfolded proteins. BiPs are replaced from binding to the ER membrane-bound kinases, such as IRE1, PERK, and ATF6, to the lumen in order to retain the proteins. Consequently, kinases become activated and send downstream signals to mediate ERAD, apoptosis, as well as other unfolded protein response-related gene signaling.

to cellular death by mediating downstream gene transcriptions of apoptosis genes, such as growth arrest and deoxyribonucleic acid (DNA) damage inducible gene 153 (Gadd153, also known as CHOP) (Rao et al., 2004).

3 OBJECTIVES

Human disease and mouse models of fibulin-4 deficiency demonstrate that fibulin-4 plays critical roles in elastogenesis. These observations are supported by numerous *in vitro* and *in vivo* studies. However, the precise mechanisms of how fibulin-4 participates in the process of elastogenesis still remain unclear. Furthermore, little is known about each functional units of fibulin-4, including two N-linked glycosylation sites at Asn^{198} and Asn^{394}. This study seeks to reveal the roles of fibulin-4 N-linked glycosylation in functional mechanisms, including elastogenesis and protein secretion.

The specific aims of this study are:

1. To biochemically explore whether N-linked glycans in fibulin-4 affect its interaction with tropoelastin.
2. To generate expression plasmids for fibulin-4 lacking N-linked glycosylation site(s) at 1) Asn^{198}, 2) Asn^{394}, and 3) both.
3. To transfect the expression plasmids into human embryonic kidney cells (HEK293H) for recombinant protein production and characterization.
4. To characterize the secretion properties of the recombinant HEK293H cell clones.
5. To perform a survey of elastogenic cell lines for the selection of a suitable cell model to test the role of N-linked glycosylation in elastogenesis.
6. To overexpress fibulin-4 wild-type and N-linked glycosylation mutant expression plasmids into the selected cell culture model to analyze the consequence in elastogenesis.
7. To generate an affinity-purified anti-fibulin-4 antibody for more specific detection of fibulin-4.

4 MATERIALS AND METHODS

4.1 Antibodies

Antibodies were used in experiments including immunofluorescence, Western blots, solid phase binding assays, dot blots, and enzyme-linked immunosorbent assays (ELISA). Fibulin-4 polyclonal antisera were generated using recombinant full-length proteins as antigen, following standard procedures (Djokic et al., 2013). The polyclonal antisera against other proteins, including fibulin-5, the C-terminal half of human fibrillin-1, fibrillin-2, and the C-terminal half of mouse fibrillin-1, fibrillin-2, were generated in a similar way (Tiedemann et al., 2001). The polyclonal mouse fibronectin antibody (Millipore, product AB2033) and the monoclonal human fibronectin antibody (FN-15; Sigma, product F7387) were purchased commercially. The polyclonal tropoelastin antibody was also commercially purchased (Elastin Product Company, product PR398). The secondary antibody used to detect the polyclonal antibodies were goat anti-rabbit antibody conjugated to either Cy3 (Jackson ImmunoResearch laboratories, product 111-165-03) or horseradish peroxidase (Agilent Technologies, product K4008) whereas the secondary antibody used to detect the monoclonal antibodies were goat anti-mouse antibodies conjugated to either Alexa 488 (Thermo Fisher Scientific, product A-11008) or horseradish peroxidase (Bio-Rad, product 1706516).

Fibulin-4 affinity-purified antibody (AP-N) was generated from a polyclonal antiserum against human fibulin-4. Initially, final bleed of the antiserum was passed over a HiTrap Protein A HP 1mL column (GE Healthcare, product 29-0485-76) using an ÄKTA avant 25 chromatography system (GE Healthcare, product 28-9308-42) to selectively enrich immunoglobulin G (IgG) antibodies. The extracted IgG antibodies were further purified through a tricorn 5/50 column (GE Healthcare, product 28-4064-09) packed with Sepharose conjugated to fibulin-4 N-terminus-cbEGF1 fragments. The specificity of fibulin-4 AP-N antibody was verified through Western blot and ELISA with full-length fibulin-4 and N-terminus-cbEGF1 fragment of fibulin-4.

4.2 Generation of fibulin-4 N-linked glycosylation site mutants

The constructs for fibulin-4 glycosylation site mutants were generated using the existing fibulin-4 wild-type construct in the pcDNA3.1+ vector (Invitrogen, product V79020) with a sequence for BM-40 signal peptide at the N-terminus, thus named pDNSP-hFBLN4 (Djokic et al., 2013; Lin et al., 2002).

The sequence for the asparagine (Asn) in the Asn^{198}-X-Ser/Thr glycosylation site of fibulin-4 was mutated by Quikchange Site-Directed Mutagenesis Kit (Agilent Technologies, product 200519), using manufacturer's protocol. Briefly, 33 nucleotides-long complementary sense and anti-sense mutagenic primers (5'-CAGCTGGGGCCTAAC**C**A**G**CGCTCCTGTCTTGAT-3' and 5'-ATCAACACAGGAGCG**C**T**G**GTTAGGCCCCAGCTG-3') were generated which contain mutated codon (**A**A**C** to **C**A**G**) with 15 correct nucleotides upstream and downstream of the site. The mutagenesis was induced through polymerase chain reaction (PCR) of pDNSP-hFBLN4 and the mutagenic primers, followed by parental DNA template digestion with *DpnI* and transformation into provided XL1-Blue supercompetent cells (pDNSP-ASNmut1).

The N-glycosylation site at position nucleotide position 1180 in fibulin-4 was mutated by cloning a synthesized DNA fragment (gBlock; Integrated DNA Technologies) into pDNSP-hFBLN4 plasmid. This 695bp double-stranded synthetic DNA fragment consisted of the fibulin-4 coding sequence from position 671 to 1329 with the desired mutation (**A**A**C** to **C**A**G**) followed by the sequence for a six histidine tag, two stop codons, and additional 86 base-pairs (bp) matching the vector sequence. Both, pDNSP-hFBLN4 plasmid and the gBlock DNA fragment were sequentially digested with *PflMI* × *EcoRI* and gel-purified, followed by subsequent ligation and transformation into competent cells and plasmid amplification. The resulting plasmid was termed pDNSP-ASNmut2.

Mutagenesis of both N-glycosylation site in fibulin-4 was performed by subcloning the mutation site at coding for p.Asn592Gln at nucleotide position 592-594 into the vector containing the mutation for the p.Asn1180Gln at nucleotide position 1180-1182. Both, pDNSP-ASNmut1 and

pDNSP-ASNmut2 were doubly digested with *Bsu36I* × *PflMI*, gel purified, followed by subsequent ligation and transformation into competent cells (pDNSP-ASNmutT). All expression plasmids were bidirectionally verified for their correct sequences by Sanger sequencing (McGill University and Génome Québec Innovation Centre).

4.3 Cell culture

4.3.1 Cell lines

Human embryonic kidney cells (HEK293H; Invitrogen, product 11631-017), human retinal pigmented epithelium (ARPE19; ATCC, product CRL-2302), and rat lung fibroblast (RFL6; ATCC, product CCL-192) were commercially purchased. Fetal bovine chondroblasts (FBC) and rat pulmonary arterial smooth muscle cells (PAC1) were generous gifts from Dr. Elaine Davis.

4.3.2 Cell transfection procedures

The expression plasmids pDNSP-hFBLN4, pDNSP-ASNmut1, pDNSP-ASNmut2, and pDNSP-ASNmutT, were linearized with *PvuI*, ethanol-precipitated for sterilization, and redissolved in sterile water. Two methods of stable transfection were performed: i) for the production of the recombinant proteins, the expression plasmids were stably transfected into HEK293H cells via calcium phosphate transfection as previously described (Lin et al., 2002); ii) for overexpression of the proteins in an elastogenic cell line, the expression plasmids were stably transfected into PAC1 cells using Lipofectamine 2000 (Invitrogen, product 11668-019) following manufacturer's protocol. For calcium phosphate transfection, cells were seeded in subconfluent dilution of 1:400, whereas for lipofectamine transfection, cells were seeded half-confluent in 100mm culture dish (Sarstedt, product 83.1802), 24h prior to the addition of 10µg DNA. For both transfection methods, transfected cells were selected through addition of 250µg/mL geneticin sulphate (G418; Wisent, product 450-130-QL) starting two days after the transfection. The cells were cultured in Dulbecco's Modified Eagle Medium with phenol red (DMEM; Wisent, product 319-005-CL), supplemented with 10% v/v fetal bovine serum (FBS; Wisent, product 080-150), 100µg/mL penicillin and streptomycin and 2mM glutamine (PSG; Wisent, product 450-202-EL). The cell incubator were maintained in 37ºC and 5% CO_2.

To analytically test the level of secretion of the recombinant proteins from HEK293H cells, the conditioned media were analyzed by sodium dodecyl sulphate-polyacrylamide gel electrophoresis (SDS-PAGE; section 4.5) and Western blotting (section 4.6) using either ~50µL conditioned media or 1mL of conditioned medium precipitated by 10% trichloroacetic acid. Both HEK293H and PAC1 cells transfected with fibulin-4 wild-type or the glycosylation site mutant constructs were also analyzed through indirect immunofluorescence assay (section 4.9).

For large scale production of recombinant secreted protein, the transfected HEK293H cells were seeded onto eight Nunc Cell Culture Treated TripleFlask with total surface area of 4000cm^2 (Thermo Fisher Scientific, product 132913). After reaching confluency, the cells were washed twice with 20mM 4-(2-hydroxyethyl)-1-1-piperazineethanesulfonic acid (HEPES), 150mM NaCl, 2.5mM $CaCl_2$, pH 7.4 to remove serum proteins. Immediately, the flasks were refilled with phenol red-free DMEM (Wisent, product 319-050-CL), supplemented with PSG, and 500mL of conditioned media were collected every two to three days until the secretion level was substantially decreased (usually up to 10 collections). After each collections, the conditioned media were centrifuged at 6000 x g for 15min at 4ºC remove cellular debris, followed by addition of 100µM phenylmethanesulphonylfluoride (PMSF) to prevent serine protease proteolysis. The collected conditioned media were stored at -20ºC until further purification.

4.4 Recombinant protein purification

Recombinantly expressed fibulin-4 wild-type and glycosylation site mutant proteins were purified through immobilized metal ion affinity chromatography with HisTrap HP 1mL columns loaded with Ni^{2+} ions (GE Healthcare, product 17-5247-01) using an ÄKTA avant 25 chromatography system as previously described (Djokic et al., 2013). Typically, 2.5L of conditioned medium was thawn at 4ºC, and cell debris was removed by filtration through a 5µm cellulose filter (Millipore, product SMWP09025). The medium was concentrated to ~40mL in pressurized ultrafiltration cells (Amicon, product 5124 and 6028), equipped with a 10 kiloDalton (kDa) membrane (Millipore, product PLGC07610) at 4ºC. Subsequently, the concentrated medium was dialyzed two times for

6h against 4L of 20mM HEPES, 500mM NaCl, pH 7.4 (running buffer) at 4ºC. Following removal of precipitation by centrifuging the dialyzed medium at 11000 x g for 15min at 4ºC, the medium was loaded into a 50mL Superloop (GE Healthcare, product 19-7850-01). The material was then passed at a flow rate of 0.5mL/min, over the Ni^{2+}-loaded HisTrap HP column equilibrated in running buffer. The column was washed with 2mL running buffer, and the bound proteins were eluted from the column with a linear 0-500mM imidazole gradient in running buffer. Eluted proteins were collected in 1mL fractions which were analyzed in 20 µL aliquots by SDS-PAGE followed by Coomassie Brilliant Blue staining. Subsequently the fractions containing fibulin-4 wild-type or glycosylation site mutants were pooled and dialyzed two times for 6h against 1L of 50mM Tris-HCl, 150mM NaCl, 2.5mM $CaCl_2$, pH 7.4 at 4ºC. The concentration of the dialyzed proteins were measured by the Pierce BCA Protein Assay Kit (Thermo Fisher Scientific, product 23225) following the manufacturer's protocol. Then the proteins were stored at -80ºC until further use.

4.5 Sodium Dodecyl Sulphate-Polyacrylamide Gel Electrophoresis

Proteins were denatured at 95ºC for 4min and separated by SDS-PAGE under non-reducing or reducing (20mM dithiothreitol (DTT)) conditions, initially at 80V (for ~15-20min) and thereafter at 110V for 2h. To prepare a 1mm 7.5% SDS-PAGE gel, the following materials were combined and poured into an assembled glass cassette (Bio-Rad, product 165-8015).

Resolving gel (7.5%) solution: 1.25mL 1.5M Tris, pH8.8, 1.25mL 30% acrylamide, 2.33mL deionized water (dH_2O), 100µL 10% sodium dodecyl sulphate (SDS), 7.5µL tetramethylethylenediamine (TEMED), 55µL 10% ammonium persulphate (APS). 200µL of isopropanol (Thermo Fisher Scientific, product A416-01) was added to generate a smooth gel surface. After polymerization, the isopropanol was removed, the gel surface was washed two times with dH2O, and the stacking gel solution detailed below was poured onto the resolving gel.

Stacking gel solution: 0.535mL 1.0M Tris, pH6.8, 0.6mL 30% acrylamide, 3.3mL dH_2O, 43.75µL 10% SDS, 9.37µL TEMED, 18.75µL 10% APS

Combs were inserted immediately to generate the loading wells.

For staining, SDS-PAGE gels were stained with Coomassie Brilliant Blue solution (1.2g Brilliant Blue G-250/100mL, 40% v/v methanol, 10% v/v acetic acid) (Thermo Fisher Scientific, product BP100-25) for 30min, followed by destaining with 40% v/v methanol, 10% v/v acetic acid. Alternatively, colloidal staining was performed in following procedure: SDS-PAGE gels were washed three times with dH_2O, and incubated with 11mL of EZBlue Gel Staining Reagent (Sigma, product G1041) for 2h, followed by several dH_2O washing.

4.6 Western blotting

Following protein samples were loaded onto 7.5% SDS-PAGE gels and separated according to their sizes as described above (section 4.5): 50µL of conditioned media, 10% trichloroacetic acid concentrates of 1mL of conditioned media, and 1µg of purified proteins. Subsequently, the proteins were blotted onto a nitrocellulose membrane (Bio-Rad, product 162-0094) in ice-cold 10mM sodium tetraborate decahydrate buffer at 0.4A for 1.5h. Proper transfer of proteins on the membrane were visualized by Ponceau Red staining (0.5% w/v in 1% acetic acid). After washing out the Ponceau Red solution with dH_2O, the membrane was incubated with 5% w/v non-fat dry milk in 50mM tris-base, 150mM NaCl, pH 7.4 or tris-buffered saline (TBS) 1h at room temperature to block unspecific antibody binding. The membrane was incubated with the primary antibody diluted at 1/500 in 5% w/v bovine serum albumin (BSA) in TBS overnight at 4ºC under constant rotation. The membrane was washed three times with 0.05% v/v Tween-20 in TBS (TBST) for 10min each, followed by incubation with the secondary goat anti-rabbit antibody conjugated with HRP diluted at 1/800 in 5% w/v BSA in TBS for 1.5h at room temperature. For this incubation, the membrane was protected against light. After another three times washing with TBST for 10min each, colour was developed by mixing 29mL TBS and 23µL H_2O_2 with 6mL methanol and 17.5mg 4-chloro-1-naphthol (Sigma, product C8890) just before pouring onto the membrane. The colour was developed for 5 to 10min at room temperature, and then the reaction was stopped with washing the membrane with TBST, followed by dH_2O.

4.7 Peptide -N-Glycosidase F deglycosylation assay

Fibulin-4 and a fragment of fibulin-4 lacking C-terminus (hFBLN4-I-II) were deglycosylated at their N-glycosylation site(s) by Peptide -N-Glycosidase F (PNGaseF, NEW ENGLNAD Biolabs, product P0704S), following the manufacturer's protocol with following minor changes. 10µg of full length fibulin-4, hFBLN4-I-II, and fibulin-4 glycosylation site mutants were incubated with 1.5µL of PNGaseF for 2h at 37ºC without provided denaturing buffers, to maintain the proteins in the most native states. Subsequently the deglycosylated proteins were subjected to denaturation at 95ºC in the presence of 20mM DTT followed by separation on 7.5% SDS-PAGE gels. Alternatively, the deglycosylated proteins were directly subjected to solid phase binding assay (section 4.8) against other proteins.

4.8 Solid phase binding assay

Solid phase binding assay was performed in order to examine the interaction of fibulin-4 wild-type and hFBLN4-I-II fragment, treated with/without PNGaseF, to tropoelastin, using previously established protocol (Djokic et al., 2013; Lin et al., 2002). Tropoelastin was commercially purchased (Elastagen, product ELA-1). 10µg/mL tropoelastin in TBS was immobilized per well in 96-well plate (Thermo Scientific, product 439454) for overnight at 4ºC. Wells were washed with TBST supplemented with 2mM $CaCl_2$ to remove unbound tropoelastin, and non-specific binding surfaces in the wells were blocked with blocking buffer (5% w/v non-fat milk in 2mM $CaCl_2$ in TBS) for 1h. All steps were performed at room temperature under rotational shaking at 550rpm, and three washes between each step with 200µL 2mM $CaCl_2$ in TBST were performed to remove any unbound ligands or antibodies. Fibulin-4 wild-type or hFBLN4_I-II fragment treated with/without PNGaseF were 1:2 serially diluted, starting from 100µg/mL, in binding buffer (2% w/v non-fat milk in TBS/2mM $CaCl_2$), and incubated in the wells for 2h. To detect bound proteins, the anti-fibulin-4 primary antibody was diluted to 1:1000 in binding buffer and incubated for 1.5h. Goat anti-rabbit secondary antibody conjugated with horseradish peroxidase was diluted 1:800 in binding buffer and incubated for 1h. The colour development was performed with 1mg/mL 5-aminosalicylic acid diluted in 20mM NaH_2PO_4 pH 6.8, filtered and mixed with 0.045% v/v H_2O_2. The reaction was terminated with 2M sodium hydroxide. The colour intensity was measured with a microplate reader (Beckman Coulter, product AD340) at 492nm.

4.9 Indirect immunofluorescence assay

The transfected and non-transfected HEK293H cells, PAC1 cells, as well as other elastogenic cell lines, including ARPE19, RFL6, and FBC (See section 4.3.1) were grown in 8-welled chamber slides (Thermo Fisher Scientific, product 154534) with 75,000 cells/well. Indirect immunofluorescence assay was performed according to a previously established protocol (Hubmacher et al., 2014) with the following varying time points of analysis for each cell types: immunofluorescence on HEK293H cells were performed three days after seeding to monitor recombinant protein expression, whereas for other cells the assay was performed 7, 11, and 14 days after seeding to analyze elastic fiber formation. Cells were washed with 137mM NaCl, 8.1mM $Na_2HPO_4 \cdot 7H_2O$, 2.7mM KCl, 1.5mM KH_2PO_4, pH 7.4 or phosphate-buffered saline (PBS) and fixed with 4% paraformaldehyde (PFA) in PBS for 10min. For intracellular protein visualization, cells were additionally washed with PBS and treated with 0.5% v/v Triton X-100 in PBS for 10min to permeabilize the cell membranes. Cells were washed with PBS, and blocked with 10% v/v normal goat serum (NGS; Jackson ImmunoResearch Laboratories, product 005-000-121) in PBS for 1h at room temperature to block unspecific antibody binding sites. All subsequent steps were followed by three washes with PBS for 5min each at room temperature. The polyclonal primary antibodies, as detailed in section 4.1, were diluted 1:500 and the FN-15 was diluted at 1/100 in 10% v/v NGS in PBS, and incubated for 2h at room temperature. Secondary antibodies, goat anti-rabbit antibody conjugated to Cy3 for polyclonal antibodies or goat anti-mouse antibody conjugated to Alexa-488 for monoclonal antibody, were diluted 1:200 in 10% v/v NGS in PBS, incubated for 1.5h at room temperature. From this step onwards, the chamber slides were protected against the light. 4', 6-diamidino-2-phenylindole (DAPI) diluted 1:8000 in PBS was incubated for 5min, and then the slides were mounted with Vectashield mounting medium (Vector Laboratories, product H-1000). Images were taken with Zen 2012 software (Zeiss) using Axio Imager.M2 microscope (Zeiss) equipped with an ORCA-flash4.0 camera (Hamamatsu, product C11440).

4.10 Enzyme-linked immunosorbent assay

An ELISA was performed to test the specificity of the fibulin-4 AP-N antibody. The protocol of solid phase binding assay was followed (section 4.8) with the following modifications. First,

10μg/mL of fibulin-4 wild-type protein or fibulin-4 N-terminus to cbEGF1 (N-1) protein fragment were immobilized per well in 96 well plates overnight at 4ºC. Second, no soluble ligands was used, only the primary antibodies against fibulin-4 and fibulin-4 N-1. Lastly, the fibulin-4 antiserum, non-purified or affinity purified, were serially diluted 1:3 in binding buffer, starting from 1:50 initial dilution.

4.11 Reverse transcription polymerase chain reaction

An RT-PCR was performed in order to semi quantitatively determine the expression levels of elastogenic components upon overexpression of fibulin-4 wild-type or glycosylation site mutants in PAC1 cells. Cells were grown in 100mm culture dish (Sarstedt, product 83.1802), and upon reaching confluency, RNA was extracted using RNeasy Plus Mini Kit (Qiagen, product 74134) according to manufacturer's protocol.

4.12 Dot blot assay

Dot blot assay was performed to examine the secreted protein levels in conditioned media of PAC1 non-transfected and transfected cells, following established protocol (Isogai et al., 2002). 50μL of conditioned media from PAC1 non-transfected and transfected cells were diluted in 450μL of TBS and were blotted directly onto the nitrocellulose membrane through vacuum suction using Bio-Dot Microfiltration Apparatus (Bio-Rad, product 170-6545). After washing with TBS, the protocol of Western blot was followed, starting from Ponceau staining. The intensity of the dots were measured and compared through densitometry analysis using ImageJ software (Schneider et al., 2012).

5 RESULTS

5.1 Fibulin-4 exhibits enhanced binding upon deglycosylation

Recombinant fibulin-4 was expressed by a mammalian cell culture system (HEK293H cells) for proper post-translational modifications including N-linked glycosylation and the correct formation of disulfide bonds. Secreted fibulin-4 in the conditioned medium was purified through immobilized metal (Ni^{2+}) affinity chromatography. When the purified protein was reduced by 20mM DTT and separated by SDS-PAGE, two bands were present at 65kDa and 61kDa; the 65kDa corresponding to fibulin-4 substituted with two N-linked glycans and the 61 kDa substituted with only one N-linked glycan as previously described (Fig. 7A) (Djokic et al., 2013). This differential fibulin-4 glycosylation pattern was supported by the fact that both bands shifted to a single band of 57kDa upon enzymatic removal N-linked glycans by PNGaseF under standard denaturing conditions (Fig. 7A). A shorter fragment of fibulin-4 which lacks the C-terminus (fibulin-4_I-II), thus only contains one glycosylation site, was also shifted to a lower mass from 50kDa to 46kDa upon PNGaseF treatment (Fig. 7A). Enzymatic deglycosylation of fibulin-4 could be also achieved under non-denaturing conditions, a pre-requisite to maintain the protein in its native conformation, necessary for the following interaction assay (Fig. 7B)

To study the functionality of the glycosylation sites in fibulin-4, solid phase binding assays were performed in the presence and absence of N-linked glycan chains. Moderate binding affinity of fibulin-4 to tropoelastin has been previously reported (Choudhury et al., 2009). Upon enzymatic deglycosylation of fibulin-4, the interaction with tropoelastin increased significantly (Fig. 7C). Similar observations were made with the fibulin-4_I-II fragment, which also exhibited significantly enhanced binding to tropoelastin upon removal of the N-linked glycan at Asn^{198} (Fig. 7C). The enhanced binding to tropoelastin upon fibulin-4 enzymatic deglycosylation was further confirmed by Biacore analysis (Fig. 7D). The interaction of PNGaseF-treated fibulin-4 with tropoelastin was about 2 fold stronger (K_d = 39nM) than the interaction of wild-type fibulin-4 with tropoelastin (K_d = 87nM). This finding demonstrates that the glycosylation sites on fibulin-4 play a regulatory roles in tropoelastin binding.

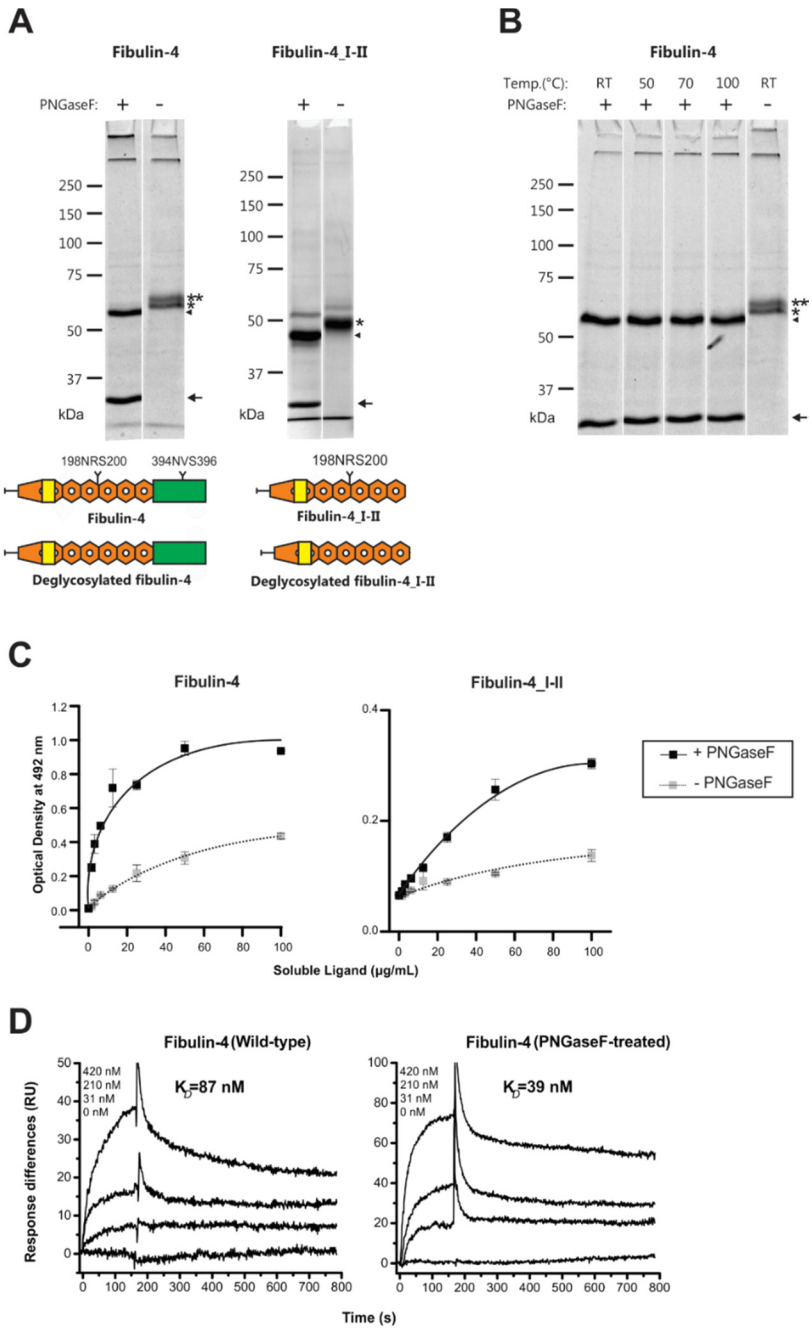

Figure 7. Enzymatically deglycosylated fibulin-4 shows enhanced binding to tropoelastin. Legends overleaf.

Figure 7. Enzymatically deglycosylated fibulin-4 shows enhanced binding to tropoelastin

(A) Enzymatically deglycosylated fibulin-4 (left panel) and fibulin-4_I-II fragment (right panel) under denaturing conditions were analyzed by SDS-PAGE. The samples were run 10μg/lane in 7.5% polyacrylamide gel under reducing condition using DTT. The double asterisk indicates fibulin-4 with double glycans and the single asterisks indicate fibulin-4 with single glycan. The arrowhead indicates deglycosylated fibulin-4 with no glycans attached. The arrow indicates PNGaseF enzyme. (B) Fibulin-4 enzymatic deglycosylation performed in various temperature without the denaturing buffers. The asterisks and the arrows indicate the same as in (A). (C) Analysis of the deglycosylated fibulin-4 (left panel) and fibulin-4_I-II fragment (right panel) by solid phase binding assay. Tropoelastin (10μg/mL) was immobilized, along with TBS as a negative control (values subtracted and plotted in the graph). Serial dilutions of fibulin-4 and fibulin-4_I-II treated with PNGaseF or TBS were applied as soluble ligands with indicated concentrations. Shown data sets represent means of the triplicates with the standard deviations. (D) Biacore analysis of the fibulin-4 wild-type (left panel) and enzymatically deglycosylated fibulin-4 (right panel) binding to tropoelastin. The concentrations of the soluble fibulin-4 are indicated in nM.

5.2 Generation of the mutants of fibulin-4 lacking N-linked glycosylation sites

To study the functional significance of N-linked glycosylation in fibulin-4, mutants lacking the glycosylation sites were generated. Fibulin-4 has two N-linked glycosylation sites at position 592-560 (amino acid position 198-200) in cbEGF domain 3 and at position 1180 (amino acid position 394-396) in the C-terminus (Fig. 7A). Both sequence match the known consensus sequence -N-X-S/T where X is any amino acids except proline (Marshall, 1972). In ER, the enzymatic addition of the N-linked glycans only occurs when the consensus sequence is present on the protein. Therefore, in order to prevent N-linked glycosylation of fibulin-4, the DNA sequences coding for the consensus N-glycosylation sequons were modified in the recombinant expression plasmid for the wild-type fibulin-4 (pDNSP-hFBLN4) by site-directed mutagenesis. The sequence for the critical asparagine was modified to glutamine which has an additional methyl group in its side chain. The following mutants were generated: one mutant plasmid (pDNSP-hFBLN4_ASNmut1) coded for Gln^{198} instead of Asn^{198}. Another mutant plasmid (pDNSP-hFBLN4_ASNmut2) contained the sequence that replaced Asn^{394} to Gln^{394}. A third plasmid was generated (pDNSP-hFBLN4_ASNmutT) that coded for both mutated N-glycosylation sites. pDNSP-hFBLN4_ASNmut1 was generated with the QuikChange site-directed mutagenesis kit using the wild-type pDNSP-hFBLN4 as a template (Fig. 8A, 9A). The mutagenesis primer pairs were designed with a melting temperature of 86ºC. The parental pDNSP-hFBLN4 plasmid was digested after the mutagenesis procedure with *DpnI* and the amplified pDNSP-hFBLN4_ASNmut1 was transformed into provided XL1-Blue supercompetent cells. This transformation produced several clones on the ampicillin-containing agar-plates. The DNA extracted from these clones were subjected to Sanger DNA sequencing, revealing that the plasmid DNA from one clone contained the desired Asn-Gln mutation without the presence of additional mutations. The attempt to mutate the second glycosylation site of fibulin-4 at amino acid position 394 failed using the QuikChange site-directed mutagenesis approach. Thus a DNA fragment was designed and commercially synthesized as a gBlock gene fragment (Integrated DNA Technologies) (Fig. 8B, 9B). gBlocks are sequence-verified synthetic double-stranded DNA which can be generated up to 2000bp. This gBlock fragment contained the Asn-Gln mutation at position 394 and appropriate restriction enzyme recognition sites (*PflMI* and *EcoRI*) at each ends for subcloning into the pDNSP-hFBLN4 plasmid (gBlock_Mut2). *PflMI* × *EcoRI* digested pDSNP-hFBLN4 and the synthetic gBlock were

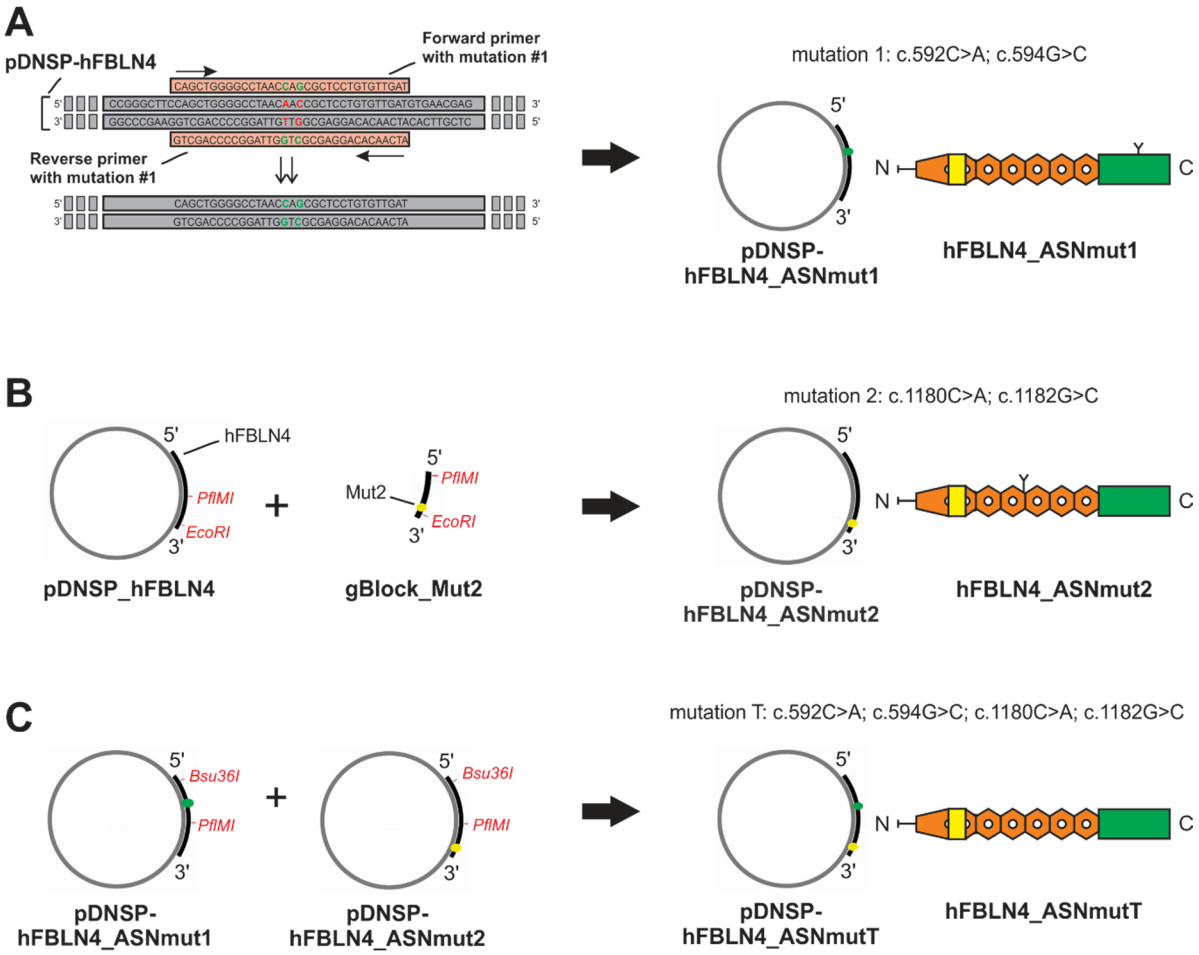

Figure 8. Schematic overview of the generation of fibulin-4 N-linked glycosylation mutants expression plasmids.

(A, left panel) In order to generate the expression plasmid containing the mutations c.592C>A; c.594G>C, the wild-type pDSNP-hFBLN4 was mutated using QuikChange site-directed mutagenesis kit. The parental wild-type DNA is shown as a double gray bar. The codon coding for 194 is highlighted in red. The mutagenesis oligonucleotides are shown on the top and bottom highlighted in orange. Mutations within the primer sequences are indicated in green. (B, left panel) The schematic shows the cloning strategy to generate pDNSP-hFBLN4_ASNmut2 via ligation of a 6296bp *PflMI* × *EcoRI* plasmid backbone of pDSNP-hFBLN4 with a 439bp *PflMI* × *EcoRI* gBlock fragment containing the mutation c.1180C>A; c.1182G>C. (C) The graphic displays the generation of the double mutant plasmid pDNSP-hFBLN4_ASNmutT via ligation of a 640bp *Bsu36I* × *PflMI* fragment from hFBLN4_ASNmut1 (insert) with the 6091bp *Bsu36I* × *PflMI* plasmid backbone from pDNSP-hFBLN4_ASNmut2. (A, B, C, right panels) The generated mutant plasmids are indicated including the relative positions of the mutations in green and yellow. The coded mutant proteins are shown on the right as a domain model with Y shape indicating the N-glycosylation sites.

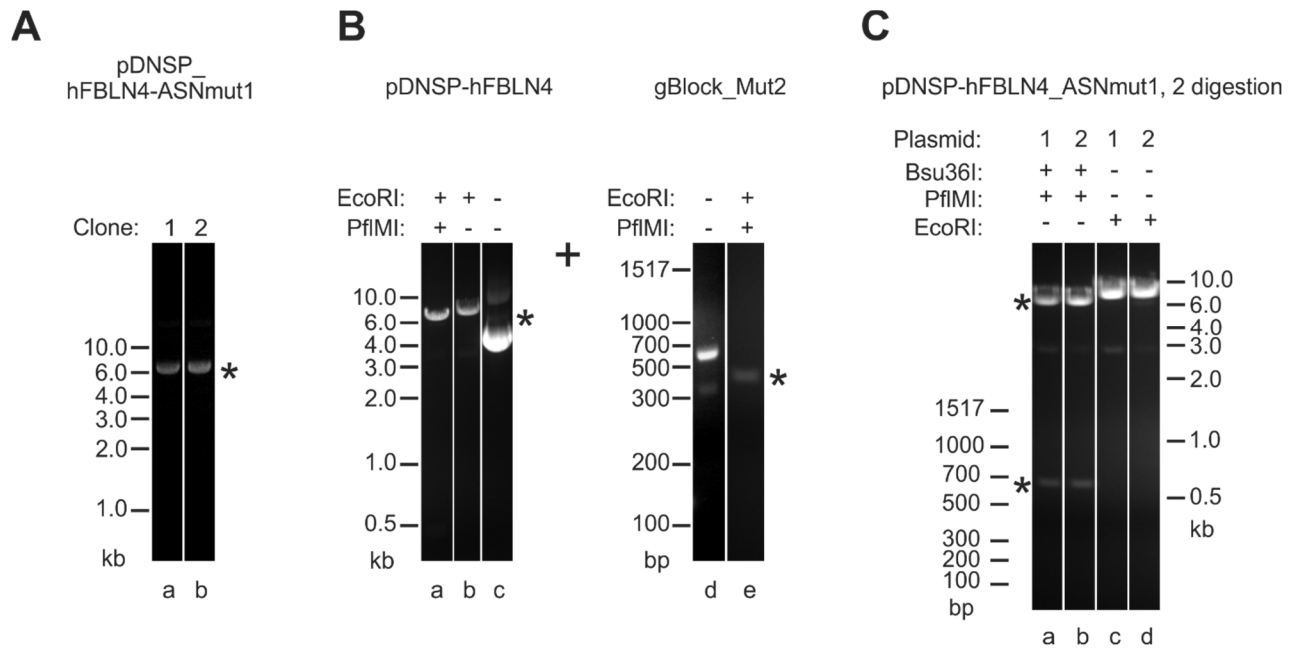

Figure 9. Experimental overview of the generation of fibulin-4 N-linked glycosylation mutants expression plasmids outlined in figure 8.

The asterisks indicate the DNA bands which corresponded to the expected sizes and further used for generation of the fibulin-4 glycosylation mutant expression plasmids (pDNSP-hFBLN4_ASNmut1 (A), pDNSP-hFBLN4_ASNmut2 (B), pDNSP-hFBLN4_ASNmutT (C)). The expected DNA bands were; in A: 6731bp; B: 6296bp in lane (a) and 429bp in lane (e); C: 640bp from lane (a) and 6091bp from lane (b). Controls are included to confirm the restriction: in B, the left panel includes single-digested (b) and non-digested (e) plasmids; the right panel includes non-digested gBlock_Mut2 (d); in C, lane (c) includes pDNSP-hFBLN4_ASNmut1 linearized with *EcoRI*, and lane (d) represents pDNSP-hFBLN4_ASNmut2 linearized with *EcoRI*.

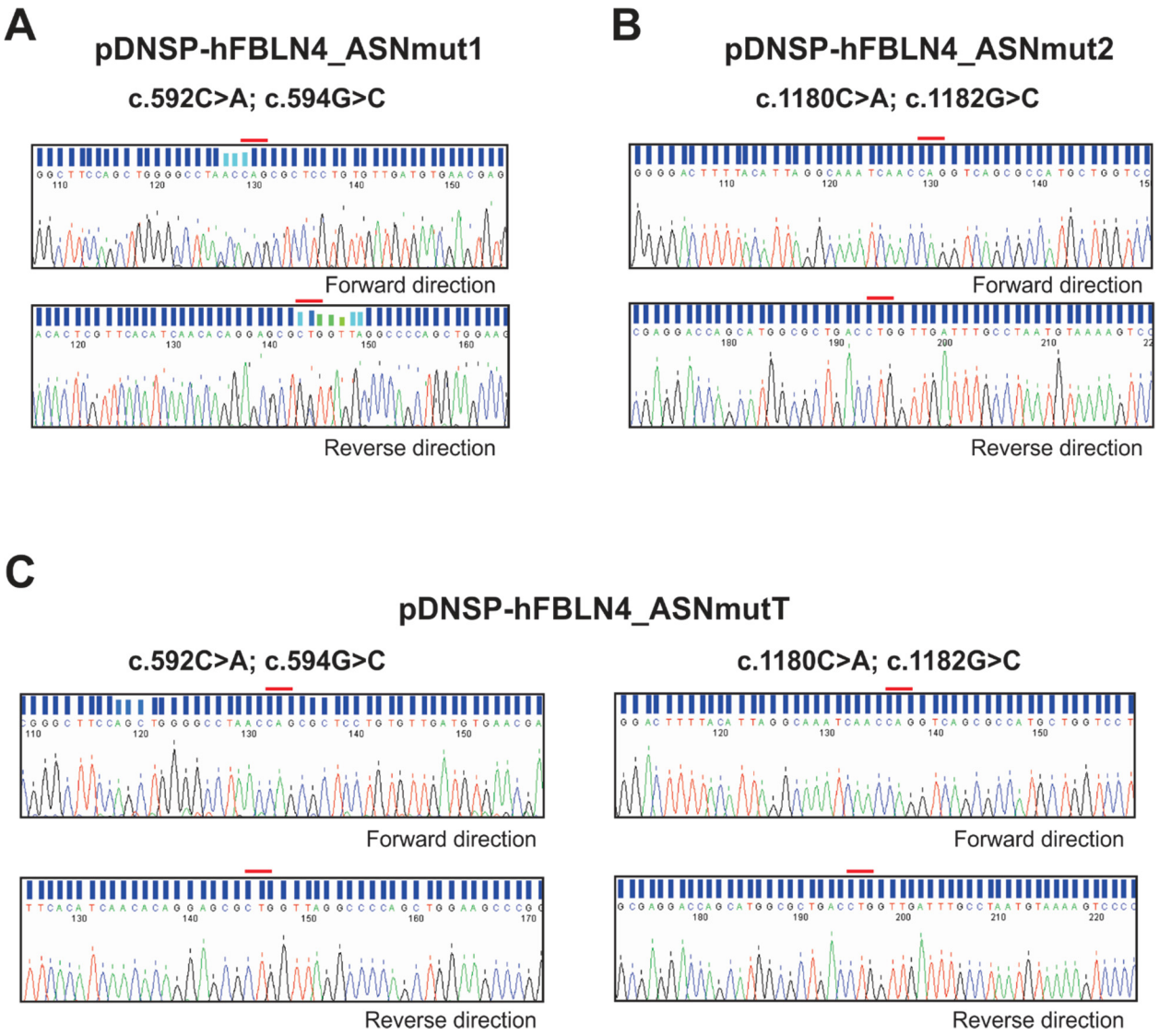

Figure 10. Confirmation of the desired Asn-Gln mutations by the Sanger sequencing chromatograms.

Shown are the chromatograms of each fibulin-4 N-linked glycosylation site mutant expression plasmids (pDNSP-hFBLN4_ASNmut1, A; pDNSP-hFBLN4_ASNmut2, B; pDNSP-hFBLN4_ASNmutT, C) using fibulin-4 oligonucleotides as forward and reverse primers. For each mutant constructs, the chromatograms are labeled with a red line on top indicating the mutated nucleotides. The Sanger sequencing was performed bi-directionally.

ligated to produce pDNSP-hFBLN4_ASNmut2 (Fig. 8B, 9B). The plasmid containing the mutations for both N-glycosylation sites (pDNSP-hFBLN4_ASNmutT) was generated by subcloning the Asn198Gln mutation site from pDNSP-hFBLN4_ASNmut1 into pDNSP-hFBLN4_ASNmut2 (Fig. 8C, 9C). All of the mutants were bi-directionally sequence-verified commercially by Sanger sequencing (Fig. 10). Large scale DNA amplification produced sufficient plasmid DNA for the subsequent transfection of cells.

5.3 Analysis of Western blotting and Coomassie blue staining of the recombinantly-expressed fibulin-4 wild-type and the N-linked glycosylation site mutants

To recombinantly produce the N-glycosylation site mutants of fibulin-4, the mutant constructs were transfected into human embryonic kidney cells (HEK293H). Stably transfected clones were selected and tested for the production of the recombinant proteins by Western blotting. About 10% of the stable clones demonstrated bands of ~60kDa in reduced condition. For each mutant construct, a representative cell clone was selected for large scale protein production. For each mutant clone, 48-h conditioned medium was produced. Typically, 2.5L of the conditioned medium was concentrated to 50mL, purified by Ni^{2+}-loaded chelating chromatography. Purified proteins (hFBLN4_ASNmut1, hFBLN4_ASNmut2, and hFBLN4_ASNmutT) were separated via SDS-PAGE and were further analyzed by Western blotting (Fig. 11A) and Coomassie blue staining (Fig. 11B) to analyze the loss of the respective glycans. Both hFBLN4_ASNmut1 and hFBLN4_ASNmut2 showed three bands of ~50kDa (monomers), ~100kDa (dimers), and above 250kDa (multimers) under non-reducing conditions, and a single band of 61kDa under reducing conditions, the molecular mass corresponding to fibulin-4 containing one glycan (Fig. 11). hFBLN4_ASNmutT, showed a single band above 250kDa under non-reducing conditions, of 57kDa which corresponded to the size of enzymatically-deglycosylated wild-type fibulin-4 (Fig. 11A, B right panel). hFBLN4_ASNmutT also showed an extra band at 43kDa (Fig. 11A, right panel). Note that there was an increase in the relative intensity of the multimeric bands versus dimeric and monomeric bands in the fibulin-4 single glycosylation site mutants as compared to the fibulin-4 wild-type (Fig. 11A, B left panel). The dimers of wild-type and mutant proteins could be completely reduced to monomers upon reduction. Whereas the higher molecular mass multimers

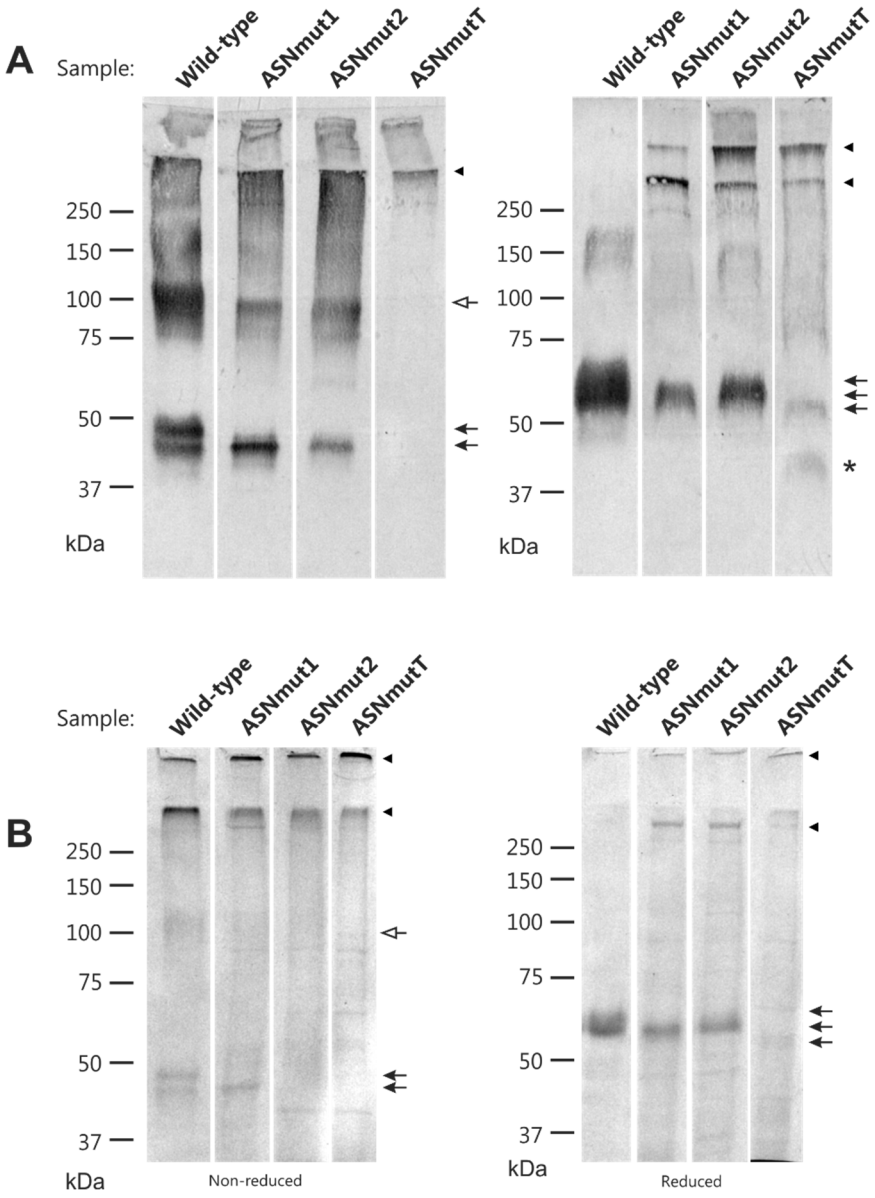

Figure 11. Comparison between fibulin-4 wild-type and N-glycosylation site mutants.

Purified recombinant wild-type fibulin-4 and N-linked glycosylation site mutants of fibulin-4 (hFBLN4_ASNmut1, 2, and T as ASNmut1, 2, and T) were analyzed by Western blotting (A, 1µg) and Coomassie blue staining (B, 5µg). Samples on the left panels were analyzed under non-reducing condition without DTT and samples on the right panels were analyzed under reducing condition in the presence of DTT. The filled-head arrows indicate monomeric proteins, the open-head arrows indicate the dimeric proteins and the arrowheads indicate proteins in multimeric conformations. Note that the multimeric proteins were not separated via DTT (right panel both A and B). Asterisk indicates an extra band from the hFBLN4_ASNmutT.

of the wild-type protein was reducible, the mutant proteins were either not or only little susceptible to DTT (Fig. 11A, arrowhead).

Whereas fibulin-4 wild-type could be purified to homogeneity, the purified mutant proteins typically showed much less homogeneity and lower band intensities, most notable for hFBLN4_ASNmutT (Fig. 11). Therefore, densitometric analysis of the fibulin-4 protein band in Coomasssie-stained gels was employed to determine the relative amounts under reducing conditions. Based on the total protein concentration measurement by the BCA kit (including impurities), 5µg of the purified fibulin-4 wild-type was compared to 15µg of the purified N-glycosylation site mutants (hFBLN4_ASNmut1 and 2) to enable relative comparisons (Fig. 12). The overall calculated densitometric band intensity measurement revealed that the hFBLN4_ASNmut1 produced ~3.5 fold less and hFBLN4_ASNmut2 produced ~4.5 fold less protein band intensities compared to the fibulin-4 wild-type (Fig. 12). Using the adjusted concentration values, it was found that the protein purification yields from the conditioned medium of wild-type fibulin-4 was ~8mg per 2.5L conditioned medium, whereas the yields of hFBLN4_ASNmut1 and 2 were ~0.8mg per 2.5L each. hFBLN4_ASNmutT could not be analytically compared and evaluated due to its extremely low protein yield.

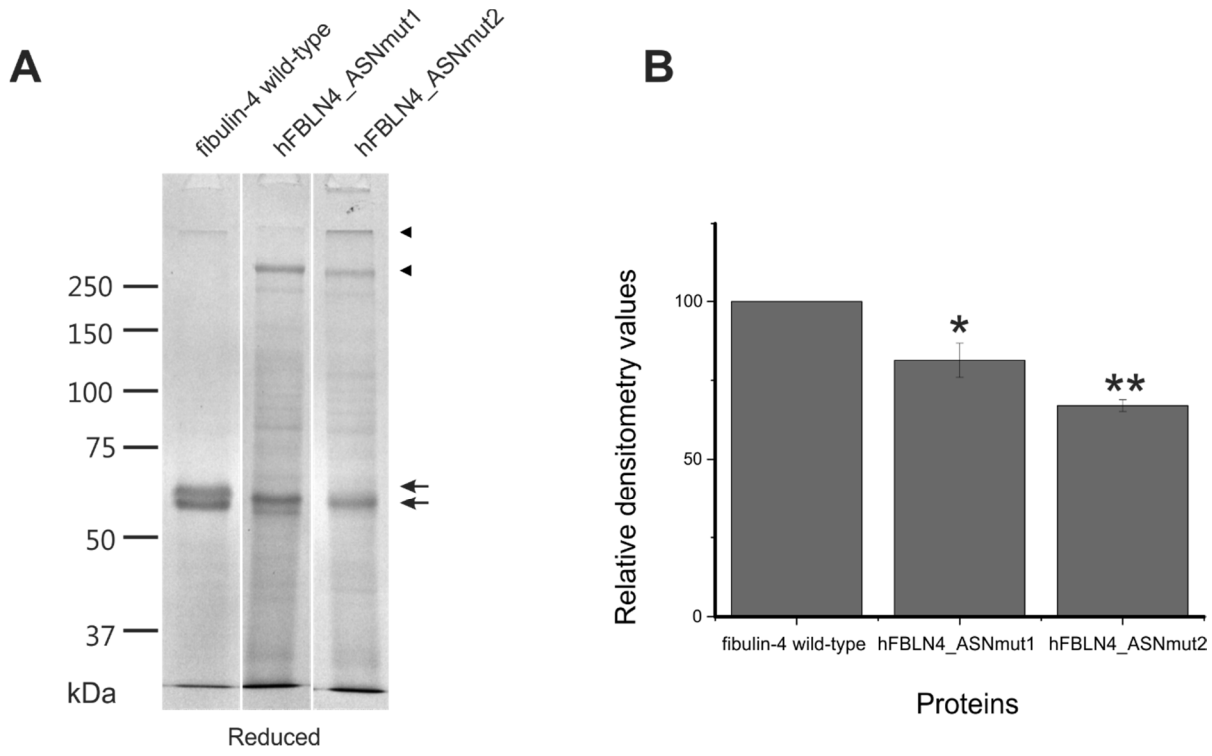

Figure 12. Densitometric comparison between fibulin-4 wild-type and the N-linked glycosylation site mutants.

Shown is the densitometric comparison between recombinantly expressed fibulin-4 wild-type (5µg) with hFBLN4_ASNmut1 and 2 (15µg) in a Coomassie-stained SDS-PAGE gel under reducing conditions (A) and the quantification of the protein bands (B). In A, the arrows indicate monomeric fibulin-4 under reducing conditions and the arrowheads represent non-reducible multimers. (B) Quantification of A using the ImageJ software. The background intensity values were subtracted from the combined intensity values of the monomeric bands and the multimeric bands. Shown data sets represent means of the triplicates with the standard deviations. *$p < 0.02$; **$p < 0.0001$

5.4 Comparison of cell surface deposition between fibulin-4 wild-type and glycosylation site mutants

Next, the transfected HEK293H cells were examined through indirect immunofluorescence assay to investigate whether the secretion was inhibited and the proteins were retained intracellularly (Fig. 13). For comparison between the amount of the secreted proteins being deposited onto the cells and the proteins being retained intracellularly, cells were either fixed only with 4% paraformaldehyde (PFA) leaving the plasma membrane intact, or fixed with 4% PFA followed by treatment with 0.5% Triton-X100 in PBS which permeabilized the membrane. The cells transfected with wild-type fibulin-4 showed more staining on the cell surface combined with strong intracellular staining (Fig. 13). These data indicate that the wild-type fibulin-4 is actively synthesized, transported through the secretory pathway and deposited on the cell surface (Fig. 13B). The cells transfected with the glycosylation site mutants, however, demonstrated only little protein staining on the cell surface combined with strong intracellular staining similar to the wild-type protein, indicating that the amount of secreted mutant fibulin-4 was substantially lower compared to the wild-type fibulin-4 (Fig. 13C-E). hFBLN4_ASNmutT rendered the least amount of protein depositions onto the cell membrane. The intracellular staining of the membrane-permeabilized cells revealed similar staining patterns and intensities for the wild-type and mutant cells (Fig. 13, right panel). These immunofluorescence experiments indicate that the secreted amount of proteins with mutant glycosylation sites is lower than that of wild-type protein, possibly due to an inhibitory mechanism in the secretory pathway.

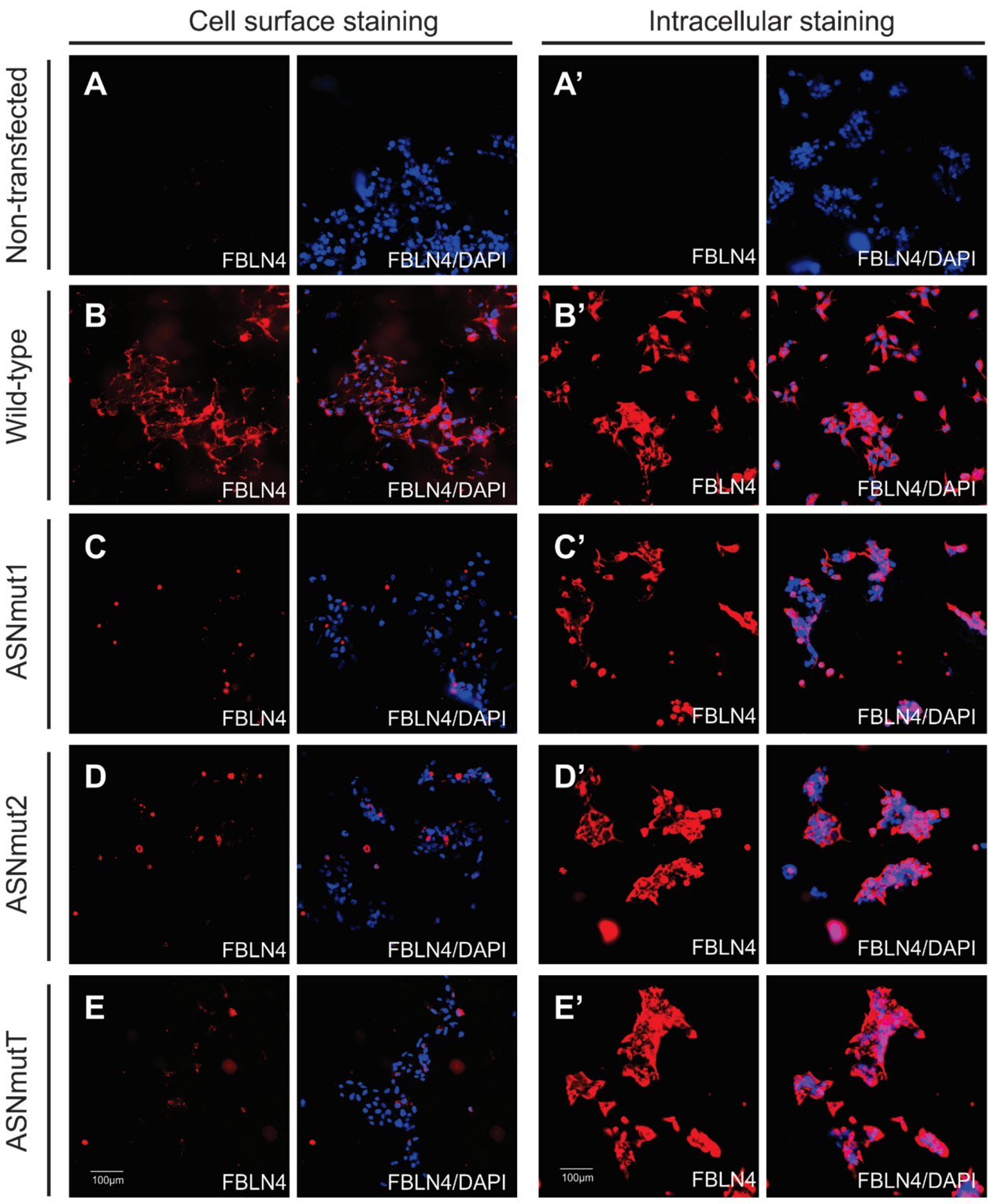

Figure 13. Fibulin-4 glycosylation site mutants exhibit less deposition onto the HEK293H cell surface. Legend overleaf.

Figure 13. Fibulin-4 glycosylation site mutants exhibit less deposition onto the HEK293H cell surface.

Recombinantly expressed fibulin-4 (Wild-type, B) fibulin-4 glycosylation site mutants (hFBLN4_ASNmut1, C; hFBLN4_ASNmut2, D; hFBLN4_ASNmutT, E) were examined for cell surface deposition (left panel, B-E) and for intracellular localization (right panel, B'-E') using an anti-fibulin-4 antibody. Cells were analyzed at day 3 post-seeding. Control staining in A and A' confirm the absence of intracellular and cell surface located fibulin-4 in non-transfected HEK293H cells (Non-transfected). Note that wild-type fibulin-4 is deposited onto the cell surface whereas the fibulin-4 glycosylation site mutants deposited much less. The amount of proteins retained inside the cells are similar between wild-type and mutant cells. The scale bars indicate 100μm; identical microscope magnification (200×) was used for all images.

5.5 Analysis of XBP1 mRNA

In order to explore whether the N-linked glycosylation mutants induced the URP in the secretory pathway, the recombinant HEK293H cell clones were analyzed for the presence of the characteristic splice variant of the XBP1 mRNA by RT-PCR (Fig. 14). It was shown by Yoshida et al. that non-transfected HEK293H cells express a XBP1 mRNA which is not cytosolically spliced, however, upon treatment with DTT, a known UPR-inducing agent which causes protein misfolding via disruption of disulfide bonds, the cells contain more of the cytosol-spliced form of the XBP1 mRNA (Yoshida et al., 2001). It was here confirmed that non-transfected HEK293H cells demonstrated a 424bp DNA band which corresponds to the non-spliced form of XBP1, whereas cells treated with DTT for 1h showed predominantly the 398bp DNA band corresponding to the spliced form of XBP1 (Fig. 14). Interestingly, HEK293H cells which were transfected with wild-type fibulin-4 construct showed XBP1 mRNA of both splice forms, although the intensity of the non-spliced XBP1 mRNA was dominant. HEK293H cells transfected with N-linked glycosylation site mutant constructs also demonstrated the presence of both splice forms of XBP1. However, the intensity of the spliced XBP1 mRNA was substantially enhanced compared to the wild-type, indicating that there had been a stronger induction of the UPR. This suggested that the removal of N-linked glycosylation sites in fibulin-4 induces UPR in the cells which in turn disrupts the secretion of the mutant protein. Consequently, less recombinant protein is enriched in the conditioned media compared to the wild-type fibulin-4.

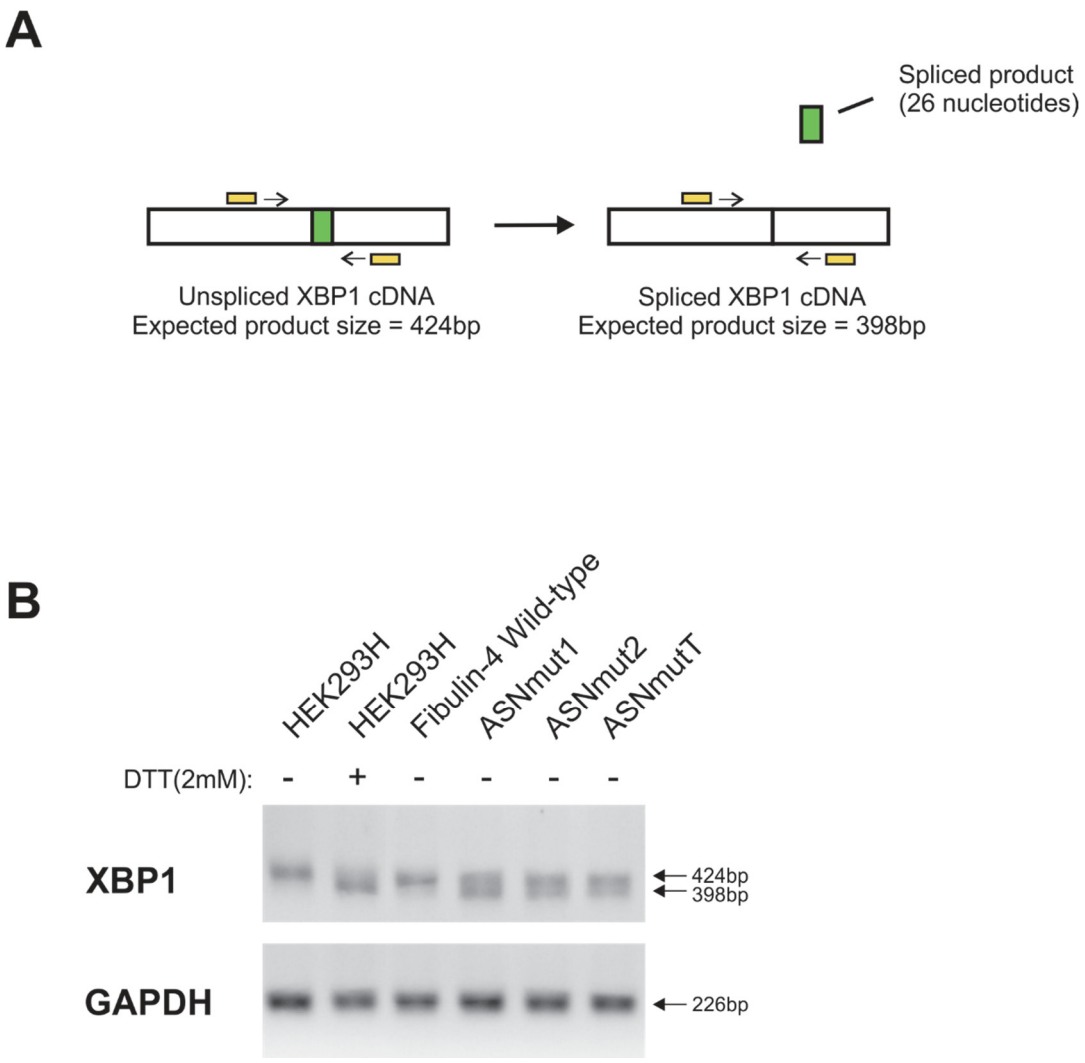

Figure 14. HEK293H cells transfected with N-linked glycosylation site mutant constructs demonstrate UPR

(A) Schematic diagram of analysis of XBP1 mRNA from HEK293H cells transfected with fibulin-4 wild-type or N-linked glycosylation site mutant constructs. Semi-quantitative RT-PCR was performed using specific primers (yellow). (B) Non-transfected HEK293H cells are characterized by the presence of a single 424bp DNA band of XBP1 (upper arrow), corresponding to unspliced XBP1 whereas HEK293H cells treated with UPR-inducing agent DTT demonstrate an additional lower 398bp DNA band, corresponding to cytosol-spliced XBP1. HEK293H cells transfected with wild-type fibulin-4 construct predominantly express unspliced XBP1 whereas HEK293H cells transfected with N-linked glycosylation site mutants constructs express splice forms, indicating UPR was induced. GAPDH was included as a loading control.

5.6 Analysis on established cell lines for their elastogenic properties

The goal to investigate the role of the N-linked glycosylation mutant protein in a cellular context required the characterization of various cell lines for their suitability to serve a recombinant elastogenic model. The focus was on the cellular expression of important elastogenic components including fibronectin, fibrillin-1 and -2, tropoelastin, and fibulin-4 and -5. The following cell lines were analyzed by indirect immunofluorescence: 1) human pigmented epithelial cells (APRE-19), 2) rat lung fibroblasts (RFL-6), 3) fetal bovine chondroblasts (FBC) and 4) rat pulmonary arterial smooth muscle cells (PAC1). The experiments were performed at various time points to observe the development of the elastic fiber-related networks over time, at day 7 and day 14. The results of these analysis are summarized in Table 1.

5.6.1 Analysis of ARPE-19

ARPE-19 cells have previously been shown to express elastogenic components such as fibrillin-1, LOX, and fibulin-5, but not tropoelastin (Wachi et al., 2005). Only upon addition of exogenous tropoelastin or after transfection the cells with a tropoelastin expression plasmid could elastic fiber assembly be observed in this study. We confirmed the previous studies by observing fibrillin-1, -2, and fibulin-5 expressions in both day 7 and 14 (Fig. 15A ii, fibrillin-2 and fibulin-5 not shown). Tropoelastin was detected in a punctuate pattern, however, it was never observed as assembled elastic fibers (Fig. 15A iv). In addition, fibronectin and fibulin-4 were expressed and formed moderately intense networks by day 14 (Fig. 15A ii and iii). In an attempt to reproduce the findings by Wachi et al., exogenous tropoelastin was added at 20µg/mL. However, indirect immunofluorescence after 7 days did not reveal the formation of elastic fibers (data not shown). Furthermore, the cells required longer seeding time for the expression and deposition of the elastogenic components in the ECM (~14days to reach similar amount of deposition compared to other cells) than what was previously shown. These findings excluded the ARPE-19 for our goal to determine the role of the N-linked glycosylation site mutants on elastic fiber formation.

Cell lines	Essential elastic fiber components				
	Tropoelastin	**Fibronectin**	**Fibrillin-1**	**Fibulin-4**	**Fibulin-5**
Human retinal pigmented epithelium (ARPE-19)	-	Moderate	Moderate	Moderate	Low
Rat lung fibroblast (RFL-6)	High	High	Moderate	High	Low
Fetal bovine chondroblast (FBC)	-	High	Low	Moderate	-
Rat pulmonary arterial smooth muscle cells (PAC1)	Moderate	High	High	Moderate	Low

Table 1. Summary of the analysis of cell lines for their elastogenic components

The expression and deposition of elastic fiber components were analyzed and visually graded for their immunofluorescence intensity in categories of 'high', 'moderate', and 'low' expression and depositions, based on the observations shown in figure 15.

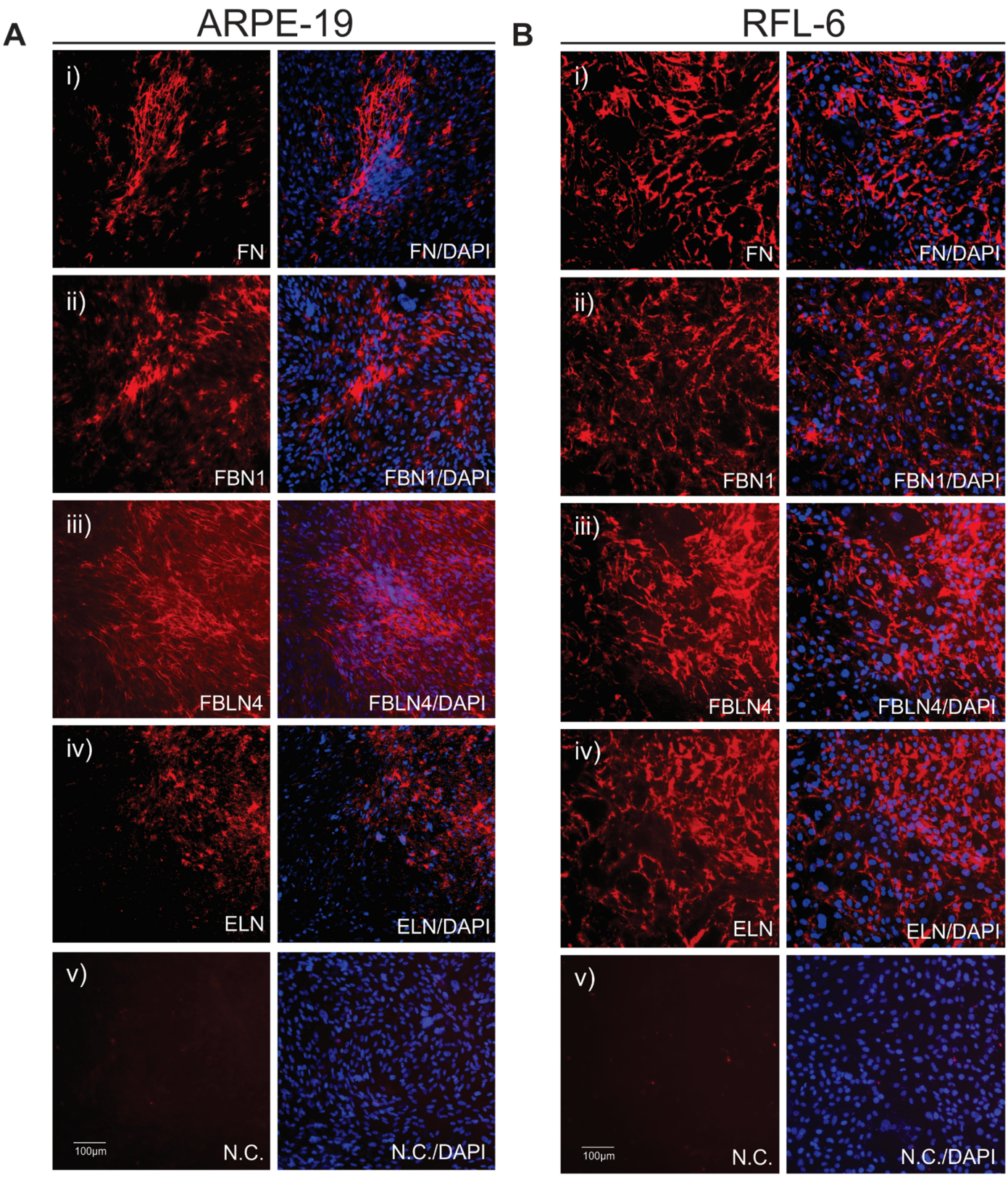

Figure 15. Analysis of cell lines for elastogenic properties. Legend overleaf.

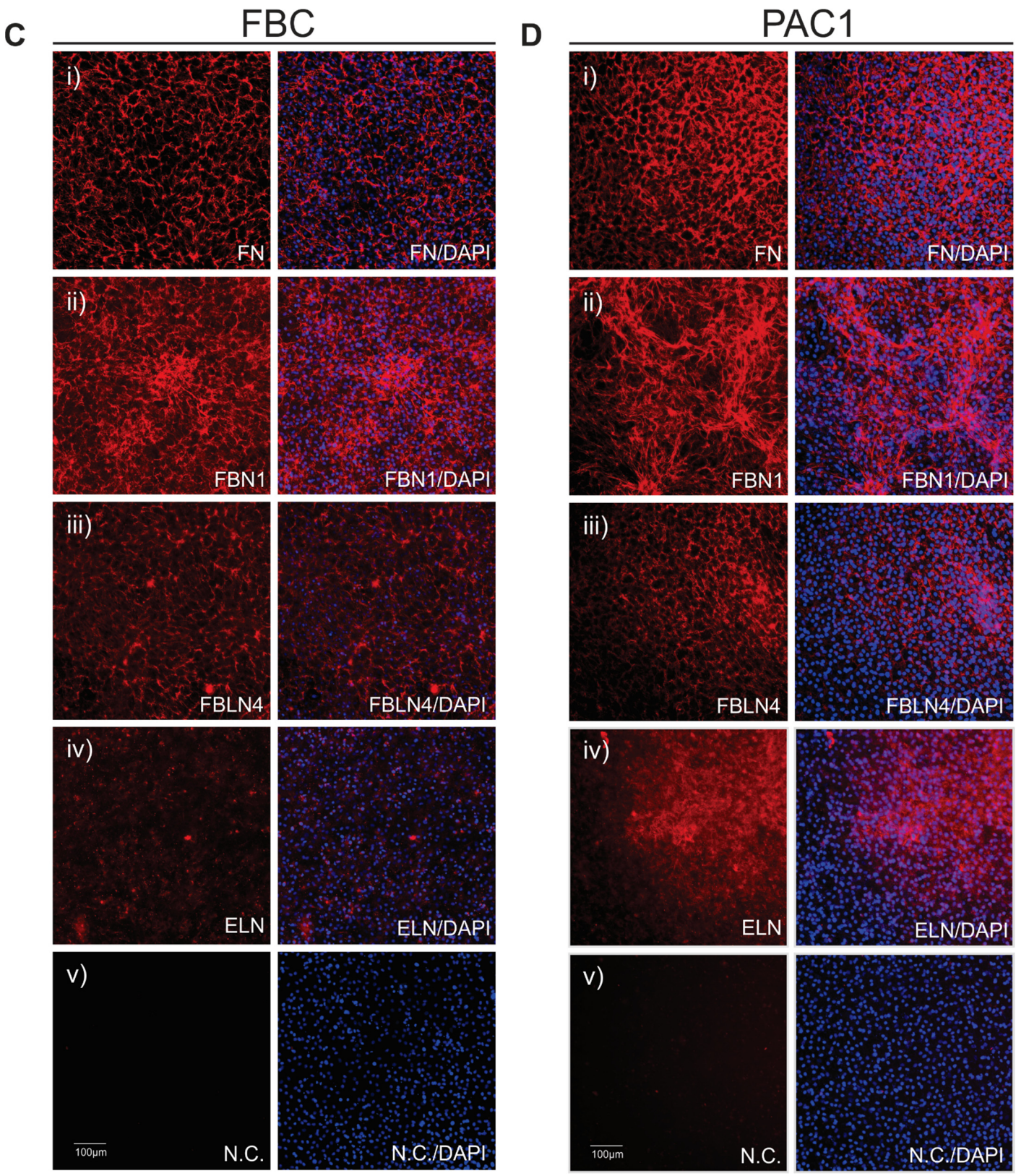

Figure 15. Analysis of cell lines for elastogenic properties. Legend overleaf.

Figure 15. Analysis of cell lines for elastogenic properties

Cell lines, including ARPE-19 (A), RFL-6 (B), FBC (C), and PAC1 (D), were examined for expression of elastic fiber components such as fibronectin (FN, i), fibrillin-1 (FBN1, ii), fibulin-4 (FBLN4, iii) and tropoelastin (ELN, iv). All cell lines were analyzed at day 7 post-seeding except of ARPE-19 which was analyzed at day 14 post-seeding due to excessive cell detachments. Note that RFL-6 cells produced an intensive fibulin-4 correlating with a significant amount of assembled elastic fibers, whereas moderate expression and deposition of fibulin-4 coincided with moderate expression and deposition of tropoelastin in PAC1 cells (B and D, iii and iv). The scale bars indicate 100μm, and same magnification (200×) was used for all images.

5.6.2 Analysis of RFL-6

RFL-6 is a well-known elastogenic cell line, known to express tropoelastin, LOX, as well as other ECM proteins such as collagen type I (Chen et al., 2005; Czirok et al., 2006). The expression of tropoelastin and deposition in typical fibrous pattern at both day 7 and day 14 was confirmed through indirect immunofluorescence (Fig. 15B iv). Additionally, a relatively high expression and deposition was observed for other elastogenic components, including fibronectin, fibrillin-1, -2, and fibulin-4 and -5 (Fig. 15B i, ii and iii). These findings provide the information for future experiments in which these elastogenic components require downregulation, for example, through siRNA approaches. However, for the current goal to analyze the fibulin-4 N-linked glycosylation site mutants, the RFL-6 cells were excluded because the tropoelastin expression and deposition was too high to analyze potential upregulation of elastic fiber formation.

5.6.3 Analysis of FBC

FBC cells were previously described to express fibrillin-1, -2, microfibril-associated glycoprotein and tropoelastin (Robb et al., 1999). In the present analysis, fibrillin-1 and fibronectin expression and deposition was observed at similar intensity at day 7 and day 14, whereas tropoelastin expression and deposition was not detected (Fig. 15C i-iv). This finding may be explained by two reasons: 1) the antibodies used were raised against human tropoelastin, and consequently may not have sufficient cross-reactivity with bovine tropoelastin, 2) tropoelastin might not be expressed anymore in the high passage number FBC (P11) we received from a collaborator.

5.6.4 Analysis of PAC1

PAC1 is known to express several smooth muscle cell markers, such as smooth muscle α-actin, myosin heavy chain, and myosin regulatory light chain (Rothman et al., 1992). However, PAC1 were not previously characterized for their expression and deposition of elastogenic proteins. Several elastic fiber formation components, including fibronectin, fibrillin-1, and tropoelastin were detected by indirect immunofluorescence after day 7 (Fig. 15D i, ii, iv). In PAC1 cells, tropoelastin was expressed in a punctuate pattern (droplets), which were assembled into fibers at slower rates compared to what was observed in RFL-6 cells (Fig. 16). Fibulin-4 was also expressed

and deposited, at moderate levels, which was comparably weaker than fibulin-4 expression and deposition in RFL-6 cells. PAC1 cells could not be evaluated at day 14 due to extensive cell detachments (data not shown). The presence of the principal components of elastic fiber formation and the formation of elastic fibers in combination with moderate fibulin-4 levels made PAC1 the ideal candidate to test the N-linked glycosylation site mutants.

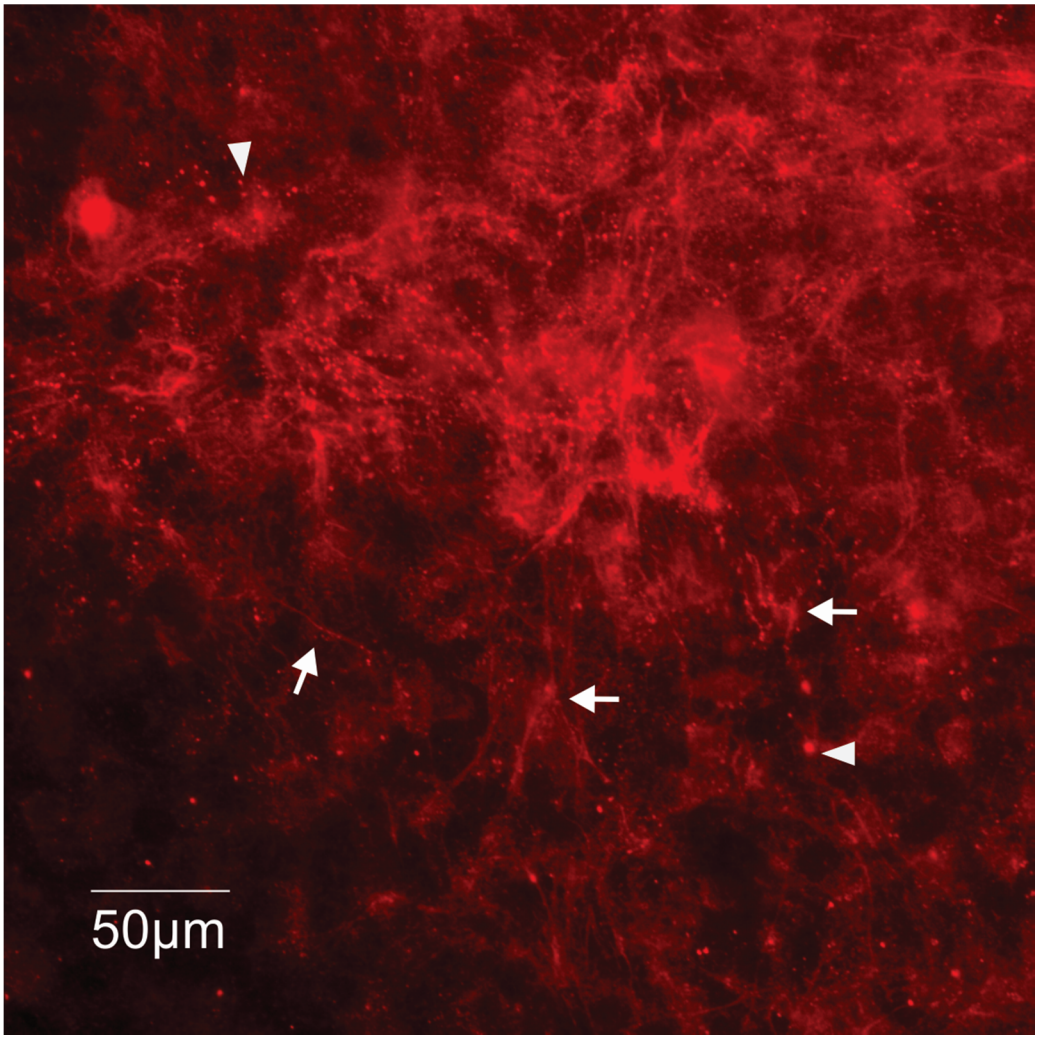

Figure 16. Elastic fiber assembly in PAC1

Shown is the zoomed-in image of figure 15D iv. Secreted tropoelastin from PAC1 cells are initially detected as droplets or aggregates (arrowheads). These aggregates get assembled together, forming elongated elastic fibers (arrows). The scale bar indicates 50µm; the image was taken at 200× magnification.

5.7 Overexpression of fibulin-4 glycosylation site mutants induces more secretion and assembly of tropoelastin into fibers

As described above, PAC1 cells express and deposit moderate level of tropoelastin which correlate with moderate level of fibulin-4 expression and deposition, whereas RFL-6 cells express high levels of tropoelastin correlating with high levels of fibulin-4 expression and deposition (Table 1). Additionally, RFL-6 cells readily assembled the highly-expressed tropoelastin into fibers whereas PAC1 cells initially deposited tropoelastin as droplets elastic fibers formed gradually presumably with the droplets as site of nucleation (Fig. 16). Therefore, the PAC1 cells were chosen to test how the N-linked glycosylation site mutants affect elastogenesis in this cell culture system. The underlying hypothesis is that N-linked glycosylation of fibulin-4 can regulate elastogenesis. In order to test this hypothesis, we overexpressed fibulin-4 wild-type and the N-linked glycosylation site mutant constructs into PAC1 cells and analyzed the elastic fiber formation including the expression and deposition of elastic fiber associated components.

PAC1 cells were stably transfected with pDNSP-hFBLN4, pDNSP-hFBLN4_ASNmut1, 2 and T expression plasmids, and were analyzed by indirect immunofluorescence after 7 days of cell culture with focus on fibronectin, fibrillin-1, fibulin-4 and elastin. The upstream regulators of elastogenesis, fibronectin and fibrillin-1 showed a typical fibrous staining pattern in non-transfected PAC1 cells (Fig. 17A i and B i). The staining pattern was very similar in PAC1 cells transfected with fibulin-4 wild-type construct (Fig. 17 A, ii and B, ii), or with all three N-linked glycosylation site mutant constructs (Fig. 17A iii-v and B iii-v). These demonstrate that the overexpression of fibulin-4 does not affect fibronectin and fibrillin-1 network formation. The deposition of fibulin-4 in all hFBLN4 constructs-overexpressed PAC1 cells appeared as fibers and bright patchy patterns which were both not observed in non-transfected PAC1 cells (Fig. 17C). These data demonstrate that the fibulin-4 positive fibers and patches represent recombinantly-expressed fibulin-4. The data further clarify that not only the recombinant wild-type fibulin-4 is secreted from the cells, but also the N-linked glycosylation site mutants. This is in stark contrast to the recombinant HEK293H cell clones that are not able to secrete the N-linked glycosylation

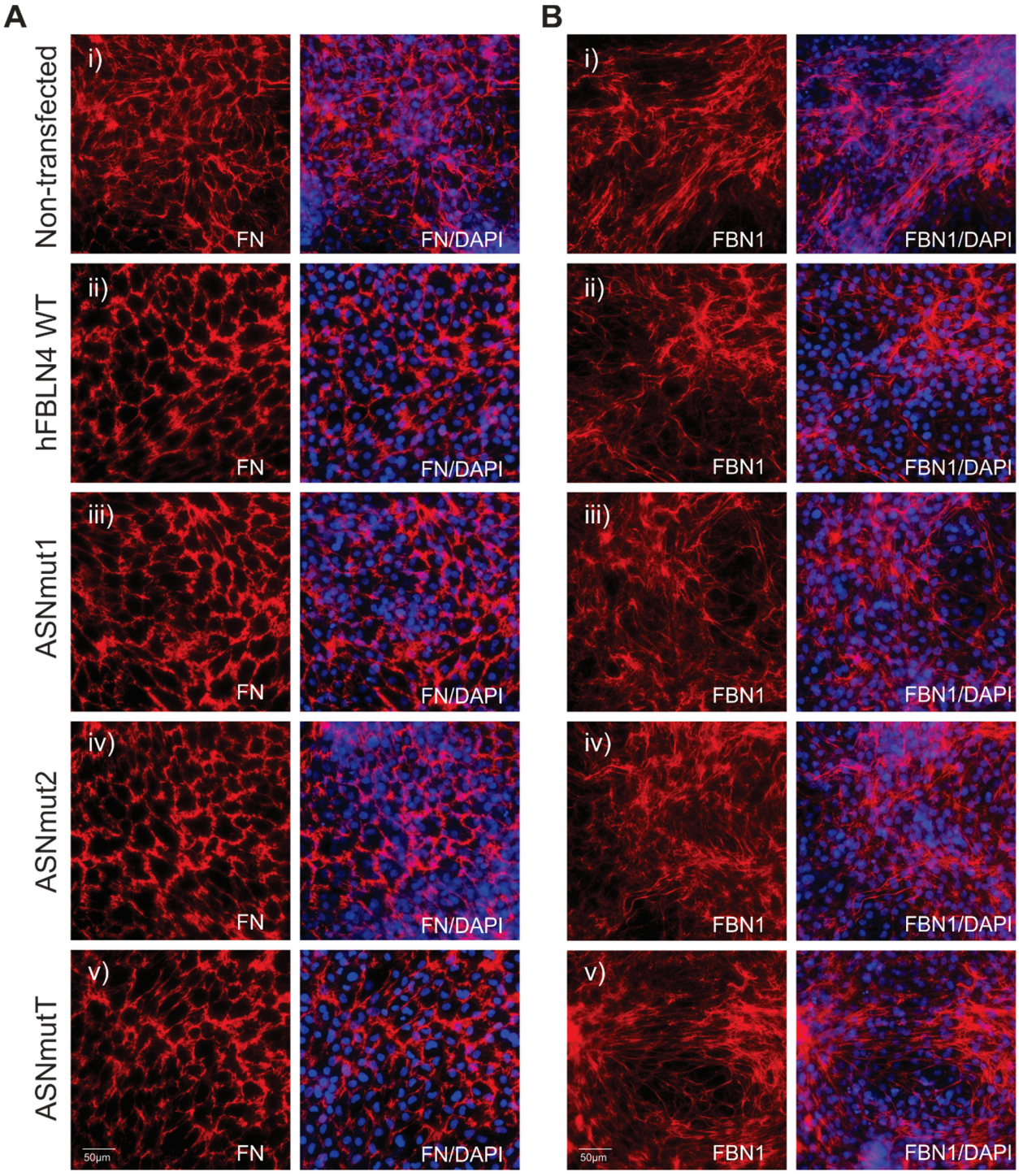

Figure 17. Analysis of recombinant overexpression of fibulin-4 wild-type and N-linked glycosylation site mutants in PAC1 cells Legend overleaf.

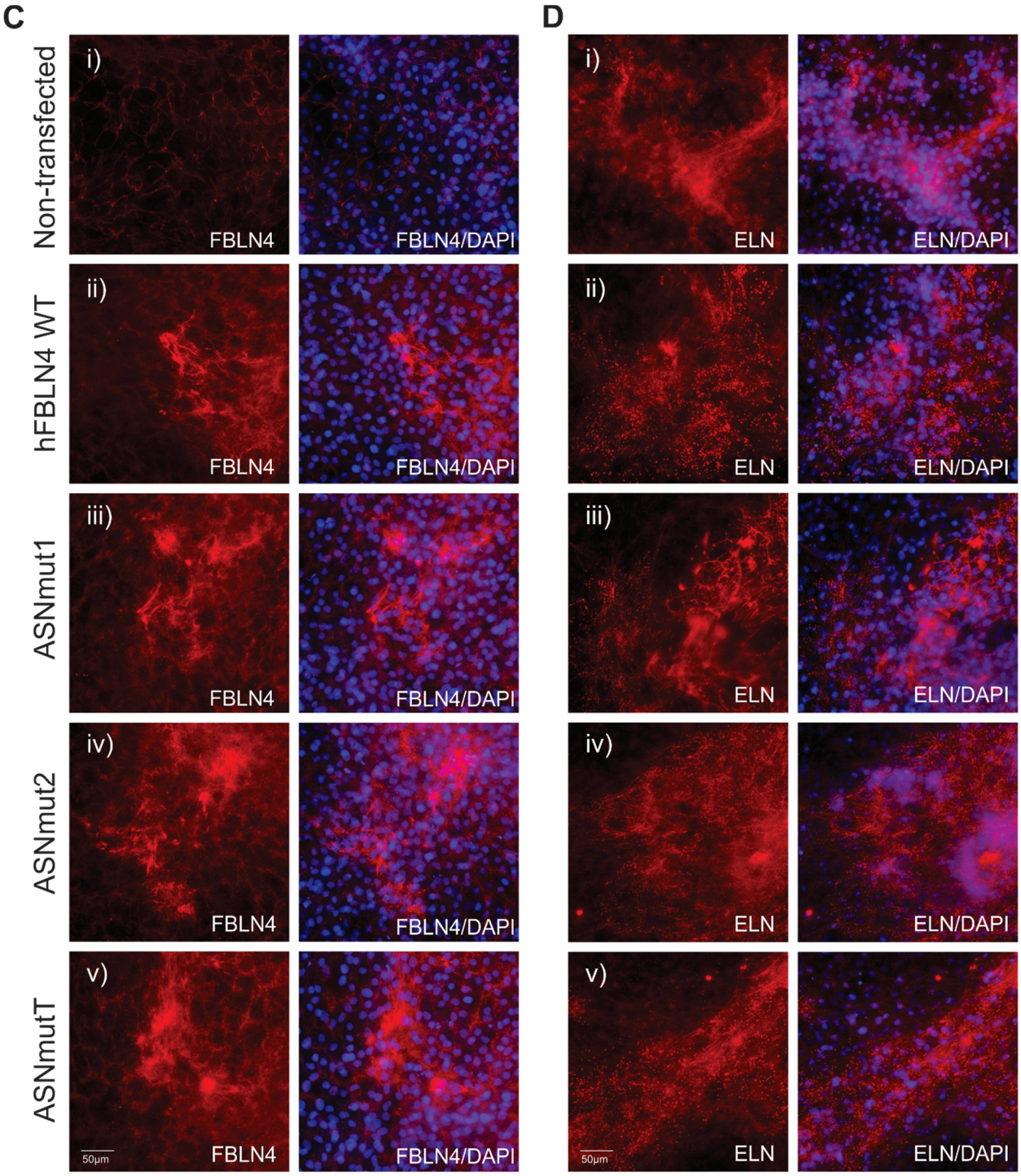

Figure 17. Analysis of recombinant overexpression of fibulin-4 wild-type and N-linked glycosylation site mutants in PAC1 cells Legend overleaf.

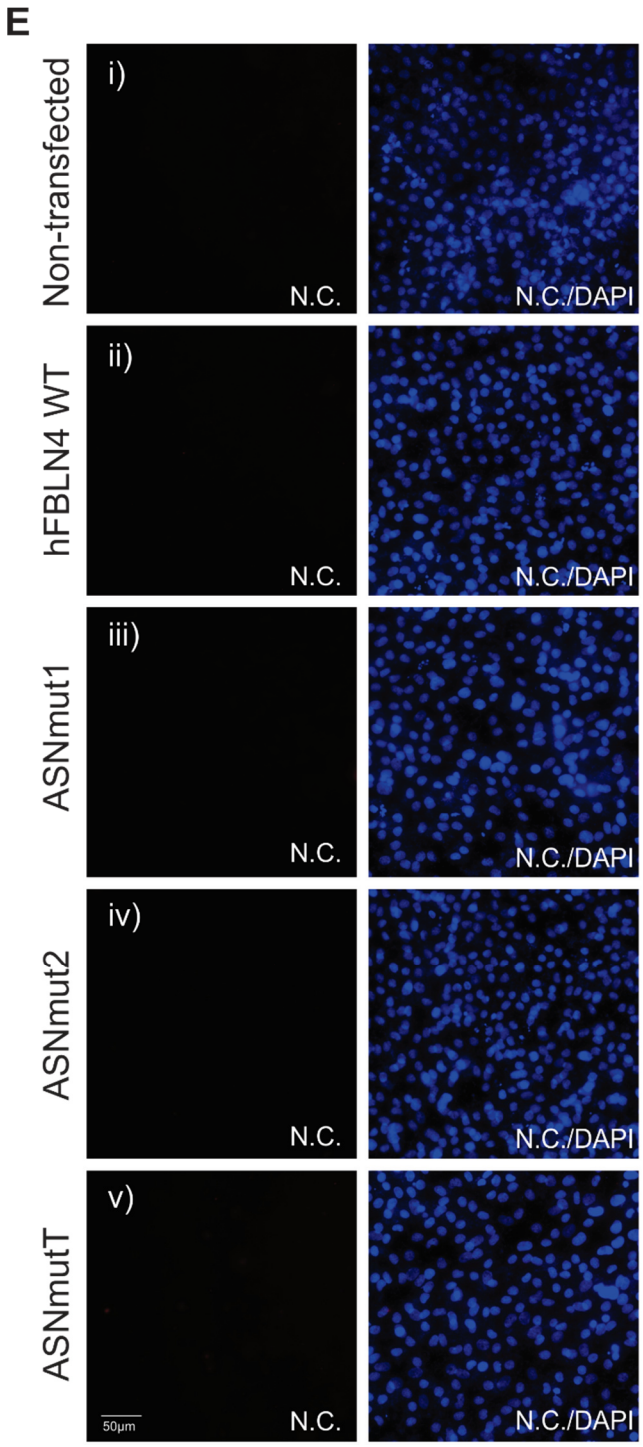

Figure 17. Analysis of recombinant overexpression of fibulin-4 wild-type and N-linked glycosylation site mutants in PAC1 cells Legend overleaf.

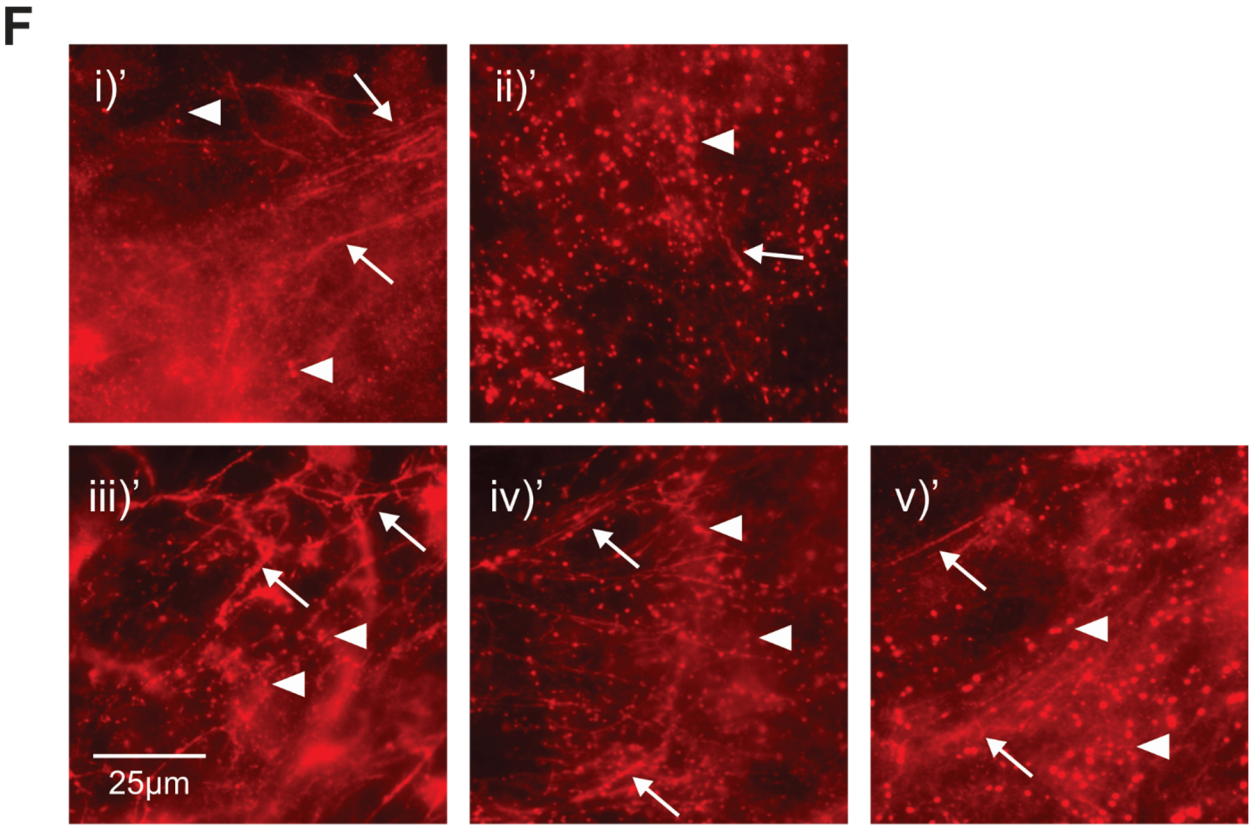

Figure 17. Analysis of recombinant overexpression of fibulin-4 wild-type and N-linked glycosylation site mutants in PAC1 cells

Shown is the analysis of PAC1 cells non-transfected (i) or stably transfected with pDNSP-hFBLN4 (hFBLN4 WT, ii), pDNSP-hFBLN4_ASNmut1 (ASNmut1, iii), pDNSP-hFBLN4_ASNmut2 (ASNmut2, iv), and pDNSP-hFBLN4_ASNmutT (ASNmutT, v) for the expression and ECM deposition of essential of elastogenic components including fibronectin (FN, A), fibrillin-1 (FBN1, B), fibulin-4 (FBLN4, C), and tropoelastin (ELN, D). Cells were analyzed at day 7 post-seeding. Negative control (N.C., E) staining was performed without addition of primary antibody. In F, note that in non-transfected PAC1 cells i)', only few tropoelastin droplets (arrowheads) and a few tropoelastin fibers (arrows) can be depicted. In ii)', the number of tropoelastin droplets substantially increased compared to i)' although the number of elastic fibers did not increase. In iii)', iv)', and v)', both the number of tropoelastin droplets and the amount of elastic fibers increased compared to the non-transfected PAC1 cells (i)'. The scale bars for A-E indicate 50µm, and the scale bar for F indicates 25µm. All images were taken with 400× magnificataion.

site mutants (see Fig. 13). Finally, the data show that the wild-type as well as all N-linked glycosylation site mutants can form fibers in the extracellular space.

The staining of tropoelastin changed substantially upon overexpression of fibulin-4 wild-type and N-linked glycosylation mutants. When fibulin-4 wild-type was overexpressed in the PAC1 cells, a drastic increase in the numbers of tropoelastin droplets was observed, although the droplets did not assemble further into fibers (Fig. 17D ii and F ii'). These data can be explained by two possible mechanisms: the overexpression of wild-type fibulin-4 either 1) enhanced the expression and/or the secretion of tropoelastin in the ECM, or 2) the presence of wild-type fibulin-4 in the ECM nucleated the formation of tropoelastin droplets. When fibulin-4 N-linked glycosylation site mutant constructs were overexpressed in PAC1 cells, similar to the wild-type fibulin-4 there were increased numbers of droplets present in the ECM compared to the non-transfected PAC1 cells (Fig. 17D iii-v and F iii'-v'). Surprisingly, all three N-linked glycosylation site mutants additionally triggered the formation of tropoelastin fibers in the ECM, which was not observed in non-transfected or wild-type fibulin-4 transfected PAC1 cells (Fig. 17D iii-v and F iii'-v'). These results clearly suggest the N-linked glycans on fibulin-4 can play a regulatory (inhibitory) role in the formation of tropoelastin fibers.

To analyze whether exogenously added fibulin-4 can trigger similar formation of tropoelastin droplets in the ECM, purified recombinant wild-type fibulin-4 (50µg/mL) was added to the PAC1 cell culture (Fig. 18). Indirect immunofluorescence analysis demonstrated that the exogenously added fibulin-4 deposited as randomly distributed large aggregates, but not as fibers as seen in the pDNSP-hFBLN4 transfected PAC1 cells (Fig. 17A iii). These data demonstrate that fibulin-4 fiber formation requires secretion through the cellular pathway. Fibrillin-1 and fibronectin staining was similar to the staining observed with the transfected PAC1 cells. Instead of the large number of tropoelastin deposits observed in the wild-type and mutant fibulin-4 constructs-transfected PAC1 cells, only few deposits were identified. Tropoelastin assembly was slightly enhanced compared to the control, however, the fibers were much shorter compared to what was observed in PAC1 cells transfected with wild-type or N-linked glycosylation site mutant constructs of fibulin-4 (Fig. 17F and 18A iv). Overall, these experiments show that endogenously expressed recombinant wild-

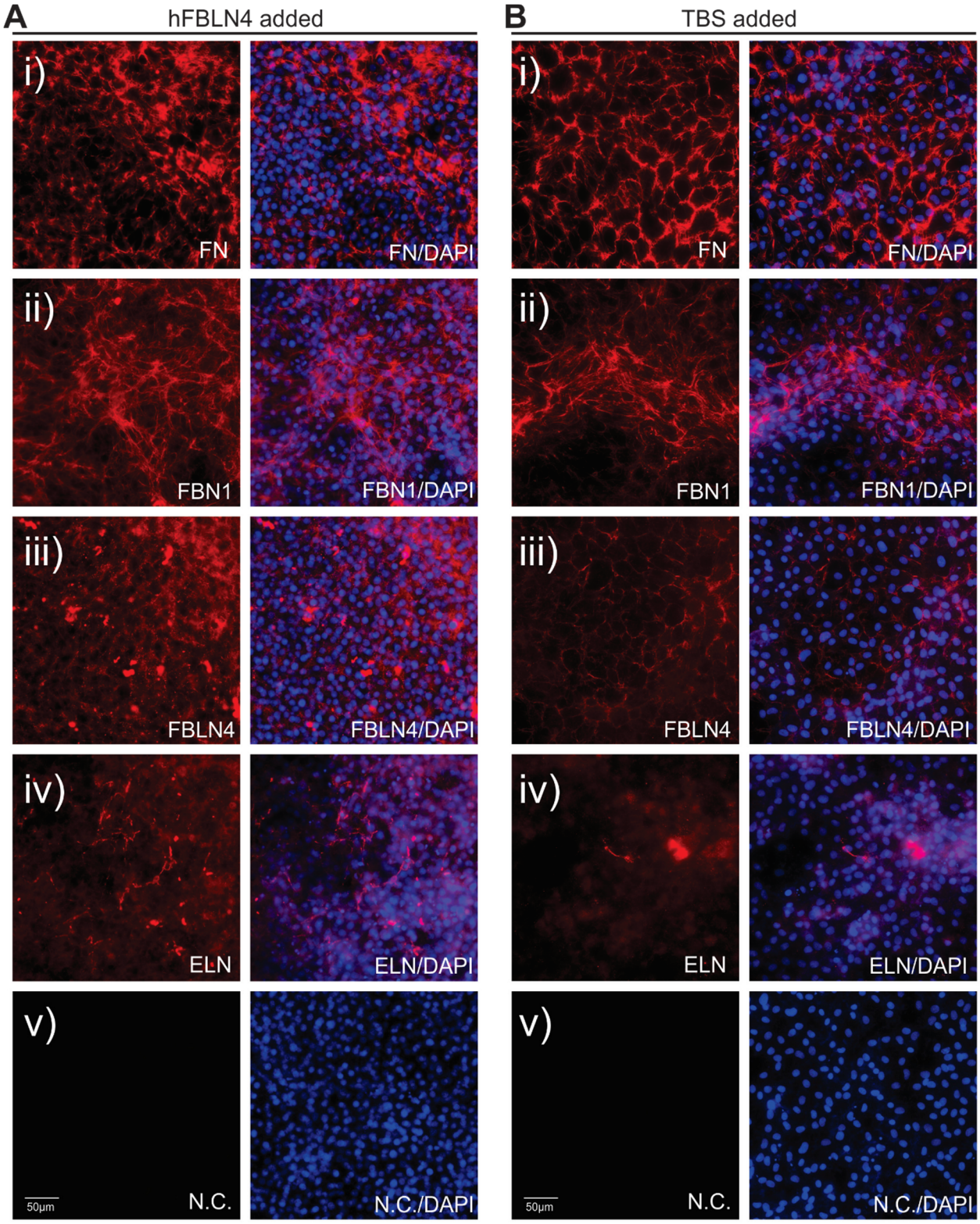

Figure 18. Addition of exogenous fibulin-4 slightly enhances elastic fiber assembly. Legend overleaf.

Figure 18. Addition of exogenous fibulin-4 slightly enhances elastic fiber assembly

PAC1 cells were grown in the presence of exogenously-added fibulin-4 (50μg/mL) or a TBS control, and were examined at day 7 post-seeding. The expression and deposition of essential elastic fiber components, including fibronectin (FN, i), fibrillin-1 (FBN1, ii), fibulin-4 (FBLN4, iii) and tropoelastin (ELN, iv) were analyzed. A negative control was included omitted the primary antibody (N.C., v). Note that exogenously-added fibulin-4 was stained as aggregates in a randomly-distributed pattern, which is not observed in the TBS control (Fig. 18A and B iii). Only few tropoelastin and few short elastic fibers were observed (Fig. 18A iv) The scale bars indicate 50μm. All the images were taken at the magnification of 400×.

type fibulin-4 induces tropoelastin droplet formation and elastic fiber formation more efficiently than exogenously added purified fibulin-4. N-linked glycosylation site mutants of fibulin-4 could not be tested in this experimental setting, because they could not be purified in sufficient high amounts (see section 5.3).

5.8 Overexpression of fibulin-4 wild-type and glycosylation site mutants enhance secretion of tropoelastin into ECM but does not increase expression of tropoelastin

To determine whether mRNA expression levels of tropoelastin and other elastic fiber components are affected upon overexpression of the fibulin-4 constructs in PAC1 cells, semi-quantitative RT-PCR was conducted (Fig. 19A). The recombinant fibulin-4 mRNA expression was only detected in the transfected PAC1 cells, whereas the endogenous fibulin-4 mRNA expression was identified in all PAC1 cells including the non-transfected control. The fibulin-4 mRNA expression level tended to be lower in transfected cells versus the non-transfected cells, similar to the fibrillin-1 and tropoelastin mRNA expression patterns. The fibronectin mRNA was similarly expressed in the non-transfected and transfected PAC1 cells. Overall, the transfection of PAC1 cells with the various fibulin-4 expression constructs did not increase the mRNA expression levels for relevant elastogenic components.

To examine whether the secreted protein levels were affected upon transfection with the fibulin-4 expression constructs, dot-blot assays were performed with using conditioned media from PAC1 non-transfected and transfected cells (Fig. 19B and C). The protein levels of the secreted essential elastic fiber components, fibronectin and fibrillin-1 did not show significant differences, except for the PAC1_Mut1 cells that showed enhanced fibrillin-1 in the medium. As expected, the amount of fibulin-4 in the medium of the transfected PAC1 cells was significantly higher than in the medium of the non-transfected PAC1 cells. The levels of secreted tropoelastin increased about 2-fold in all transfected PAC1 cells compared to the non-transfected cells (Fig. 19B and C). These results suggest that recombinant overexpression of fibulin-4 constructs facilitated tropoelastin secretion from the cells. The enhanced secretion of tropoelastin may account for increased number of tropoelastin droplets, and potentially elastic fibers, observed in the immunofluorescence assay.

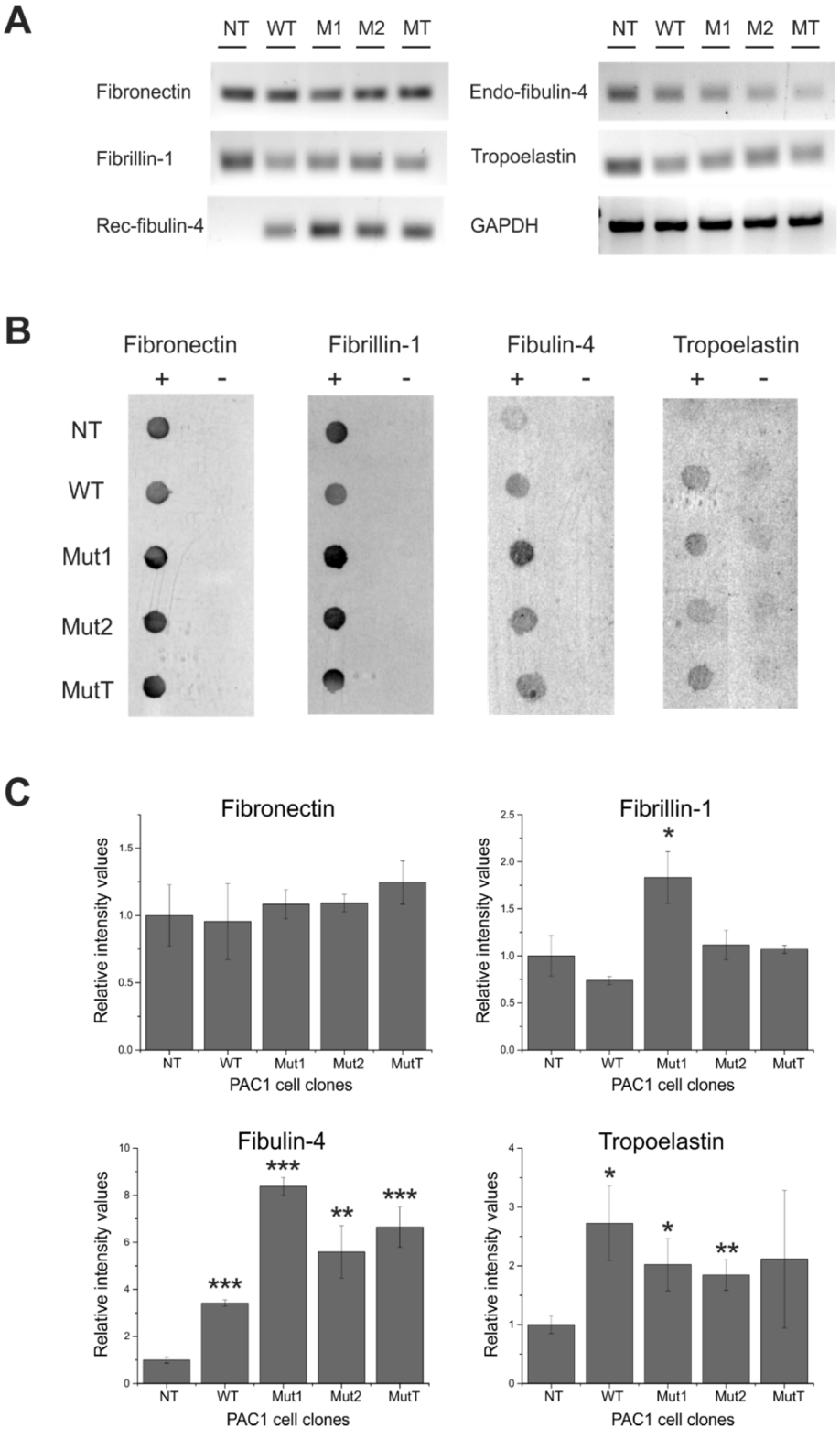

Figure 19. Analysis of mRNA and secreted protein levels in transfected PAC1 cells. Legend overleaf.

Figure 19. Analysis of mRNA and secreted protein levels in transfected PAC1 cells

Shown is the analysis of mRNA and secreted protein level in PAC1 cells non-transfected and transfected with fibulin-4 wild-type and N-linked glycosylation mutants. (A) RT-PCR was performed with primers generated for the complementary DNA (cDNA) of fibronectin, fibrillin-1, fibulin-4, tropoelastin, and GAPDH. Two sets of primers for the fibulin-4 cDNA were used to differentiate between recombinant (rec) and endogenous (endo) fibulin-4 mRNA. Only transfected cells exhibited expression of rec-fibulin-4 mRNA. (B) Dot-blot assay of conditioned media from non-transfected and transfected PAC1 cells. For the analysis of fibronectin, fibrillin-1, and fibulin-4, 50μL of conditioned media were applied and for tropoelastin, 500μL of conditioned media were applied. The experiment was performed in triplicates with TBS as a negative control. (C) Quantification of figure 19B by densitometry. *$p < 0.02$; **$p < 0.01$; ***$p < 0.0001$

5.9 Additional results related to the project

An affinity-purified anti-fibulin-4 antibody (anti-fibulin-4_AP-N antibody) was generated using a column packed with sepharose conjugated with the fibulin-4 N-terminus to cbEGF1 (fibulin-4_N-1) protein fragment for more specific detection of fibulin-4. The goal was to obtain antibodies with a higher specificity for fibulin-4. The specificity of the anti-fibulin-4_AP-N antibody was verified compared to the anti-fibulin-4 antibody by ELISA using fibulin-4 wild-type and fibulin-4_N-1 fragment (Fig. 20).

The tested antibodies include two polyclonal antisera against human fibulin-4 (non-purified, ID166 and ID122), the first and the second flow-through of the extracted IgG antibodies of one of the polyclonal antiserum (ID122) from the sepharose column conjugated to fibulin-4_N-1 fragment (Flow-through 1 and Flow-through 2), as well as the anti-fibulin-4_AP-N antibody. As expected, the fibulin-4 wild-type revealed similar binding levels of all antibodies (Fig. 20). The fibulin-4_N-1 fragment showed strong binding with the two non-purified fibulin-4 antibodies and the anti-fibulin-4_AP-N antibody (Fig. 20). However, the flow-through did not bind to the fibulin-4_N-1 fragment, indicating that there were no more specific antibodies against the fibulin-4_N-1 fragment present (Fig. 20). These data verified the affinity-purified anti-fibulin-4_AP-N binds specifically against the N-terminus of the fibulin-4.

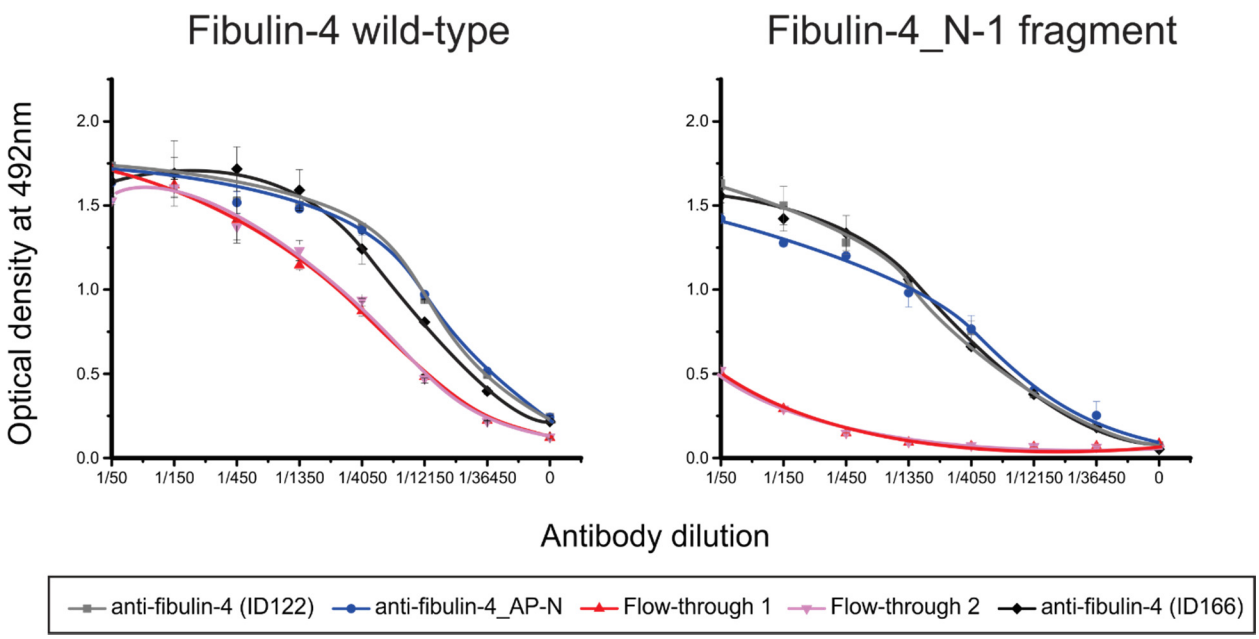

Figure 20. ELISA analysis using different antibodies against fibulin-4 wild-type and the fibulin-4_N-1 fragment

Shown is a representative ELISA analysis performed on 96-well plates coated with fibulin-4 wild-type (left panel) or fibulin-4_N-1 fragment (right panel) using two polyclonal antisera against human fibulin-4 (ID166 and ID122), the first and the second flow-through of the extracted IgG antibodies from one of the polyclonal antiserum (ID122) against the sepharose column conjugated to fibulin-4_N-1 fragment (Flow-through 1 and Flow-through 2), and the anti-fibulin-4_AP-N antibody (anti-fibulin-4_AP-N). Shown data sets represent means of triplicates with standard deviations.

Further validation of the affinity-purified antibodies was performed by Western blotting, using several recombinantly expressed fibulin-4 proteins, including fibulin-4 wild-type, monomeric and multimeric preparations (which were gel-filtrated based on their molecular weights), and fibulin-4 N-linked glycosylation site mutants including hFBLN4_ASNmut1, 2, and T (Djokic et al., 2013) (Fig. 21). Under non-reducing conditions, the observed banding patterns were similar between the anti-fibulin-4 antibody and the anti-fibulin-4_AP-N antibody (Fig. 21, left panels) The monomer preparation of fibulin-4 showed predominantly monomeric (~50kDa, filled arrows) and dimeric (~100kDa, open arrows) bands, whereas the fibulin-4 multimer preparations showed at all three bands corresponding to monomer, dimer and multimer (above 250kDa, arrowheads), with a stronger band at the multimeric region (Fig. 21, left panel). Under reducing conditions, using anti-fibulin-4 antibody, almost all fibulin-4 proteins were reduced to ~60-65kDa in fibulin-4 wild-type and the monomer preparation (Fig. 21A). However, in the fibulin-4 multimer preparation and the N-glycosylation site mutants, there were still bands detected in the multimeric regions above 250kDa, indicating that these proteins may form intermolecular bonds which are not reducible by DTT (Fig, 21A, right panel, arrowheads). The anti-fibulin-4_AP-N antibody produced similar bands in reduced conditions compared to the anti-fibulin-4 antibody (Fig. 21B, right panel). One exception was that the lower bands of the non-reducible multimers were substantially decreased compared to the anti-fibulin-4 antibody (Fig. 21B, right panel, arrowheads). These observations suggested that the multimers may form in a way which sterically obstructs the N-terminal region of the fibulin-4, and renders it thus less detectable with the anti-fibulin-4_AP-N antibody.

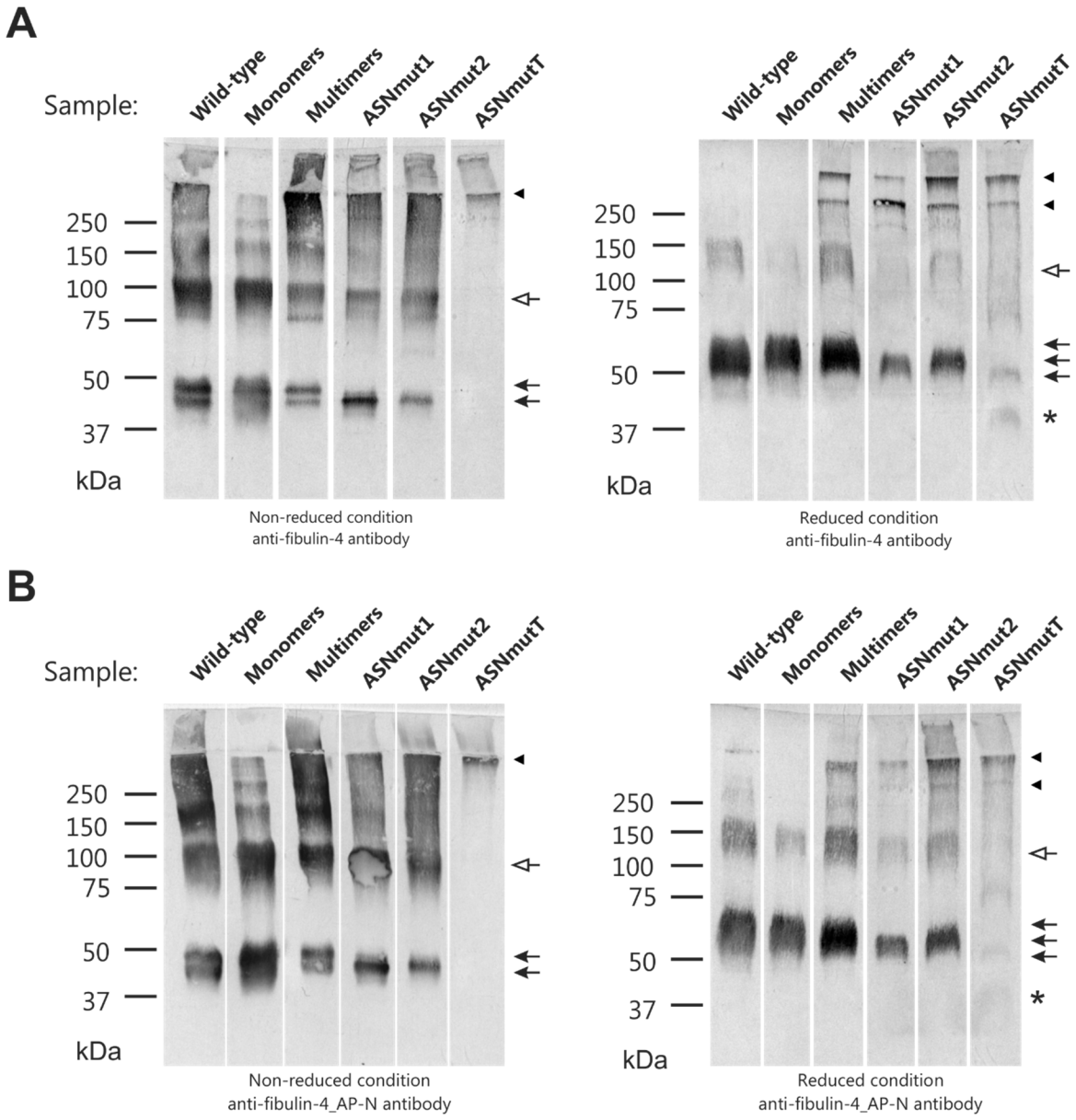

Figure 21. Western blotting comparison between the anti-fibulin-4 antibody and affinity purified anti-fibulin-4_AP-N antibody

Shown are the Western blotting membranes of fibulin-4 proteins (1μg per lane), including fibulin-4 wild-type, a monomer and a multimer preparation by gel filtration, and the N-glycosylation site mutants (hFBLN4_ASNmut1, 2, and T as ASNmut1, 2, and T), using anti-fibulin-4 antibody (A) or anti-fibulin-4_AP-N antibody (B). On the left panel, the proteins were analyzed under non-reducing conditions and on the right panel, the proteins were analyzed under reducing conditions with 20mM DTT. The filled arrows represent monomeric, the open arrows represent dimeric, and the arrowheads represent multimeric bands of fibulin-4 wild-type and the N-glycosylation site mutants. The asterisks indicate a 43kDa band observed in hFBLN4_ASNmutT, which is likely a degradation product.

6 RATIONALE, DISCUSSIONS, AND FUTURE DIRECTIONS

6.1 Rationale

Initially, fibulin-4 was recognized for its potential oncogenic properties and as a binding partner of p53, a tumor suppressor gene, and thus named as mutant p53 binding protein 1 (MBP1) (Gallagher et al., 1999). From a structural point of view, MBP1 resembled EGF-containing fibulin-like extracellular matrix protein 1 (EFEMP1 or fibulin-3); it contains six tandem arrays of cbEGF domains and the fibulin-type module at the C-terminus, thus named as EFEMP2 or fibulin-4 (Giltay et al., 1999; Katsanis et al., 2000). Electron microscopic analysis of fibulin-4 after rotary shadowing revealed that it possesses a rod-shape with association to one or two globular structures (Giltay et al., 1999). Tissue localization and the fibulin-4 complete KO mouse model revealed that its expression is predominant in elastic tissues, such as heart and large and small blood vessels (Kobayashi et al., 2007; McLaughlin et al., 2006). Patients reported of rare human fibulin-4 mutations were diagnosed with defects in elastic tissues at varying degrees, including cutis laxa, cardiovascular defects including aortic aneurysms, dilatations, and tortuosity, and developmental lung emphysema, supporting the concept of fibulin-4 as a critical molecule in elastogenesis (Hoyer et al., 2009; Hucthagowder et al., 2006; Renard et al., 2010).

As outlined in detail in the introduction, several studies have been performed to delineate the function of fibulin-4, including analyses of how fibulin-4 may participate in elastogenesis process (Giltay et al., 1999; Kobayashi et al., 2007). However, little is known about the functional domains/entities of fibulin-4 involved in elastogenesis. Fibulin-4 contains two predicted N-linked glycosylation sites which are conserved in evolution (Segade, 2010). Recombinantly-expressed fibulin-4 contains either contains either one or two N-linked glycans (Djokic et al., 2013; Giltay et al., 1999). In the present study, we aimed to characterize the functions of the fibulin-4 N-glycosylation sites. Two principal methods were employed to obtain deglycosylated fibulin-4: i) purified human recombinant fibulin-4 was enzymatically deglycosylated by PNGaseF; ii) site-directed mutagenesis was employed to mutagenize the asparagine in the N-glycosylation consensus sequence (Asn-X-Ser/Thr) to glutamine which contains only an additional methyl group. This prevented attachment of N-glycans at the consensus sites and minimized the

conformational changes in the protein. With this methodological setup, the roles of N-linked glycosylation sites in fibulin-4 were studied, with focus on the secretory pathway and the elastogenesis.

6.2 Disrupted secretory pathway

The pDNSP plasmid coding for full length human fibulin-4 and for single and double N-linked glycosylation site mutants were generated, with the sequence for an N-terminal signal peptide, and for a hexa-histidine tag at the C-terminus. The plasmids were transfected into mammalian cells (HEK293H) for proper post-translational modifications in the secretory pathway, including N-linked glycosylation and disulfide bond formation. Formation of correct intra-domain disulfide bonds confers stability and functionality of the proteins when they are exposed to the ECM (Bulleid, 2012). The hexa-histidine tag was utilized to facilitate purification of the secreted proteins from the conditioned medium by immobilized metal ion chromatography (Ni^{2+}-loaded) (Djokic et al., 2013).

After purification of the wild-type fibulin-4 and the single and double fibulin-4 N-linked glycosylation site mutants, significant differences were observed for the protein yields. The glycosylation site mutants yielded substantially lower amounts (~10 folds less) compared to the wild-type fibulin-4, resulting in protein pools containing less of the N-linked mutant proteins and more non-specific proteins (see section 5.3). This suggested that the removal of the N-linked glycosylation site(s) could have affected either the expression or the secretion of the fibulin-4. In order to differentiate between the two possibilities, indirect immunofluorescence analyses were performed using the transfected HEK293H cells to visualize and compare the localization of fibulin-4 inside the cells versus on the cell surface (Fig. 13). The immunofluorescence analyses revealed that the amount of cell surface-localized fibulin-4 was markedly reduced from the cells expressing the N-linked glycosylation site mutants, compared to the cells expressing the wild-type (Fig. 13). Interestingly, the intracellular staining level was observed to be similar between each recombinant cell clones (Fig. 13, right panel). These data, together with the reduced yields from the protein purifications, indicate that removal of the N-glycosylation site in fibulin-4 decreases the secretion through inhibiting the secretory pathway of the protein. One possible mechanism for

reduced protein secretion is through activation of the UPR which causes retention of unfolded or misfolded proteins (Tjeldhorn et al., 2011). One of the consequences of the UPR is the cytosolic splicing of the XBP1 mRNA which is known to be involved in further downstream signaling of protein retention and degradation pathway (Yoshida et al., 2001). The hypothesis was that the transfection of HEK293H cells with the fibulin-4 N-glycosylation site mutant constructs has activated the UPR, and analysis of the cytosolic mRNA of XBP1 was employed to address this hypothesis. Semi-quantitative RT-PCR revealed that the HEK293H cells transfected with the fibulin-4 N-linked glycosylation site mutant constructs contained significantly higher amount of the spliced XBP1 mRNA, compared to the cells transfected with the fibulin-4 wild-type construct, indicating that the UPR was indeed induced in the recombinant HEK293H cells. These data suggest that fibulin-4 requires complete N-linked glycosylation for the proper secretion of the protein into the ECM. Examining other molecular machineries, including the cleavage product of ATF6 in the cytosol from ATF6 kinase and the GADD34 expression from PERK kinase, would further confirm the activation of the UPR in the cells (see fig.6). Several previous studies have revealed the important regulatory roles of the N-linked glycosylation of extracellular proteins, including thrombospondin, extracellular matrix protein 1 and hyaluronidase1 (Goto et al., 2014; Uematsu et al., 2014; Vischer et al., 1985). Conversely, other studies have found that the N-linked glycosylation do not affect the secretion of the extracellular proteins such as fibulin-3, LOX propeptide, and matrillin-1 (Fresquet et al., 2010; Grimsby et al., 2010; Hulleman and Kelly, 2015). Overall, the findings suggest that N-linked glycosylation of fibulin-4 may play an important role in protein secretion.

The Western blot analysis of fibulin-4 wild-type under non-reduced conditions showed bands of three different molecular weight groups: monomers of about 50kDa, dimers of about 100kDa, and multimers above 250kDa (Fig. 11) (Djokic et al., 2013). Similar results were observed with both fibulin-4 single glycosylation site mutants showing monomers, dimers, and multimers (Fig. 11). However, there was an increase in the relative intensity of the multimeric bands versus dimeric and monomeric bands in the fibulin-4 single glycosylation site mutants as compared to the fibulin-4 wild-type, suggesting that the removal of a single glycan promoted multimerization of fibulin-4 (Fig. 11). The double unglycosylated fibulin-4 showed only multimeric under non-reducing conditions but not monomers and dimers (Fig. 11, left panel). This suggested that removal of both

N-glycosylation sites in fibulin-4 further enhanced self-interaction leading to the predominant multimers. When the disulfide bonds were reduced in wild-type fibulin-4, the monomeric, dimeric and multimeric bands merged together into a 61-65kDa band (Fig. 11, right panel). Interestingly, the addition of 20mM and DTT in the fibulin-4 N-glycosylation site mutants could not entirely reduce the proteins as they still occurred as multimeric bands above 250kDa (Fig.11, right panel). This suggested that upon prevention of N-glycosylation, fibulin-4 undergoes pre-mature multimerization which are non-reducible, possibly mediated through transglutaminases (Chen et al., 2000; Tyrrell et al., 1988). Consequently, the pre-mature multimerization of fibulin-4 N-glycosylation site mutants may interfere with proper secretion due to its molecular mass, which in turn would lead to a lower amount of secreted proteins in the extracellular environment compared to the wild-type fibulin-4. Interestingly, Djokic et al. have reported a gain of function upon multimerization of the recombinant fibulin-4 which showed enhanced binding to heparin, a model for cell surface heparan sulphate (Djokic et al., 2013). Analysis of fibulin-4 N-glycosylation mutant interaction partners, including extracellular proteins and relevant cell types may further unveil the functional role of the N-linked glycosylation in fibulin-4 through multimerization.

6.3 Impact on elastogenesis

Recombinantly expressed fibulin-4 has been previously reported to bind tropoelastin with a moderate binding affinity (Choudhury et al., 2009). The enzymatically deglycosylated fibulin-4 showed significantly enhanced binding to tropoelastin compared to the N-glycosylated wild-type fibulin-4 (Fig.7C). Similarly, PNGaseF-treated fibulin-4_I-II fragment also exhibited significantly enhanced binding to tropoelastin compared to the untreated protein. These observations led to hypothesize that the two N-linked glycans of fibulin-4 (Asn^{198} and Asn^{394}) may play regulatory roles in elastogenesis by inhibiting the binding to tropoelastin. Therefore, the expression plasmids of the N-linked glycosylation site mutants of fibulin-4 were generated to further test this hypothesis in cell culture.

PAC1 cells were chosen as a cell culture model to examine the functional roles of the fibulin-4 N-linked glycosylation site mutants in cell culture after surveying a panel of established elastogenic cell lines, including ARPE-19, RFL-6 and FBC (see section 5.6). PAC1 cells showed strong

expressions and depositions of both fibronectin and fibrillin-1 which are the pre-requisite components of the elastogenesis. PAC1 cells further showed moderate expression and deposition of fibulin-4 and tropoelastin, a requisite property to observe potential up- and down-regulation under the experimental conditions (Fig. 15D, 16). Interestingly in PAC1 cells, tropoelastin was observed as aggregates or droplets which appeared to gradually assemble into fibers. This observation correlates with how tropoelastin assembles in other cell lines (Czirok et al., 2006). In RFL-6 cells, high expression of tropoelastin was observed which readily formed fibers and this coincided with high expression of fibulin-4 (Fig. 15B). These observations suggested that the expression of tropoelastin and the assembly of tropoelastin aggregates into elastic fibers may be dependent on the expression level of fibulin-4. To confirm this hypothesis, either fibulin-4 overexpression or knock-down by siRNA could clarify the role of fibulin-4 in tropoelastin assembly in PAC1 cells. In the present study, fibulin-4 wild-type and the N-linked glycosylation site mutants constructs were overexpressed in PAC1 cells to analyze their roles in elastogenesis.

Fibulin-4 wild-type and the N-linked glycosylation site mutant overexpression in PAC1 cells revealed that all recombinant cell clones showed similar strong expression and deposition of both fibronectin and fibrillin-1 compared to the non-transfected controls. This demonstrated that overexpression of fibulin-4 wild-type or N-linked glycosylation site mutants do not influence fibronectin and fibrillin-1 fibers (Fig. 17A and B). As a previous study reported, fibulin-4 interacts with fibrillin-1 (Choudhury et al., 2009). Together with the findings presented here, demonstrating that overexpression of fibulin-4 does not enhance the fibrillin-1 fibers in the ECM, the data suggest that fibulin-4 may participate in elastogenesis after the formation of fibrillin-1 and fibronectin fibers.

Fibulin-4 in the matrix of the non-transfected PAC1 cells was observed as assembled network-like patterns, indicating that fibulin-4 may either form independent fibers or that is deposited on other pre-existing fibers such as fibrillin-1 or fibronectin fibers (Fig. 15D iii and 17C i). For interaction with fibronectin, however, fibulin-4 would require an adaptor molecule because it cannot interact directly with fibronectin (Kobayashi et al., 2007). All transfected PAC1 cells deposited recombinant fibulin-4 in bright patches and in significant higher amounts of fibulin-4 fibers

compared to the non-transfected PAC1 cells (Fig. 17C ii-v). From this experiment, it was not conclusive whether the recombinantly expressed fibulin-4 proteins were incorporated into the endogenous fibulin-4 network or whether they were deposited onto these networks.

PAC1 cells transfected with the wild-type fibulin-4 or the N-linked glycosylation site mutants showed substantially increased numbers of small globular tropoelastin aggregates compared to the non-transfected PAC1 cells (Fig. 17D and F). Furthermore, the PAC1 cells transfected with fibulin-4 mutant constructs displayed enhanced elastic fiber formations likely using the tropoelastin aggregates as nucleation sites (Fig. 17D and F). These results demonstrate that fibulin-4 overexpression influenced the number of the tropoelastin aggregates in the ECM and that the N-linked glycosylation site mutants further influenced the assembly of the aggregates into elastic fibers. As enzymatically deglycosylated fibulin-4 clearly showed enhanced binding to tropoelastin compared to the wild-type fibulin-4 (Fig. 7), it is likely that the overexpressed fibulin-4 proteins lacking one or two N-linked glycans interacted more readily with tropoelastin in the ECM, thus accelerating elastogenesis. Furthermore, semi-quantitative RT-PCR and dot-blot analysis revealed that the overexpression of wild-type fibulin-4 or the N-linked glycosylation site mutants enhanced the secretion of the tropoelastin but not the mRNA expression (Fig. 19). Analysis of expression levels of other tropoelastin interaction partners, including fibulin-5 and LTBP-4, would provide further information if the enhanced secretion is directly or indirectly related to fibulin-4 overexpression. The overall observations from this study suggest that fibulin-4 enhances the secretion of tropoelastin and fibulin-4 N-glycosylation site mutants further enhance the assembly of the secreted tropoelastin into elastic fibers.

If this concept is true, there are two critical questions which need to be solved: 1) how can the cellular machinery effectively secrete N-glycosylation deficient fibulin-4 to the ECM?, and 2) how can the enhanced binding to tropoelastin eventually be dissociated for further deposition of the nascent elastic fibers onto microfibrils?

It has been demonstrated that exogenously added recombinant wild-type fibulin-4 did neither affect the number of tropoelastin aggregates nor the assembly of elastic fibers by PAC1 cells (Fig. 18). Therefore, the increased number of the tropoelastin droplets observed with the transfected PAC1 cells might be due to the interaction of tropoelastin and the overexpressed fibulin-4 within the secretory pathway. In fact, little is known about the intracellular binding partners of tropoelastin. Known tropoelastin binding proteins include elastin binding protein and FK506-binding protein (FKBP65) (Davis et al., 1998; Hinek et al., 1995). Elastin binding protein and FKBP65 interact with tropoelastin in the ER, and are known to assist tropoelastin in folding, prepare tropoelastin to undergo coacervation, and help it to be properly secreted to the ECM as chaperones (Cheung et al., 2010; Miao et al., 2013). Similarly, when fibulin-4 N-linked glycosylation site mutants are overexpressed, they may assist tropoelastin for extracellular secretion as chaperones through the enhanced interaction with tropoelastin. Simultaneously, through this interaction with tropoelastin, fibulin-4 mutant proteins themselves may be chaperoned and secreted more efficiently to the ECM even in the absence of the proper N-linked glycosylation. To prove these possibilities, cell lysate pull-down assays of the tropoelastin against fibulin-4 need to be performed to reveal if there is any interaction between the two proteins. Also the analysis of the UPR in the PAC1 non-transfected and transfected cells should demonstrate if there is any change in the UPR activation levels.

The dissociation of tropoelastin from fibulin-4 and the deposition onto microfibrils must occur properly because elastogenesis is a timely and spatially-regulated process (Kozel et al., 2006). Building up from the previous hypothesis, tropoelastin and fibulin-4 N-linked glycosylation site mutants are secreted to the ECM in a cooperative chaperoning complex. Thereafter, immediate dissociations of the complex following the delivery of the tropoelastin aggregates onto the microfibrils would be expected. Note that hFBLN4_ASNmutT generated an additional fragment of 43kDa band when observed by Western blotting, which could potentially be a degradation product due to the absence of the N-linked glycans (Fig. 11A, right panel). From these observations, it is hypothesized that fibulin-4 N-linked glycosylation site mutants proteins are degraded at faster rates compared to the wild-type fibulin-4. The ECM is an environment full of various proteases, including matrix metalloproteinases (MMPs), A disintegrin-like and metalloprotease (reprolysin type) with thrombospondin type 1 motif (ADAMTS) proteases, and

meprins, which constantly degrade and remodel the extracellular environment (Apte, 2009; Kruse et al., 2004; Lind et al., 2006; Lu et al., 2011). Additionally, several previous studies have reported that upon deletion/removal of the N-linked glycosylation sites of extracellular proteins, including fibulin-3 and thrombospondin, the stabilities of the proteins becomes altered and are more prone to degradations (Hulleman and Kelly, 2015; Vischer et al., 1985). If this is true, it would also explain the reason for such a low protein purification yields from the conditioned media of the HEK293H cells transfected with the fibulin-4 N-linked glycosylation site mutants constructs (see section 5.3). To prove this hypothesis, proteolytic cleavage assays using various metalloproteinases would reveal if the fibulin-4 N-linked glycosylation site mutant proteins are more prone to cleavages than to the wild-type fibulin-4 (Djokic et al., 2013). Additionally, N-terminal sequencing of the 43kDa protein band observed in hFBLN4_ASNmutT would be required to verify if the band is a degradation fragment of fibulin-4.

6.4 Working models

Based on the observations in this study, we propose working models suggesting the role of fibulin-4 N-linked glycosylation sites in HEK293H cells (Fig.22) and in PAC1 cells (Fig. 23). These proposed models are meant to guide future work to elucidate the mechanism in which fibulin-4 participates in the elastogenesis. However, they still lack numerous major and minor experiments to prove the hypothesis.

In HEK293H cells, the transfected wild-type fibulin-4 is expressed and secreted through the secretory pathway. The protein undergoes proper post-translational modifications in the ER, including disulfide-bond formation and N-linked glycosylation, and are secreted to the extracellular environment. Fibulin-4 N-linked glycosylation site mutants are also translocated into the ER as the wild-type fibulin-4. However, the mutant proteins are recognized for not possessing a proper N-linked glycosylation sites and this activates the UPR. Thus, the protein secretion is stalled within the secretory pathway and remain intracellularly.

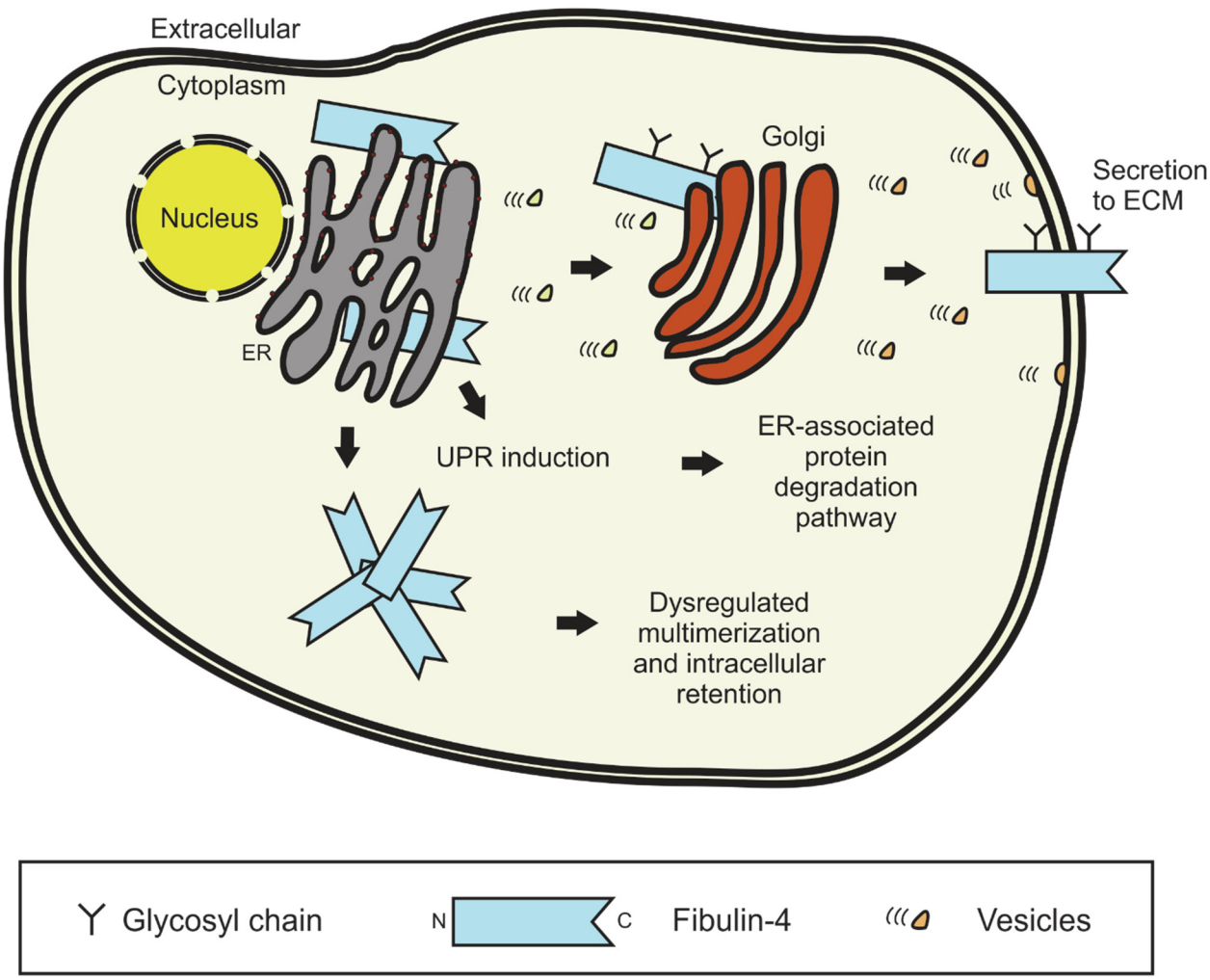

Figure 22. Working model of fibulin-4 wild-type and the N-linked glycosylation site mutant secretory pathway in HEK293H cells

Fibulin-4 wild-type undergoes proper post-translational modifications, including N-linked glycosylation, and is secreted to the ECM. When N-linked glycosylation cannot take place, UPR is activated which cause retention of fibulin-4 in the ER. Unglycosylated fibulin-4 may also undergo dysregulated multimerization which additionally inhibit the secretory pathway.

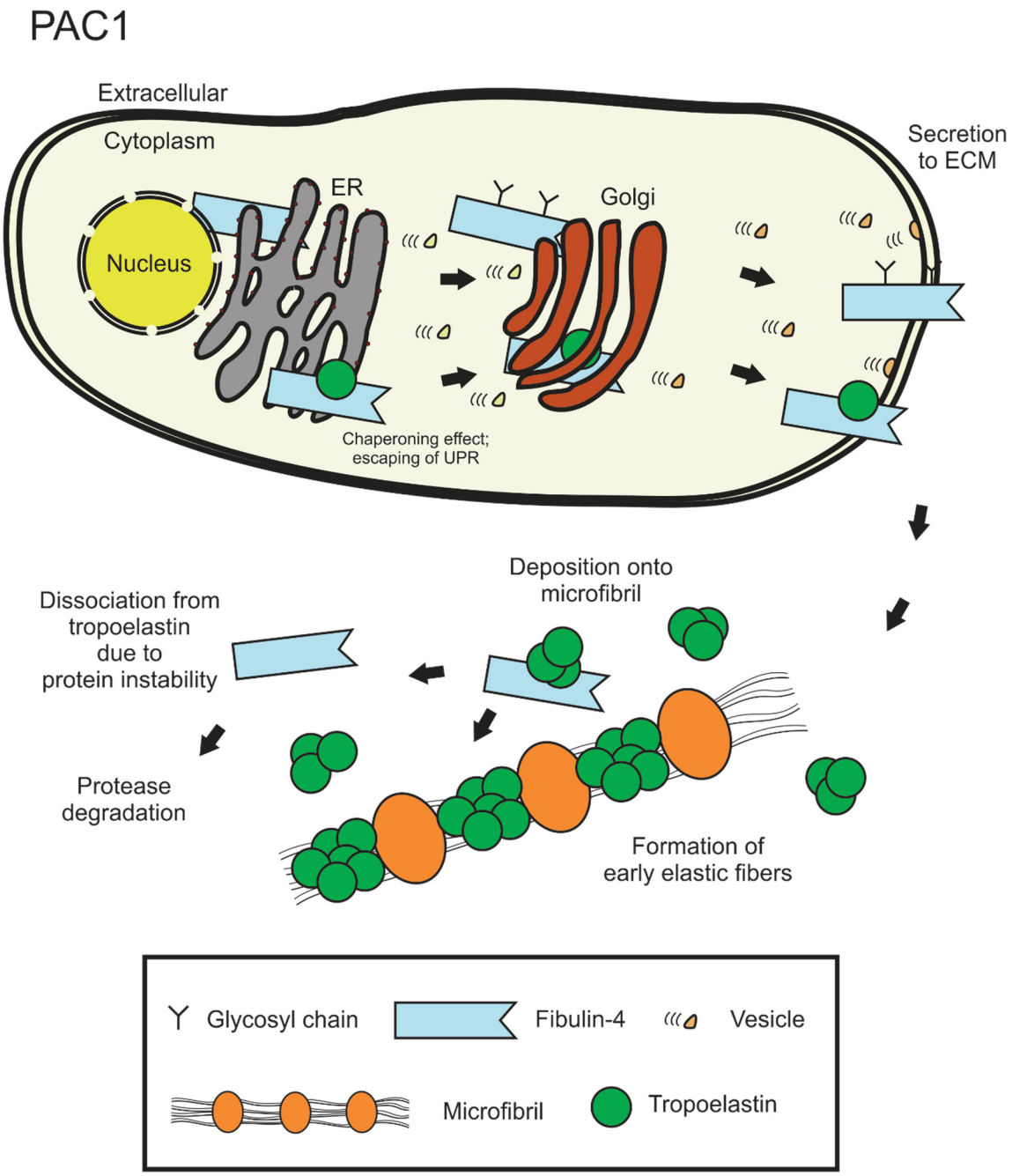

Figure 23. Working model of fibulin-4 wild-type and the N-linked glycosylation site mutant secretory pathway in PAC1 cells

In PAC1 cells where tropoelastin is expressed, the unglycosylated fibulin-4 may interact with tropoelastin within the secretory pathway, and act as a chaperone for tropoelastin to aid its secretion to the ECM. Likewise, tropoelastin also acts as a chaperone for unglycosylated fibulin-4 and bypass the UPR. The secreted tropoelastin-fibulin-4 complex may dissociate faster due to elevated susceptibility of the fibulin-4 against ECM proteases.

In PAC1 cells, the presence of tropoelastin chaperones the fibulin-4 N-linked glycosylation site mutants from being stalled at the ER. With the enhanced binding affinity, fibulin-4 N-linked glycosylation site mutants bind to tropoelastin inside the cells and, in turn, enhance the tropoelastin secretion to the ECM. However, due to the absence of the N-linked glycans, fibulin-4 mutants become more prone to proteolytic degradation by ECM proteases. This may release the tropoelastin from the fibulin-4-tropoelastin complex and subsequently tropoelastin may become deposited onto microfibrils, the next step in the formation of elastic fibers.

6.5 Conclusions

The overall analysis of fibulin-4 N-linked glycosylation sites reveals that they play important roles for two biological events: 1) proper secretion of the protein to the extracellular environment, and 2) elastic fiber formation. Fibulin-4 requires a proper N-linked glycosylation at the ER to be secreted, and N-glycosylation deficiencies activate UPR. In the presence of tropoelastin, unglycosylated fibulin-4 may escape the retention at the level of the ER by forming a complex with tropoelastin, and simultaneously enhance the secretion to the ECM. Subsequently, tropoelastin may be deposited onto the microfibrils and unglycosylated fibulin-4 may be degraded by extracellular proteases. In future, their roles may be further investigated by *in vivo* studies, as well as to other aspects, including cancers.

7 REFERENCES

1) **Apte, S.S.** (2009). A disintegrin-like and metalloprotease (reprolysin-type) with thrombospondin type 1 motif (ADAMTS) superfamily: functions and mechanisms. **Journal of Biological Chemistry** *284*, 31493-31497.

2) **Aumailley, M., and Gayraud, B.** (1998). Structure and biological activity of the extracellular matrix. **Journal of Molecular Medicine (Berlin, Germany)** *76*, 253-265.

3) **Bertolotti, A., Zhang, Y., Hendershot, L.M., Harding, H.P., and Ron, D.** (2000). Dynamic interaction of BiP and ER stress transducers in the unfolded-protein response. **Nature Cell** *2*, 326-332.

4) **Bulleid, N.J.** (2012). Disulfide bond formation in the mammalian endoplasmic reticulum. **Cold Spring Harbor Perspectives in Biology** *4*. a013219

5) **Bultmann-Mellin, I., Conradi, A., Maul, A.C., Dinger, K., Wempe, F., Wohl, A.P., Imhof, T., Wunderlich, F.T., Bunck, A.C., Nakamura, T., *et al.*** (2015). Modeling autosomal recessive cutis laxa type 1C (ARCL1C) in mice reveals distinct functions of Ltbp-4 isoforms. **Disease Models & Mechanisms**. *8*, 403-415

6) **Cannon, K.S., and Helenius, A.** (1999). Trimming and readdition of glucose to N-linked oligosaccharides determines calnexin association of a substrate glycoprotein in living cells. **Journal of Biological Chemistry** *274*, 7537-7544.

7) **Carta, L., Pereira, L., Arteaga-Solis, E., Lee-Arteaga, S.Y., Lenart, B., Starcher, B., Merkel, C.A., Sukoyan, M., Kerkis, A., Hazeki, N., *et al.*** (2006). Fibrillins 1 and 2 perform partially overlapping functions during aortic development. **Journal of Biological Chemistry** *281*, 8016-8023.

8) **Chen, L.J., Zhao, Y., Gao, S., Chou, I.N., Toselli, P., Stone, P., and Li, W.** (2005). Downregulation of lysyl oxidase and upregulation of cellular thiols in rat fetal lung fibroblasts treated with cigarette smoke condensate. **Toxicological Sciences** *83*, 372-379.

9) **Chen, R., Gao, B., Huang, C., Olsen, B., Rotundo, R.F., Blumenstock, F., and Saba, T.M.** (2000). Transglutaminase-mediated fibronectin multimerization in lung endothelial matrix in response to TNF-alpha. **American Journal of Physiology: Lung Cellular and Molecular Physiology** *279*, L161-174.

10) **Cheung, K.L., Bates, M., and Ananthanarayanan, V.S.** (2010). Effect of FKBP65, a putative elastin chaperone, on the coacervation of tropoelastin in vitro. **Biochemistry and Cell Biology** *88*, 917-925.

11) **Choudhury, R., McGovern, A., Ridley, C., Cain, S.A., Baldwin, A., Wang, M.C., Guo, C., Mironov, A., Jr., Drymoussi, Z., Trump, D., *et al.*** (2009). Differential regulation of

elastic fiber formation by fibulin-4 and -5. **Journal of Biological Chemistry** *284*, 24553-24567.

12) **Corson, G.M., Charbonneau, N.L., Keene, D.R., and Sakai, L.Y.** (2004). Differential expression of fibrillin-3 adds to microfibril variety in human and avian, but not rodent, connective tissues. **Genomics** *83*, 461-472.

13) **Curran, M.E., Atkinson, D.L., Ewart, A.K., Morris, C.A., Leppert, M.F., and Keating, M.T.** (1993). The elastin gene is disrupted by a translocation associated with supravalvular aortic stenosis. **Cell** *73*, 159-168.

14) **Czirok, A., Zach, J., Kozel, B.A., Mecham, R.P., Davis, E.C., and Rongish, B.J.** (2006). Elastic fiber macro-assembly is a hierarchical, cell motion-mediated process. **Journal of Cellular Physiology** *207*, 97-106.

15) **Davis, E.C., Broekelmann, T.J., Ozawa, Y., and Mecham, R.P.** (1998). Identification of tropoelastin as a ligand for the 65-kD FK506-binding protein, FKBP65, in the secretory pathway. **Journal of Cell Biology** *140*, 295-303.

16) **Djokic, J., Fagotto-Kaufmann, C., Bartels, R., Nelea, V., and Reinhardt, D.P.** (2013). Fibulin-3, -4, and -5 are highly susceptible to proteolysis, interact with cells and heparin, and form multimers. **Journal of Biological Chemistry** *288*, 22821-22835.

17) **Ellgaard, L., and Helenius, A.** (2003). Quality control in the endoplasmic reticulum. **Nature Reviews: Molecular Cell Biology** *4*, 181-191.

18) **Ewart, A.K., Morris, C.A., Atkinson, D., Jin, W., Sternes, K., Spallone, P., Stock, A.D., Leppert, M., and Keating, M.T.** (1993). Hemizygosity at the elastin locus in a developmental disorder, Williams syndrome. **Nature Genetics** *5*, 11-16.

19) **Fresquet, M., Jowitt, T.A., Stephen, L.A., Ylostalo, J., and Briggs, M.D.** (2010). Structural and functional investigations of Matrilin-1 A-domains reveal insights into their role in cartilage ECM assembly. **Journal of Biological Chemistry** *285*, 34048-34061.

20) **Gallagher, W.M., Argentini, M., Sierra, V., Bracco, L., Debussche, L., and Conseiller, E.** (1999). MBP1: a novel mutant p53-specific protein partner with oncogenic properties. **Oncogene** *18*, 3608-3616.

21) **Galli, C., Bernasconi, R., Solda, T., Calanca, V., and Molinari, M.** (2011). Malectin participates in a backup glycoprotein quality control pathway in the mammalian ER. **PloS One** *6*, e16304.

22) **Gething, M.J.** (1999). Role and regulation of the ER chaperone BiP. **Seminars in Cell and Developmental Biology** *10*, 465-472.

23) **Gibson, M.A., Hatzinikolas, G., Davis, E.C., Baker, E., Sutherland, G.R., and Mecham, R.P.** (1995). Bovine latent transforming growth factor beta 1-binding protein 2:

molecular cloning, identification of tissue isoforms, and immunolocalization to elastin-associated microfibrils. **Molecular and Cellular Biology** *15*, 6932-6942.

24) **Giltay, R., Timpl, R., and Kostka, G.** (1999). Sequence, recombinant expression and tissue localization of two novel extracellular matrix proteins, fibulin-3 and fibulin-4. **Matrix Biology** *18*, 469-480.

25) **Goto, Y., Niwa, Y., Suzuki, T., Uematsu, S., Dohmae, N., and Simizu, S.** (2014). N-glycosylation is required for secretion and enzymatic activity of human hyaluronidase1. **FEBS Open Bio** *4*, 554-559.

26) **Grimsby, J.L., Lucero, H.A., Trackman, P.C., Ravid, K., and Kagan, H.M.** (2010). Role of lysyl oxidase propeptide in secretion and enzyme activity. **Journal of Cellular Biochemistry** *111*, 1231-1243.

27) **Hanada, K., Vermeij, M., Garinis, G.A., de Waard, M.C., Kunen, M.G., Myers, L., Maas, A., Duncker, D.J., Meijers, C., Dietz, H.C.*, et al.*** (2007). Perturbations of vascular homeostasis and aortic valve abnormalities in fibulin-4 deficient mice. **Circulation Research** *100*, 738-746.

28) **Hart, G.W., Brew, K., Grant, G.A., Bradshaw, R.A., and Lennarz, W.J.** (1979). Primary structural requirements for the enzymatic formation of the N-glycosidic bond in glycoproteins. Studies with natural and synthetic peptides. **Journal of Biological Chemistry** *254*, 9747-9753.

29) **Hebson, C., Coleman, K., Clabby, M., Sallee, D., Shankar, S., Loeys, B., Van Laer, L., and Kogon, B.** (2014). Severe aortopathy due to fibulin-4 deficiency: molecular insights, surgical strategy, and a review of the literature. **European Journal of Pediatrics** *173*, 671-675.

30) **Hinek, A., Keeley, F.W., and Callahan, J.** (1995). Recycling of the 67-kDa elastin binding protein in arterial myocytes is imperative for secretion of tropoelastin. **Experimental Cell Research** *220*, 312-324.

31) **Hirai, M., Horiguchi, M., Ohbayashi, T., Kita, T., Chien, K.R., and Nakamura, T.** (2007). Latent TGF-beta-binding protein 2 binds to DANCE/fibulin-5 and regulates elastic fiber assembly. **EMBO Journal** *26*, 3283-3295.

32) **Holzenberger, M., Lievre, C.A., and Robert, L.** (1993). Tropoelastin gene expression in the developing vascular system of the chicken: an in situ hybridization study. **Anatomy and Embryology** *188*, 481-492.

33) **Horiguchi, M., Inoue, T., Ohbayashi, T., Hirai, M., Noda, K., Marmorstein, L.Y., Yabe, D., Takagi, K., Akama, T.O., Kita, T.*, et al.*** (2009). Fibulin-4 conducts proper elastogenesis via interaction with cross-linking enzyme lysyl oxidase. **Proceedings of the National Academy of Sciences of the United States of America** *106*, 19029-19034.

34) **Hoyer, J., Kraus, C., Hammersen, G., Geppert, J.P., and Rauch, A.** (2009). Lethal cutis laxa with contractural arachnodactyly, overgrowth and soft tissue bleeding due to a novel homozygous fibulin-4 gene mutation. **Clinical Genetics** *76*, 276-281.

35) **Hu, Q., Loeys, B.L., Coucke, P.J., De Paepe, A., Mecham, R.P., Choi, J., Davis, E.C., and Urban, Z.** (2006). Fibulin-5 mutations: mechanisms of impaired elastic fiber formation in recessive cutis laxa. **Human Molecular Genetics** *15*, 3379-3386.

36) **Huang, J., Davis, E.C., Chapman, S.L., Budatha, M., Marmorstein, L.Y., Word, R.A., and Yanagisawa, H.** (2010). Fibulin-4 deficiency results in ascending aortic aneurysms: a potential link between abnormal smooth muscle cell phenotype and aneurysm progression. **Circulation Research** *106*, 583-592.

37) **Hubbard, S.C., and Robbins, P.W.** (1979). Synthesis and processing of protein-linked oligosaccharides in vivo. **Journal of Biological Chemistry** *254*, 4568-4576.

38) **Hubmacher, D., El-Hallous, E.I., Nelea, V., Kaartinen, M.T., Lee, E.R., and Reinhardt, D.P.** (2008). Biogenesis of extracellular microfibrils: Multimerization of the fibrillin-1 C terminus into bead-like structures enables self-assembly. **Proceedings of the National Academy of Sciences of the United States of America** *105*, 6548-6553.

39) **Hubmacher, D., and Reinhardt, D.** (2011). Microfibrils and Fibrillin. In The Extracellular Matrix: an Overview, R.P. Mecham, ed. **(Springer Berlin Heidelberg)**, pp. 233-265.

40) **Hubmacher, D., Bergeron, E., Fagotto-Kaufmann, C., Sakai, L.Y., and Reinhardt, D.P.** (2014). Early fibrillin-1 assembly monitored through a modifiable recombinant cell approach. **Biomacromolecules** *15*, 1456-1468.

41) **Hucthagowder, V., Sausgruber, N., Kim, K.H., Angle, B., Marmorstein, L.Y., and Urban, Z.** (2006). Fibulin-4: a novel gene for an autosomal recessive cutis laxa syndrome. **American Journal of Human Genetics** *78*, 1075-1080.

42) **Hulleman, J.D., and Kelly, J.W.** (2015). Genetic ablation of N-linked glycosylation reveals two key folding pathways for R345W fibulin-3, a secreted protein associated with retinal degeneration. **FASEB Journal** *29*, 565-575.

43) **Ihn, H.** (2002). Pathogenesis of fibrosis: role of TGF-beta and CTGF. **Current Opinion in Rheumatology** *14*, 681-685.

44) **Isogai, Z., Aspberg, A., Keene, D.R., Ono, R.N., Reinhardt, D.P., and Sakai, L.Y.** (2002). Versican interacts with fibrillin-1 and links extracellular microfibrils to other connective tissue networks. **Journal of Biological Chemistry** *277*, 4565-4572.

45) **Jones, R.P., Ridley, C., Jowitt, T.A., Wang, M.C., Howard, M., Bobola, N., Wang, T., Bishop, P.N., Kielty, C.M., Baldock, C.*, et al.*** (2010). Structural effects of fibulin 5 missense mutations associated with age-related macular degeneration and cutis laxa. **Investigative Ophthalmology and Visual Science** *51*, 2356-2362.

46) **Kagan, H.M., and Sullivan, K.A**. (1982). [35] Lysyl oxidase: Preparation and role in elastin biosynthesis. In Methods in Enzymology, D.W.F. Leon W. Cunningham, ed. **(Academic Press)**, pp. 637-650.

47) **Katsanis, N., Venable, S., Smith, J.R., and Lupski, J.R.** (2000). Isolation of a paralog of the Doyne honeycomb retinal dystrophy gene from the multiple retinopathy critical region on 11q13. **Human Genetics** *106*, 66-72.

48) **Keeley, F.W.** (1979). The synthesis of soluble and insoluble elastin in chicken aorta as a function of development and age. Effect of a high cholesterol diet. **Canadian Journal of Biochemistry** *57*, 1273-1280.

49) **Keene, D.R., Maddox, B.K., Kuo, H.J., Sakai, L.Y., and Glanville, R.W.** (1991). Extraction of extendable beaded structures and their identification as fibrillin-containing extracellular matrix microfibrils. **Journal of Histochemistry and Cytochemistry** *39*, 441-449.

50) **Kielty, C.M.** (2006). Elastic fibres in health and disease. **Expert Reviews in Molecular Medicine** *8*, 1-23.

51) **Kobayashi, N., Kostka, G., Garbe, J.H., Keene, D.R., Bachinger, H.P., Hanisch, F.G., Markova, D., Tsuda, T., Timpl, R., Chu, M.L.*, et al.*** (2007). A comparative analysis of the fibulin protein family. Biochemical characterization, binding interactions, and tissue localization. **Journal of Biological Chemistry** *282*, 11805-11816.

52) **Kornfeld, R., and Kornfeld, S.** (1985). Assembly of asparagine-linked oligosaccharides. **Annual Review of Biochemistry** *54*, 631-664.

53) **Kozel, B., Mecham, R., and Rosenbloom, J.** (2011). Elastin. In The Extracellular Matrix: an Overview, R.P. Mecham, ed. **(Springer Berlin Heidelberg)**, pp. 267-301.

54) **Kozel, B.A., Rongish, B.J., Czirok, A., Zach, J., Little, C.D., Davis, E.C., Knutsen, R.H., Wagenseil, J.E., Levy, M.A., and Mecham, R.P.** (2006). Elastic fiber formation: a dynamic view of extracellular matrix assembly using timer reporters. **Journal of Cellular Physiology** *207*, 87-96.

55) **Kriz, W., Elger, M., Lemley, K., and Sakai, T.** (1990). Structure of the glomerular mesangium: a biomechanical interpretation. **Kidney International Supplement** *30*, S2-9.

56) **Kruse, M.N., Becker, C., Lottaz, D., Kohler, D., Yiallouros, I., Krell, H.W., Sterchi, E.E., and Stocker, W.** (2004). Human meprin alpha and beta homo-oligomers: cleavage of basement membrane proteins and sensitivity to metalloprotease inhibitors. **Biochemical Journal** *378*, 383-389.

57) **Li, D.Y., Brooke, B., Davis, E.C., Mecham, R.P., Sorensen, L.K., Boak, B.B., Eichwald, E., and Keating, M.T.** (1998a). Elastin is an essential determinant of arterial morphogenesis. **Nature** *393*, 276-280.

58) **Li, D.Y., Faury, G., Taylor, D.G., Davis, E.C., Boyle, W.A., Mecham, R.P., Stenzel, P., Boak, B., and Keating, M.T.** (1998b). Novel arterial pathology in mice and humans hemizygous for elastin. **Journal of Clinical Investigation** *102*, 1783-1787.

59) **Lin, G., Tiedemann, K., Vollbrandt, T., Peters, H., Batge, B., Brinckmann, J., and Reinhardt, D.P.** (2002). Homo- and heterotypic fibrillin-1 and -2 interactions constitute the basis for the assembly of microfibrils. **Journal of Biological Chemistry** *277*, 50795-50804.

60) **Lind, T., Birch, M.A., and McKie, N.** (2006). Purification of an insect derived recombinant human ADAMTS-1 reveals novel gelatin (type I collagen) degrading activities. **Molecular and Cellular Biochemistry** *281*, 95-102.

61) **Liu, X., Zhao, Y., Gao, J., Pawlyk, B., Starcher, B., Spencer, J.A., Yanagisawa, H., Zuo, J., and Li, T.** (2004). Elastic fiber homeostasis requires lysyl oxidase-like 1 protein. **Nature Genetics** *36*, 178-182.

62) **Loeys, B., Van Maldergem, L., Mortier, G., Coucke, P., Gerniers, S., Naeyaert, J.M., and De Paepe, A.** (2002). Homozygosity for a missense mutation in fibulin-5 (FBLN5) results in a severe form of cutis laxa. **Human Molecular Genetics** *11*, 2113-2118.

63) **Loeys, B.L., Gerber, E.E., Riegert-Johnson, D., Iqbal, S., Whiteman, P., McConnell, V., Chillakuri, C.R., Macaya, D., Coucke, P.J., De Paepe, A.*, et al.*** (2010). Mutations in fibrillin-1 cause congenital scleroderma: stiff skin syndrome. **Science Translational Medicine** *2*, 23ra20.

64) **Lomas, A.C., Mellody, K.T., Freeman, L.J., Bax, D.V., Shuttleworth, C.A., and Kielty, C.M.** (2007). Fibulin-5 binds human smooth-muscle cells through alpha5beta1 and alpha4beta1 integrins, but does not support receptor activation. **Biochemical Journal** *405*, 417-428.

65) **Lu, P., Takai, K., Weaver, V.M., and Werb, Z.** (2011). Extracellular matrix degradation and remodeling in development and disease. **Cold Spring Harbor Perspectives in Biology** *3*. a005058

66) **Marshall, R.D.** (1972). Glycoproteins. **Annual Review of Biochemistry** *41*, 673-702.

67) **McLaughlin, P.J., Chen, Q., Horiguchi, M., Starcher, B.C., Stanton, J.B., Broekelmann, T.J., Marmorstein, A.D., McKay, B., Mecham, R., Nakamura, T.*, et al.*** (2006). Targeted disruption of fibulin-4 abolishes elastogenesis and causes perinatal lethality in mice. **Molecular and Cellular Biology** *26*, 1700-1709.

68) **Mecham, R.P., and Davis, E.C.** (1994). Elastic Fiber Structure and Assembly. In Extracellular Matrix Assembly and Structure, P.D.Y.E.B.P. Mecham, ed. **(San Diego: Academic Press)**, pp. 281-314.

69) **Miao, M., Reichheld, S.E., Muiznieks, L.D., Huang, Y., and Keeley, F.W.** (2013). Elastin binding protein and FKBP65 modulate in vitro self-assembly of human tropoelastin. **Biochemistry** *52*, 7731-7741.

70) **Milewicz, D.M., Grossfield, J., Cao, S.N., Kielty, C., Covitz, W., and Jewett, T.** (1995). A mutation in FBN1 disrupts profibrillin processing and results in isolated skeletal features of the Marfan syndrome. **Journal of Clinical Investigation** *95*, 2373-2378.

71) **Mithieux, S.M., and Weiss, A.S.** (2005). Elastin. **Advances in Protein Chemistry** *70*, 437-461.

72) **Muschler, J., and Streuli, C.H.** (2010). Cell-matrix interactions in mammary gland development and breast cancer. **Cold Spring Harbor Perspectives in Biology** *2*, a003202.

73) **Nakamura, T., Ruiz-Lozano, P., Lindner, V., Yabe, D., Taniwaki, M., Furukawa, Y., Kobuke, K., Tashiro, K., Lu, Z., Andon, N.L.*, et al.*** (1999). DANCE, a novel secreted RGD protein expressed in developing, atherosclerotic, and balloon-injured arteries. **Journal of Biological Chemistry** *274*, 22476-22483.

74) **Nakamura, T., Lozano, P.R., Ikeda, Y., Iwanaga, Y., Hinek, A., Minamisawa, S., Cheng, C.F., Kobuke, K., Dalton, N., Takada, Y.*, et al.*** (2002). Fibulin-5/DANCE is essential for elastogenesis in vivo. **Nature** *415*, 171-175.

75) **Noda, K., Dabovic, B., Takagi, K., Inoue, T., Horiguchi, M., Hirai, M., Fujikawa, Y., Akama, T.O., Kusumoto, K., Zilberberg, L.*, et al.*** (2013). Latent TGF-beta binding protein 4 promotes elastic fiber assembly by interacting with fibulin-5. **Proceedings of the National Academy of Sciences of the United States of America** *110*, 2852-2857.

76) **Nonaka, R., Onoue, S., Wachi, H., Sato, F., Urban, Z., Starcher, B.C., and Seyama, Y.** (2009). DANCE/fibulin-5 promotes elastic fiber formation in a tropoelastin isoform-dependent manner. **Clinical Biochemistry** *42*, 713-721.

77) **Papke, C.L., and Yanagisawa, H.** (2014). Fibulin-4 and fibulin-5 in elastogenesis and beyond: Insights from mouse and human studies. **Matrix Biology** *37*, 142-149.

78) **Parks, W.C.** (1997). Posttranscriptional regulation of lung elastin production. **American Journal of Respiratory Cell and Molecular Biology** *17*, 1-2.

79) **Partridge, S.M., Elsden, D.F., and Thomas, J.** (1963). Constitution of the cross-linkages in elastin. **Nature** *197*, 1297-1298.

80) **Ramirez, F., and Sakai, L.Y.** (2010). Biogenesis and function of fibrillin assemblies. **Cell and Tissue Research** *339*, 71-82.

81) **Rao, R.V., Ellerby, H.M., and Bredesen, D.E.** (2004). Coupling endoplasmic reticulum stress to the cell death program. **Cell Death and Differentiation** *11*, 372-380.

82) **Rapaka, R.S., and Urry, D.W.** (1978). Coacervation of sequential polypeptide models of tropoelastin. Synthesis of H-(Val-Ala-Pro-Gly)n-Val-OMe and H-(Val-Pro-Gly-Gly)n-Val-OMe. **International Journal of Peptide and Protein Research** *11*, 97-108.

83) **Raviola, G.** (1971). The fine structure of the ciliary zonule and ciliary epithelium. With special regard to the organization and insertion of the zonular fibrils. **Investigative Ophthalmology** *10*, 851-869.

84) **Renard, M., Holm, T., Veith, R., Callewaert, B.L., Ades, L.C., Baspinar, O., Pickart, A., Dasouki, M., Hoyer, J., Rauch, A., *et al.*** (2010). Altered TGFbeta signaling and cardiovascular manifestations in patients with autosomal recessive cutis laxa type I caused by fibulin-4 deficiency. **European Journal of Human Genetics** *18*, 895-901.

85) **Robb, B.W., Wachi, H., Schaub, T., Mecham, R.P., and Davis, E.C.** (1999). Characterization of an in vitro model of elastic fiber assembly. **Molecular Biology of the Cell** *10*, 3595-3605.

86) **Robinson, P.N., Arteaga-Solis, E., Baldock, C., Collod-Beroud, G., Booms, P., De Paepe, A., Dietz, H.C., Guo, G., Handford, P.A., Judge, D.P., *et al.*** (2006). The molecular genetics of Marfan syndrome and related disorders. **Journal of Medical Genetics** *43*, 769-787.

87) **Ron, D., and Walter, P.** (2007). Signal integration in the endoplasmic reticulum unfolded protein response. **Nature Reviews: Molecular Cell Biology** *8*, 519-529.

88) **Rothman, A., Kulik, T.J., Taubman, M.B., Berk, B.C., Smith, C.W.J., and Nadalginard, B.** (1992). Development and Characterization of a Cloned Rat Pulmonary Arterial Smooth-Muscle Cell-Line That Maintains Differentiated Properties through Multiple Subcultures. **Circulation** *86*, 1977-1986.

89) **Rozario, T., and DeSimone, D.W.** (2010). The extracellular matrix in development and morphogenesis: a dynamic view. **Developmental Biology** *341*, 126-140.

90) **Sabatier, L., Chen, D., Fagotto-Kaufmann, C., Hubmacher, D., McKee, M.D., Annis, D.S., Mosher, D.F., and Reinhardt, D.P.** (2009). Fibrillin assembly requires fibronectin. **Molecular Biology of the Cell** *20*, 846-858.

91) **Sakai, L.Y., Keene, D.R., and Engvall, E.** (1986). Fibrillin, a new 350-kD glycoprotein, is a component of extracellular microfibrils. **Journal of Cell Biology** *103*, 2499-2509.

92) **Schallus, T., Jaeckh, C., Feher, K., Palma, A.S., Liu, Y., Simpson, J.C., Mackeen, M., Stier, G., Gibson, T.J., Feizi, T., *et al.*** (2008). Malectin: a novel carbohydrate-binding protein of the endoplasmic reticulum and a candidate player in the early steps of protein N-glycosylation. **Molecular Biology of the Cell** *19*, 3404-3414.

93) **Schneider, C.A., Rasband, W.S., and Eliceiri, K.W.** (2012). NIH Image to ImageJ: 25 years of image analysis. **Nature Methods** *9*, 671-675.

94) **Schroder, M., and Kaufman, R.J.** (2005). ER stress and the unfolded protein response. **Mutation Research** *569*, 29-63.

95) **Segade, F.** (2010). Molecular evolution of the fibulins: implications on the functionality of the elastic fibulins. **Gene** *464*, 17-31.

96) **Shang, J., and Lehrman, M.A.** (2004). Discordance of UPR signaling by ATF6 and Ire1p-XBP1 with levels of target transcripts. **Biochemical and Biophysical Research Communications** *317*, 390-396.

97) **Shapiro, S.D., Endicott, S.K., Province, M.A., Pierce, J.A., and Campbell, E.J.** (1991). Marked longevity of human lung parenchymal elastic fibers deduced from prevalence of D-aspartate and nuclear weapons-related radiocarbon. **Journal of Clinical Investigation** *87*, 1828-1834.

98) **Sideek, M.A., Menz, C., Parsi, M.K., and Gibson, M.A.** (2014). LTBP-2 competes with tropoelastin for binding to fibulin-5 and heparin, and is a negative modulator of elastinogenesis. **Matrix Biol** *34*, 114-123.

99) **Stone, E.M., Braun, T.A., Russell, S.R., Kuehn, M.H., Lotery, A.J., Moore, P.A., Eastman, C.G., Casavant, T.L., and Sheffield, V.C.** (2004). Missense variations in the fibulin 5 gene and age-related macular degeneration. **New England Journal of Medicine** *351*, 346-353.

100) **Tannous, A., Pisoni, G.B., Hebert, D.N., and Molinari, M.** (2014). N-linked sugar-regulated protein folding and quality control in the ER. **Seminars in Cell and Developmental Biology**. 1084-9521

101) **Tassabehji, M., Metcalfe, K., Hurst, J., Ashcroft, G.S., Kielty, C., Wilmot, C., Donnai, D., Read, A.P., and Jones, C.J.** (1998). An elastin gene mutation producing abnormal tropoelastin and abnormal elastic fibres in a patient with autosomal dominant cutis laxa. **Human Molecular Genetics** *7*, 1021-1028.

102) **Tiedemann, K., Batge, B., Muller, P.K., and Reinhardt, D.P.** (2001). Interactions of fibrillin-1 with heparin/heparan sulfate, implications for microfibrillar assembly. **Journal of Biological Chemistry** *276*, 36035-36042.

103) **Tjeldhorn, L., Iversen, N., Sandvig, K., Bergan, J., Sandset, P.M., and Skretting, G.** (2011). Protein C mutation (A267T) results in ER retention and unfolded protein response activation. **PloS One** *6*, e24009.

104) **Trombetta, E.S., and Helenius, A.** (2000). Conformational requirements for glycoprotein reglucosylation in the endoplasmic reticulum. **Journal of Cell Biology** *148*, 1123-1129.

105) **Tyrrell, D.J., Sale, W.S., and Slife, C.W.** (1988). Isolation of a sodium dodecyl sulfate-insoluble transglutaminase substrate from liver plasma membranes. **Journal of Biological Chemistry** *263*, 1946-1951.

106) **Uematsu, S., Goto, Y., Suzuki, T., Sasazawa, Y., Dohmae, N., and Simizu, S.** (2014). N-Glycosylation of extracellular matrix protein 1 (ECM1) regulates its secretion, which is unrelated to lipoid proteinosis. **FEBS Open Bio** *4*, 879-885.

107) **Viljoen, D., Ramesar, R., and Behari, D.** (1991). Beals syndrome: clinical and molecular investigations in a kindred of Indian descent. **Clinical Genetics** *39*, 181-188.

108) **Vischer, P., Beeck, H., and Voss, B.** (1985). Synthesis, intracellular processing and secretion of thrombospondin in human endothelial cells. **European Journal of Biochemistry** *153*, 435-443.

109) **Wachi, H., Sato, F., Murata, H., Nakazawa, J., Starcher, B.C., and Seyama, Y.** (2005). Development of a new in vitro model of elastic fiber assembly in human pigmented epithelial cells. **Clinical Biochemistry** *38*, 643-653.

110) **Wachi, H., Nonaka, R., Sato, F., Shibata-Sato, K., Ishida, M., Iketani, S., Maeda, I., Okamoto, K., Urban, Z., Onoue, S.,** ***et al.*** (2008). Characterization of the molecular interaction between tropoelastin and DANCE/Fibulin-5. **Journal of Biochemistry** *143*, 633-639.

111) **Wess, T.J., Purslow, P.P., Sherratt, M.J., Ashworth, J., Shuttleworth, C.A., and Kielty, C.M.** (1998). Calcium determines the supramolecular organization of fibrillin-rich microfibrils. **Journal of Cell Biology** *141*, 829-837.

112) **Wormald, M.R., and Dwek, R.A.** (1999). Glycoproteins: glycan presentation and protein-fold stability. **Structure** *7*, R155-160.

113) **Yanagisawa, H., Davis, E.C., Starcher, B.C., Ouchi, T., Yanagisawa, M., Richardson, J.A., and Olson, E.N.** (2002). Fibulin-5 is an elastin-binding protein essential for elastic fibre development in vivo. **Nature** *415*, 168-171.

114) **Yanagisawa, H., and Davis, E.C.** (2010). Unraveling the mechanism of elastic fiber assembly: The roles of short fibulins. **International Journal of Biochemistry and Cell Biology** *42*, 1084-1093.

115) **Yoshida, H., Matsui, T., Yamamoto, A., Okada, T., and Mori, K.** (2001). XBP1 mRNA is induced by ATF6 and spliced by IRE1 in response to ER stress to produce a highly active transcription factor. **Cell** *107*, 881-891.

116) **Zanetti, M., Braghetta, P., Sabatelli, P., Mura, I., Doliana, R., Colombatti, A., Volpin, D., Bonaldo, P., and Bressan, G.M.** (2004). EMILIN-1 deficiency induces elastogenesis and vascular cell defects. **Molecular and Cellular Biology** *24*, 638-650.

117) **Zhang, H., Apfelroth, S.D., Hu, W., Davis, E.C., Sanguineti, C., Bonadio, J., Mecham, R.P., and Ramirez, F.** (1994). Structure and expression of fibrillin-2, a novel microfibrillar component preferentially located in elastic matrices. **Journal of Cell Biology** *124*, 855-863.

118) **Zheng, Q., Davis, E.C., Richardson, J.A., Starcher, B.C., Li, T., Gerard, R.D., and Yanagisawa, H.** (2007). Molecular analysis of fibulin-5 function during de novo synthesis of elastic fibers. **Molecular and Cellular Biology** *27*, 1083-1095.